UC Berkeley
UC Berkeley Electronic Theses and Dissertations

Title

Factors that Contribute to Protective CD8+ T Cell Responses to Chronic Infection

Permalink

https://escholarship.org/uc/item/1h79880q

Author

Tsitsiklis, Alexandra

Publication Date

2020

Peer reviewed|Thesis/dissertation

eScholarship.org Powered by the California Digital Library
University of California

Factors that Contribute to Protective CD8+ T Cell Responses to Chronic Infection

By

Alexandra Tsitsiklis

A dissertation submitted in partial satisfaction of the

requirements for the degree of

Doctor of Philosophy

in

Infectious Diseases and Immunity

in the

Graduate Division

of the

University of California, Berkeley

Committee in charge:

Professor Ellen Robey, Chair
Professor Sarah Stanley
Professor Laurent Coscoy
Professor David Raulet

Spring 2020

Abstract

Factors that Contribute to Protective CD8+ T Cell Responses to Chronic Infection

by

Alexandra Tsitsiklis

Doctor of Philosophy in Infectious Disease and Immunity

University of California, Berkeley

Professor Ellen Robey, Chair

The CD8+ T cell response to the intracellular parasite *Toxoplasma gondii* varies dramatically between mouse strains, resulting in differences in control of the parasite. This difference is linked to MHC haplotype, and protection in BALB/c mice has been attributed to an unusually strong MHC-1 L^d-restricted CD8+ T cell response directed against a peptide derived from the parasite protein GRA6. Our lab has previously shown that the GRA6-L^d specific response is maintained by a proliferative intermediate population that gives rise to large numbers of armed effector T cells throughout chronic infection and shows no signs of functional exhaustion. To further investigate this robust CD8+ T cell response, we characterized the TCR repertoire of GRA6-L^d specific CD8+ T cells after *T. gondii* infection. We showed that the GRA6-L^d specific T cell response displays a TCR repertoire dominated by the Vβ2 variable chain, limited clonal diversity, a strongly selected CDR3β motif, and a public TCR. Additionally, we showed that another L^d-restricted CD8+ T cell response specific for the F2 peptide from Vaccinia virus also has a preference for Vβ2 and a similarly focused TCR repertoire.

The MHC-1 L^d molecule has limited peptide binding compared to conventional MHC molecules such as K^b or D^b, which correlates with polymorphisms associated with "elite control" of HIV in humans. To investigate the link between this unusual MHC-1 molecule and the generation of "elite controller" CD8+ T cell responses, we compared the GRA6-L^d specific T cell response to the OVA-K^b specific response restricted to the conventional MHC-1 K^b molecule. GRA6-L^d specific T cells are significantly more protective and resistant to exhaustion in chronic *T. gondii* infection. Next, we used CRISPR/Cas9 to generate mice with a point mutation (W97R) in the peptide-binding groove of L^d that results in broader peptide binding and investigated the effect of this L^d W97R mutation on another robust L^d-restricted response against the IE1 peptide during Murine Cytomegalovirus (MCMV) infection. We observed an increase in exhaustion marker expression on the IE1-L^d specific CD8+ T cells during chronic MCMV infection. In both systems, T cells restricted to MHC-1 L^d exhibited resistance to exhaustion compared to T cells restricted to an MHC-1 with broader peptide binding, supporting a model in which limited peptide binding my MHC favors protective responses during chronic infection.

Table of Contents

Chapter 1: Introduction……1
1.1 CD8+ T cell responses to chronic infection……..……1
1.2 CD8+ T cell responses to *Toxoplasma gondii:* lessons from a successful parasite…...5
1.3 Function of T cells with high and low self-reactivity……..18
1.4 References……...20

Chapter 2: TCR Repertoire Analysis of Ld-Restricted CD8+ T Cells.....30
2.1 Introduction.....30
2.2 Results and Discussion.....30
2.3 Materials and Methods.....33
2.4 References.....34

Chapter 3: An Unusual MHC Molecule Generates Protective CD8+ T Cell Responses to Chronic Infection.....43
3.1 Abstract.....43
3.2 Introduction.....43
3.3 Results.....45
3.4 Discussion.....49
3.5 Materials and Methods.....52
3.6 References.....54

Chapter 4: Studying CD8+ T Cells with High or Low Self-Reactivity.....72
4.1 Introduction.....72
4.2 Results and Discussion.....72
4.3 References.....76

List of Figures

Chapter 1

Table 1.1: Natural CD8+ T cell epitopes in *T. gondii*.....13

Table 1.2: Engineered CD8+ T cell antigens.....14

Figure 1.1: Modes of MHC-1 presentation of vacuolar antigens.....16

Figure 1.2: CD8+ T cell fate during *T. gondii* infection.....17

Chapter 2

Figure 2.1: Expansion of *T. gondii* epitope specific CD8+ T cells after peptide immunization.....36

Figure 2.2: Vβ usage in epitope specific CD8+ T cells after *T. gondii* infection.....37

Figure 2.3: Peptide binding strength, T cell expansion and Vβ usage of other L^d-restricted CD8+ T cell responses.....38

Figure 2.4: Clonal analyses of TCR α and β chains of GRA6-L^d specific T cells.....40

Figure 2.5: Clonal analyses of TCR α and β chains of F2-L^d specific T cells.....42

Chapter 3

Figure 3.1: TG6 T cells are more protective and resistant to exhaustion compared to OT-1 T cells.....59

Figure 3.2: The OVA-K^b specific CD8+ T cell response to *T. gondii* infection shows signs of functional exhaustion.....60

Figure 3.3: The L^d-restricted MCMV IE1 response has a proliferative intermediate population.....62

Figure 3.4: Polymorphism in H2-L^d increases self-peptide binding and correlates with increased expression of exhaustion markers on IE1-L^d specific CD8+ T cells.....63

Supplemental Figure 3.1: TG6 T cells are more protective compared to OT-1 T cells....65

Supplemental Figure 3.2: OT-1 T cells express higher levels of PD1 after infection.....66

Supplemental Figure 3.3: TG6 and OT-1 T cells experience similar levels of antigenic stimulation after transfer to infected mice.....67

Supplemental Figure 3.4: H2-L^d expression in L^d 97W mice is stabilized by peptide in different cell types.....68

Supplemental Figure 3.5: IE1-L^d specific CD8+ T cells express higher levels of CD69 in the lymph nodes compared to the spleen in L^d 97W and L^d 97R mice.....69

Supplemental Figure 3.6: Antigen levels are similar between L^d 97W and L^d 97R mice after MCMV infection.....70

Supplemental Figure 3.7: Model for MHC-1 specialists and CD8+ elite control.....71

Chapter 4

Figure 4.1: Analysis of CD5 expression on naïve GRA6-L^d specific T cells and bulk T cells from different mouse strains.....77

Figure 4.2: Survival and proliferation of naïve TG6 and OT-1 T cells *in vitro* with and without IL7.....78

Figure 4.3: Survival and proliferation of antigen experienced TG6 and OT-1 T cells *in vitro* with and without IL7.....79

Figure 4.4: Tracking GRA6-L^d and OVA-K^b specific CD8+ T cell populations in the blood after peptide-DC immunization.....80

Figure 4.5: GRA6-L^d and OVA-K^b specific T cells in $CD5^{high}$ or $CD5^{low}$ CD8+ T cell transfer.....81

Figure 4.6: Ratio of $CD5^{high}$ to $CD5^{low}$ transferred CD8+ T cells in blood over time.....82

Figure 4.7: Activation and PD1 expression of transferred $CD5^{high}$ and $CD5^{low}$ T cells in *T. gondii* infected mice.....83

Acknowledgements

First and foremost, I would like to thank my mentor Ellen Robey, for all of her support, guidance and mentorship throughout my time in the lab.

Special thanks to the Robey lab members who have been great coworkers and amazing friends and have made the lab an incredibly fun and supportive place for the past 5 years: Derek Bangs, Lydia Lutes, Michael Manoharan-Valerio, Nadia Kurd, and Laura McIntyre. Having you all in the lab has make the challenges and stresses of graduate school much easier to handle.

Special thanks to Shiao Chan for everything you do for the lab. None of this work would have been possible without your help.

I would also like to thank Hamlet Chu for getting me started on this project and teaching me everything I needed to know in the short time that we overlapped in the lab, as well as for all of your experiment and career advice over the years.

I would also like to thank my thesis committee, Sarah Stanley, Laurent Coscoy and David Raulet for their feedback and advice. Special thanks to Sarah Stanley for bringing me along to teach an immunology workshop in Uganda, and for always being available for additional advice.

Special thanks to everyone in the IDI PhD program for your friendship. It's been great being surrounded by people with the same passions as me, and we've had a lot of fun together over the past 6 years. You've all made my graduate school experience better.

Finally, I would like to thank my family and friends for all of their love and support. I would not have survived graduate school without all of you.

Chapter 1: Introduction

1.1: CD8+ T cell responses to chronic infection

During the adaptive immune response, antigen-presenting cells (APC) present pathogen derived peptides on major histocompatibility complex (MHC) class I molecules to CD8+ T cells to generate an antigen-specific CD8+ T cell response. CD8+ T cell responses are critical for the control of many intracellular pathogens. During acute infection, naïve T cells become activated, proliferate and differentiate into relatively short-lived effector T cells. Following pathogen clearance, the majority of activated T cells die, leaving behind a stem-like quiescent memory T cell population, which can rapidly generate new effector T cells upon secondary challenge (Kaech and Wherry 2007). In contrast, effective control of chronic pathogens requires continual replenishment of the effector T cell population to maintain balance between host and pathogen. However, persistent antigen and inflammation during chronic infection often causes T cells to become dysfunctional, or "exhausted" (Wherry 2011).

The maintenance of CD8+ T cell mediated control of chronic infections in mice has been widely studied in viral infection models such as lymphocytic choriomeningitis virus (LCMV) and mouse cytomegalovirus (MCMV). Additional studies conducted by our lab have also investigated protective CD8+ T cells during chronic *T. gondii* infection in mice (Chu et al. 2016). CD8+ T cell responses to *T. gondii* will be described in detail in Section 1.2.

CD8+ T cell exhaustion

A significant barrier to long-term protection against many infectious diseases and cancers is the functional exhaustion of T cells that results from persistent stimulation by antigen or inflammatory signals. T cell exhaustion involves a progressive loss of effector functions and the up-regulation and co-expression of multiple inhibitory receptors such as PD-1, Tim3, and Lag3 (Wherry 2011). This loss of "polyfunctionality", or ability to perform multiple effector functions, is characterized by a hierarchical loss of functions such as cytokine production, cytotoxicity, and proliferation, leading to subsequent deletion of many antigen-specific T cells (Zajac et al. 1998; Wherry et al. 2003). T cell exhaustion functions to limit immunopathology while balancing pathogen control, in order to promote survival of the host. However, in many infections severe CD8+ T cell exhaustion can lead to inefficient control and eventual host mortality.

Persistent antigen exposure is a primary factor leading to T cell exhaustion. Severity of exhaustion has been shown to correlate with the level of antigenic stimulation in both mice and humans (Wherry et al. 2003; Streeck et al. 2008; Blackburn et al. 2009; Bucks et al. 2009). Additional factors such as inflammatory signals, strength of TCR stimulation, and lack of CD4+ T cell help (Matloubian et al. 1994) also contribute to and determine the extent of exhaustion (Wherry 2011).

T cell exhaustion has been studied extensively in chronic viral infections with high levels of persisting viremia such as LCMV Clone 13 in mice. T cell exhaustion was first described in this model (Gallimore et al. 1998; Zajac et al. 1998), and it was later shown that functionality of exhausted CD8+ T cells is rescued by blockade of the PD-1-PD-L1 pathway in LCMV-infected mice (Barber et al. 2006). After PD-1 blockade, a subset of CD8+ T cells experience a "proliferative burst", recover some of their effector functions, and provide better control against infection (Barber et al. 2006). Importantly, not all exhausted T cells are able to respond to PD1 blockade. Subsequent studies demonstrated that the cells that are responsive to PD1 blockade have intermediate expression of PD1, while cells with the highest expression of PD1 cannot be rescued (Blackburn et al. 2008).

Immunotherapies targeting the PD-1 pathway have since shown to be effective in certain human cancer patients (Pardoll 2012; Pauken and Wherry 2015). In addition to PD-1, exhausted T cells simultaneously up-regulate multiple other inhibitory receptors and the expression of multiple exhaustion markers correlates with the severity of exhaustion (Blackburn et al. 2009). Combination immunotherapy has therefore been designed to target T cells co-expressing multiple inhibitory receptors in human chronic infections and cancer (Wolchok et al. 2013).

CD8+ T cell differentiation

Recently, several studies have aimed to characterize the memory, proliferative, and effector T cell subsets that arise during chronic infection with LCMV Clone 13. First, a stem-like memory population was identified, distinguished by CXCR5 and TCF1 co-expression (He et al. 2016; Im et al. 2016; Leong et al. 2016; Utzschneider et al. 2016). Further studies identified a proliferative CD8+ T cell subset which is an intermediate between the stem-like memory population and terminally differentiated cells and depends on CD4+ T cell help in the form of IL-21 production (Hudson et al. 2019; Zander et al. 2019). Importantly, the stem-like memory population was responsive to checkpoint blockade, indicating potential therapeutic benefits in studying this T cell subset. Similar T cell subsets present in chronic *T. gondii* infection are discussed in Section 1.2.

In contrast to LCMV Clone 13 infection, during chronic infection with MCMV the virus is well controlled and kept at a low level, with viral reservoirs maintained in the salivary glands (Krmpotic et al. 2003). Within the MCMV specific CD8+ T cell response, a unique phenomenon of memory inflation has been described, where certain antigen-specific T cell responses increase in magnitude over time and retain functionality despite chronic stimulation (Holtappels et al. 2000; Karrer et al. 2003; Munks et al. 2006). Studies of CD8+ T cells to MCMV have identified a memory-like progenitor population responsible for the continuous generation of effector T cells (Snyder 2008; Quinn 2015; Delpoux et al. 2017). Additional studies have described a population of highly proliferative cells (Smith et al. 2014). Further studies should compare these populations to those identified in LCMV infection.

CD8+ T cell responses to chronic infection in humans

Chronic infections are a significant burden to human health and a major public health concern. In many cases, current treatments can only control, but not eliminate, the pathogen, and new vaccines and therapeutics are needed. CD8+ T cells play an important role in the immune response against persistent viral infections, so understanding these responses will aid in the development of vaccines or immunotherapeutic strategies to combat these diseases.

While CD8+ T cell exhaustion was first described in mouse models, the effects of T cell exhaustion in viral infection have also been appreciated in many human infections such as HIV, hepatitis B virus (HBV), and hepatitis C virus (HCV) (Bowen and Walker 2005; Day et al. 2006; Trautmann et al. 2006; Urbani et al. 2006; Boni et al. 2007; Radwiezicz et al. 2007). Importantly, checkpoint blockade has been shown to have an effect on viral specific T cells in HIV, HBV, and HCV infection in humans, opening up opportunities for immunotherapy (Sharpe et al. 2007).

CD8+ T cell responses to HIV

CD8+ T cells are critical for the control of HIV infection, and a polyfunctional CD8+ T cell response is associated with viral control. Rapid activation of a potent CD8+ T cell response during the acute infection is associated with better control of viremia (Ndhlovu et al. 2015), but this response is not always effectively maintained during the chronic phase of infection, so disease outcome varies widely between individuals. Due to persistent viremia and chronic immune activation, CD8+ T cells become functionally exhausted in most individuals during later phases of HIV infection, evidenced by an increase in expression of inhibitory molecules, a reduction in cytokine production and proliferative capacity, and an increase in cell death (Day et al. 2006; Petrovas et al. 2006).

Interestingly, rare HIV-infected individuals are able to control the HIV virus to undetectable levels without antivirals and are therefore called HIV “elite controllers”. Several studies have identified specific HLA-B alleles, like HLA-B*27 and HLA-B*57, which correlate strongly with viral control (Kaslow et al. 1996; Migueles et al. 2000; Taborda-Vanegas et al. 2011), implicating CD8+ T cells in control of disease progression. These HLA-B alleles present immunodominant epitopes derived from the HIV Gag protein, and many studies have linked disease outcome to T cells targeting this viral protein (Goulder and Walker 2012). Control of SIV in rhesus macaques has also been shown to correlate with specific HLA alleles (Loffredo et al. 2007). The association between specific HLA alleles and protection against chronic infections is poorly understood.

CD8+ T cells in HIV controllers have been shown to exhibit greater cytotoxicity, proliferation, and polyfunctionality compared with responses in progressors (Migueles et al. 2002; Betts et al. 2006; Migueles et al. 2008; Hersperger et al. 2011). Additional studies have demonstrated that CD8+ T cell responses in elite controllers may be more

cross-reactive to variant epitopes resulting from viral mutants, effectively suppressing the replication of viruses with escape mutations (Ladell et al. 2013; Pohlmeyer et al. 2013). Furthermore, analysis of specific TCR in controllers revealed that the protective effect in "controllers" is associated with distinct TCR clonotypes that more effectively control the virus *in vitro*, are more cross-reactive, and have enhanced perforin activity (Chen et al. 2012). The factors that may select for more effective TCRs in this context are not known. Interestingly, these same alleles also correlate with susceptibility to autoimmune conditions such as ankylosing spondylitis (AS), which may be the cost of such robust CD8+ T cell responses (Sorrentino et al. 2013).

Analysis of the HLA alleles associated with control or progression has revealed that viral control is associated with individual amino acid positions that influence how these alleles present peptides. Specifically, the strongest correlation with control and progression is position 97 within the peptide-binding groove of HLA-B (Pereyra et al. 2010). Variability at this position influences the structure and flexibility of the peptide-binding groove (Blanco-Gelaz et al. 2006; Fagerberg et al. 2006). A computational study analyzed the specific polymorphisms identified in this study and demonstrated that the protective "controller" alleles are predicted to bind fewer self-peptides compared to the "progressor" alleles (Kosmrjl et al. 2010). The authors predicted that the protective HLA alleles should select for more cross-reactive T cells due to lower self-peptide presentation by these alleles in the thymus, which alters thymic selection (Kosmrjl et al. 2010).

Despite numerous studies demonstrating differences between CD8+ T cells in "controllers" versus "progressors", the precise mechanism allowing for robust control of HIV in these individuals is not known. Importantly, not all individuals with protective alleles are able to control the virus, and many factors may play a role in modulating this effect (Goulder and Walker 2012). Understanding the role of distinct MHC-1 alleles in generating protective CD8+ T cell responses may have important implications in the development of vaccines or immunotherapies for HIV, as well as for other persistent infections or cancers.

1.2: CD8+ T cell responses to *Toxoplasma gondii*: lessons from a successful parasite

The following section was adapted and/or reprinted with permission from: Tsitsiklis, A., Bangs, D.J, and Robey, E.A. (2019) CD8+ T cell responses to *Toxoplasma gondii*: lessons from a successful parasite. Trends in Parasitology, 35(11): 887-898

T. gondii infection in mice provides an excellent model for the study of CD8+ T cell responses. Natural and engineered *T. gondii* antigens have led the way to understanding the factors regulating antigen presentation from vacuolar pathogens. *T. gondii* infection of resistant and sensitive mouse strains provides unique models to study both effective CD8+ T cell function and protection in a well-controlled infection attributed to a novel T cell population, and T cell exhaustion in a progressing chronic infection. Additionally, the long-term persistence of the parasite in the brain provides a unique model of neurotropic infection used to study CD8+ T cell entry, retention and function in the brain. Here we discuss recent advances in each of these areas.

CD8+ T cell responses to *T. gondii*

The protozoan intracellular parasite, *Toxoplasma gondii (T. gondii)*, is a highly successful pathogen. It is found world-wide in a variety of birds and mammals, including an estimated 20-50% of humans. Its success is largely achieved by the parasite's ability to establish a stable balance with the host immune response, thus allowing the parasite to rapidly spread through the body and establish persistent infection, while also maintaining the viability of the host. A key part of this balance involves CD8+ T cells, the primary cell type that controls the parasite in the mammalian adaptive immune response.

Experimental *T. gondii* infection of mice (a natural host) provides an outstanding model for understanding CD8+ T cell responses. Propagating the parasite in the lab is relatively safe and easy, and a large variety of genetically engineered parasite strains are available. The parasite spreads systemically, allowing for the study of CD8+ T cell responses in a variety of lymphoid and nonlymphoid tissues, including the brain, the primary site of long-term persistence. Finally, the CD8+ T cell response differs dramatically in different inbred mouse strains, leading to differential control of the parasite during chronic infection, and providing an opportunity to explore the factors that determine CD8+ T cell efficacy. Recent progress using the mouse-*T. gondii* infection model has uncovered various aspects of CD8+ T cell responses, including antigen presentation and effector T cell differentiation.

How CD8+ T cells detect vacuolar pathogens

In many viral and intracellular bacterial infections, pathogen-derived antigens are present in the host cell cytosol and can be processed and presented to CD8+ T cells via the classical Major Histocompatibility Complex Class I (MHC-I) presentation pathway. However, vacuolar pathogens such as *T. gondii* pose particular challenges for MHC-I presentation, since their antigens do not have access to the host cytosol. Nevertheless, *T. gondii* infection elicits a robust and protective CD8+ T cell response. That fact, together

with a collection of several natural antigens that have been identified (Table 1), and the ability to generate parasites expressing engineered antigens (Table 2), makes *T. gondii* a valuable model for the study of CD8+ T cell responses to vacuolar pathogens.

Although in some settings inert, phagocytosed antigens can be cross-presented by certain antigen presenting cells (APC**)** (Joffre et al. 2012), presentation of *T. gondii* antigens requires interactions of live parasites with APC (Gubbels et al. 2005; Dupont et al. 2014). Moreover, presentation of *T. gondii* antigens is strongly affected by their mode of secretion from the parasite into host cells, and their location and membrane topology within the host cell (Table 1). For example, constitutive secretion via organelles termed dense granules favors antigen presentation, whereas retention of the antigen within the parasite prevents presentation (Gubbels et al. 2005; Kwok et al. 2003; Gregg et al. 2011). In addition, soluble antigens that are secreted into the parasitophorous vacuole (PV) lumen appear to enter the MHC-I presentation pathway via a Sec22b-dependent ER to Golgi intermediate compartment (ERGIC) pathway (Goldszmid et al. 2009; Cebrian et al. 2011; Joffre et al. 2012), and are processed in a proteasome/TAP dependent manner (Gubbels et al. 2005; Bertholet et al. 2006) (Figure 1). In contrast, the immunodominant GRA6 antigen, which is also secreted via dense granules, does not require Sec22b (Buaillon 2017). After secretion, the GRA6 protein associates with the PV membrane (PVM) with its C-terminal epitope protruding into the host cytosol, and this orientation favors efficient presentation (Feliu et al. 2013; Lopez et al. 2015; Buaillon et al. 2017) (Figure 1). Presentation of the HF10-GRA6 epitope has been shown to require components of the classical MHC-I pathway such as the proteasome, TAP, and ERAAP (Blanchard et al. 2008), however it is unknown how the epitope is released from the PVM to access this pathway. It has been hypothesized that an unidentified protease may cleave the C-terminal epitope which protrudes into the host cell cytosol. Interestingly, some host proteins involved in cross-presentation, such as Rab22a and Sec61, associate directly with the PV (Cebrian et al. 2016; Goldszmid et al. 2009), suggesting there may be direct access of parasite antigens to the cross-presentation pathway. On the other hand, for some antigens, access to the cytosol may be accomplished through damage to the PVM by host defense mechanisms such as immunity-related GTPases (IRGs) (Dzierszinski et al. 2007; Lee et al. 2015).

In addition to constitutive secretion via dense granules, *T. gondii* also possess a distinct secretory pathway via organelles termed rhoptries. Rhoptries directly discharge their contents into host cells during the invasion process, and during abortive invasion events (Koshy et al. 2012, reviewed in Boothroyd and Dubremetz 2008). This model of secretion might be expected to favor MHC-I presentation, since the antigens have direct access to the host cytosol and the classic MHC-I presentation machinery (Figure 1). However, rhoptry targeted antigens are relatively weak antigens (Frickel et al. 2008), and antigenicity can be improved by retargeting a rhoptry epitope for dense granule secretion (Grover et al. 2014) (Table 2). This may reflect the transient nature of rhoptry secretion, and failure to accumulate sufficient parasite antigen in the cytosol.

A model for effector CD8+ T cell responses

Most of our knowledge about CD8+ T cell responses to persistent infections comes from studies with Lymphocytic choriomeningitis virus (LCMV), in which chronic infection and persistently high antigen load leads to functional impairment of T cells, or T cell exhaustion (Barber et al. 2006, Virgin et al. 2009; Wherry et al. 2011). HIV, one of the most medically important chronic viral infections, also results in T cell exhaustion (Shankar et al. 2000, Goepfert et al. 2000, Day et al. 2006) but is difficult to study due to lack of an appropriate mouse model. Well-controlled viral infections can be complicated by factors such as periods of viral latency or the phenomena of epitope switching and "memory inflation" observed in Mouse Cytomegalovirus (MCMV) infection (Karrer et al. 2003, Snyder et al. 2008). Therefore, our understanding of the mechanisms that maintain effective control during infection with persistent pathogens is limited and could benefit from additional mouse models. Studies focusing on T cell responses during *T. gondii* infection have provided insights into T cell function and differentiation.

Features of the CD8+ response to T. gondii

CD8+ T cells are critical for effective control of many intracellular pathogens, including *T. gondii* (Gigley et al. 2011). Early work utilizing depletion or knockout studies demonstrated that CD8+ T cells are the most protective adaptive immune cell type during infection (Suzuki and Remington 1988; Parker et al. 1991; Schaeffer et al. 2009). IFNγ has been identified as a key mediator of protection (Suzuki et al. 1988; Suzuki and Remington 1990; Norose et al. 2001), and CD8+ T cells, in addition to CD4+ T cells, serve as important cytokine producers. CD8+ T cells can also mediate lysis of infected cells, and recently direct lysis of parasites through granulysin secretion in the acute stage has been demonstrated as well (Dotiwala et al. 2016).

The observation that BALB/c (H-2^d) mice are better at controlling *T. gondii* infection compared to C57BL/6 mice (H-2^b) led to this trait being mapped to the MHC-I L^d gene in BALB/c mice (Brown et al. 1995). We and our colleagues have shown that this is due to the induction of an immunodominant and protective CD8+ T cell response directed against a peptide from the parasite protein GRA6 (Blanchard et al. 2008). BALB/c mice are able to establish effective long-term control of the parasite, while C57/BL6 mice, which lack L^d and therefore cannot present the GRA6 peptide, develop progressing disease. These two contrasting settings provide a unique opportunity to study the differentiation, exhaustion, and maintenance of CD8+ T cell responses to infection in the context of a well-controlled infection versus a poorly-controlled progressing infection.

CD8+ T cell differentiation during acute infection

During an immune response, naive pathogen-specific CD8+ T cells differentiate into functionally heterogeneous populations characterized by distinct memory potential and effector functions (Williams et al. 2007). This differentiation is regulated by various signals, including T cell receptor signaling, co-stimulatory signals, and cytokine signals received from APC or other bystander cells. In particular, inflammatory cytokines such as

IL-12 and type-I interferons have been shown to function as a "signal 3", directly signaling activated CD8+ T cells to promote proliferation and effector functions *in vitro* and *in vivo*. (Curtsinger et al. 1999, Curtsinger et al. 2005; Kolumam et al. 2005).

The specific cytokines that drive early effector differentiation can vary between models, and studies examining CD8+ T cell fate during acute *T. gondii* infection in C57BL/6 mice have identified a critical role for IL-12 in this system. IL-12 knockout mice fail to generate large numbers of effector CD8+ T cells and show reduced expression of KLRG1 (Wilson et al. 2008; Wilson et al. 2010), a widely used marker of effector differentiation. Co-infection of mice with *T. gondii* and an intestinal helminth can promote the type-II cytokine IL-4, which together with IL-10 suppresses IL-12 responses and dampens effector CD8+ differentiation (Marple et al. 2017). IL-12 impacts the different stages of effector T cell differentiation both by signaling directly to the T cell or through activating other cell types to make IFNγ (Shah et al. 2015) (Figure 2).

As CD8+ T cells differentiate during acute infection, their localization within lymphoid tissues changes. Shah et al. (2015) tracked the location of T cell populations in the spleen as they progressed through various stages of differentiation after vaccination with an attenuated parasite strain. As cells matured from naïve to terminally differentiated effectors, they moved from the white pulp through the marginal zone into the red pulp. This migration into the red pulp appears to be regulated by the chemokine receptor CXCR3 and its ligands CXCL9 and CXCL10, similar to the role of CXCR3 on CD8+ T cells in other models (Kurachi et al. 2011, Hu et al. 2011). This relationship between fate and location suggests there may be environmental signals promoting distinct fates in these different regions.

CD8+ T cells in progressing chronic infection

Although C57/BL6 mice are able to mount effective CD8+ T cell responses during acute infection, they are ultimately unable to control the parasite in chronic stages of infection, resulting in mouse mortality due to toxoplasmic encephalitis (TE). In this setting, CD8+ T cells upregulate the inhibitory receptor PD-1, a marker of T cell exhaustion typically upregulated in chronic viral infections (Bhadra et al. 2011). These CD8+ T cells also lose effector functions and become more susceptible to apoptosis (Bhadra et al. 2012). *In vivo* blockade of the receptor for PD-1, PD-L1, referred to as checkpoint blockade, rescues PD-1+ CD8+ T cells, leading to improved CD8+ T cell responses and prevention of TE-associated mortality (Bhadra et al. 2011). However, the infection model may impact the efficacy of this treatment, as neutralization of inhibitory receptors failed to reverse CD8+ T cell exhaustion and rescue infected mice after challenge with hyper-virulent strains (Splitt et al. 2018).

Recently, a progenitor-like CD8+ T cell population that responds to checkpoint blockade in certain models of chronic infection and tumors has been identified and characterized (Im et al. 2016; Utzschneider et al. 2016; Kurtulus et al. 2019). These cells share some common features across models, the most prominent being expression of *Tcf7*/TCF1, a transcription factor associated with self-renewal capacity. It will be interesting to

determine whether a similar progenitor-like CD8+ T cell population is present in mice chronically infected by *T. gondii,* and whether its presence or absence correlates with the response of mice to checkpoint blockade.

CD4+ T cell help plays a role in preventing or reversing CD8+ T cell exhaustion during infection with *T. gondii* and other chronic viral pathogens. Expression of the transcription factor Blimp-1 in CD4+ T cells correlates with CD4+ T cell exhaustion during *T. gondii* infection (Figure 2), and deletion of Blimp-1 restores function of these CD4+ T cells (Hwang et al. 2016). Boosting CD4+ T cell function by deletion of Blimp-1 or adoptive transfer of functional CD4+ T cells into chronically infected mice can also restore CD8+ T cell function after exhaustion (Hwang et al. 2016). IL-21 is a key cytokine produced by follicular helper CD4+ T cells (Tfh) that has an important role in proper B cell activation. Interestingly, IL-21 also appears to be critical in maintaining CD8+ T cell functionality during chronic *T. gondii* infection. Exhausted CD4+ T cells lose IL-21 production but re-gain production after Blimp-1 ablation (Moretto et al. 2017; Hwang et al. 2016). In addition, IL-21 knockout mice have impaired CD8+ responses and reduced ability to control the parasite compared to wild-type mice (Moretto et al. 2017).

CD8+ T cells in a well-controlled chronic infection

Utilizing the unique model of parasite control in H-2^d-expressing mice allows for investigations of the factors regulating CD8+ T cells in a well-controlled chronic infection and provides an interesting contrast to the H-2^b model of susceptibility. H-2^d-linked protection is mediated by an immunodominant CD8+ T cell response against the parasite protein GRA6 (Blanchard et al. 2008). Investigations into the processing and presentation of the GRA6 epitope have advanced our understanding of MHC-I presentation (see above), and this unique response has begun to provide key insights into novel features of CD8+ T cell function as well. Unlike T cells in most chronic infections, GRA6-specific CD8+ T cells do not upregulate PD-1 or other inhibitory receptors and retain cytotoxic capacity and cytokine production throughout chronic infection (Chu et al. 2016). Investigating the exact mechanisms behind this may provide novel therapeutic targets to prevent or reverse T cell exhaustion.

The protective capacity of CD8+ T cell responses against GRA6 have also been demonstrated by other groups. Sanecka et al (2016) showed that GRA6-specific transnuclear CD8+ T cells significantly reduced parasite burden during the acute phase of infection, while Sa et al (2017) provided evidence that GRA6-specific CD8+ T cells play a role in cyst removal during chronic infection.

The GRA6 response also develops a unique differentiation profile. GRA6-specific T cells maintain a balance between three functionally distinct populations defined by surface expression of CXCR3 and KLRG1 (Chu et al. 2016). A long-lived memory population (T_{MEM}) gives rise to a highly proliferative intermediate population (T_{INT}) that allows the generation of a large number of terminally differentiated effectors (T_{EFF}). Modeling studies demonstrated the importance of this novel T_{INT} population in rapidly producing new T_{EFF} cells without depleting the T_{MEM} population, and subdominant responses

lacking this T_{INT} population were not maintained well throughout the chronic stages of infection.

Certain similarities exist between the wave of effector T cell differentiation that occurs following *T. gondii* vaccination and the continuous production of effector T cells that occurs during well-controlled *T. gondii* infection (Figure 2). In both settings, CXCR3 is expressed early but is subsequently lost as cells progress to terminal differentiation. KLRG1 expression is regulated inversely, with initial upregulation being observed during the intermediate stages of differentiation and high expression continuing through terminal differentiation. Both models also feature proliferation specifically within a CXCR3+ KLRG1+ population (Shah et al. 2015; Chu et al. 2016). In light of these similarities it will be important to investigate the location of each GRA6-specific population within the spleen during chronic infection and the role of inflammatory cytokines like IL-12 and IFNγ.

CD8+ T Cell Responses in the Brain

During infection, *T. gondii* crosses the blood-brain barrier and establishes brain cysts that allow the parasite to persist into the chronic phase. Control of the parasite necessitates an ongoing immune response in the brain, providing a unique opportunity to study CD8+ T cell entry, retention, and function in the brain.

T cell entry into the brain

T cell entry into the brain is a multi-step process (reviewed in Landrith et al. 2015) mediated by interactions with endothelial cells and dependent on an array of adhesion molecules and chemokine receptors. *T. gondii* infection induces endothelial cells to express increased amounts of integrins and selectins like PECAM-1, ICAM-1 and VCAM-1. These integrins appear to be critical for T cell entry, as antibody blocking of VLA-4, the ligand for VCAM-1, prevents entry (Wilson et al. 2009). Infection also increases the expression of the inflammatory chemokines CXCL9 and CXCL10 in the brain (Harris et al. 2012), which function as ligands for the chemokine receptor CXCR3. CXCR3 plays a critical role in T cell entry in the brain in other viral and parasitic infection models (Klein et al. 2005; Zhang et al. 2008; Campanella et al. 2008). Antibody blockade of CXCL9 (Ochiai et al. 2015) or CXCL10 (Harris et al. 2012) during infection dramatically reduces the numbers of brain-infiltrating CD8+ T cells, supporting a vital role of this axis during *T. gondii* infection as well. Together, these studies indicate that inflammation appears to be a key element regulating T cell infiltration into the brain. Anti-PDL1 treatment also results in increases in CD3+ and CD8+ cells in the brains of *T. gondii* infected mice (Xiao et al. 2018). While the exact mechanisms remain unclear, it is possible that increased inflammation following checkpoint blockade mediates this increase in T cell infiltration in the brain.

T cell retention in the brain

While inflammatory signals are sufficient to mediate the initial entry of antigen-experienced T cells into the brain, only T cells with the appropriate antigen specificity are efficiently retained in the brain. OVA-specific CD8+ T cells activated *in vitro* and then transferred into mice infected with *T. gondii* were observed in the brain, despite the absence of the OVA epitope in this model (Schaeffer et al. 2009). While these OVA-specific T cells were capable of entering the brain, their numbers rapidly declined in this setting. T cells' affinity for their antigen may also regulate their retention. Two T cell clones with different affinities for the same epitope were shown to enter the brain in similar numbers, but the lower affinity clone exhibited more rapid contraction in the brain five weeks post-infection (Sanecka et al. 2018).

T cell-mediated protection in the brain

While antigen recognition appears to promote T cell retention and effector function in the brain, the nature of the brain cells that present parasite antigens to T cells remains incompletely understood. Static imaging of brain sections revealed that parasite-specific T cells interacted with granuloma-like aggregates of CD11b+ cells harboring parasite material (Schaeffer et al. 2009). In contrast, no interaction was observed between T cells and intact cysts (Schaeffer et al. 2009), which were likely contained within neurons (Ferguson et al. 1994; Cabral et al. 2016). However, recent evidence suggests that neurons can present antigen directly to T cells, and that this presentation is critical for parasite control in the brain (Salvioni et al. 2019). L^d-expressing mice with a neuron-specific L^d knockout had dramatically increased numbers of brain cysts and increased amounts of parasite DNA despite high numbers of antigen-specific CD8+ T cells. Restricting the expression of the immunodominant antigen specifically to the tachyzoite stage did not significantly reduce the CD8+ T cell response, nor reduce their ability to protect from encephalitis (Table 2). Together with the previous imaging data, this suggests that tachyzoite recognition within neurons may result in critical T cell:neuron interactions, while bradyzoites within cysts remain relatively invisible to T cells.

Resident memory T cells

Resident memory T cells (T_{RM}) are a distinct lineage of cells that confer protection directly in the relevant tissues rather than within the lymphatic system. Traditionally, tissue residence has been defined by an inability of these cells to recirculate in the mouse as shown by parabiosis experiments. CD8+ T cells that remain in the brain during *T. gondii* infection appear to adopt a T_{RM} phenotype, evidenced by surface expression of CD69 and CD103 (Chu et al. 2016, Sanecka et al. 2018). Supporting their status as bona-fide T_{RM} cells, CD8+ T cells in the brains of *T. gondii* infected mice also have a transcriptional profile resembling a T_{RM} signature (Landrith et al. 2017), though parabiosis experiments have not demonstrated their tissue residence status using the classic definition. *T. gondii* infection may provide a unique opportunity to study these cells, and future work investigating the development and protective capacity of these cells will be of great interest.

Concluding Remarks and Future Perspectives

Studies of *T. gondii* infection in mice have led to seminal discoveries in the filed of CD8+ T cell biology and our understanding of how CD8+ T cells detect and respond to intracellular pathogens. The *T. gondii*-mouse infection model will be instrumental in addressing additional questions in the field.

The *T. gondii* parasite provides us with a unique model to investigate the requirements for presentation of vacuolar antigens, which cannot be studied with a viral model in which antigens are translated in the cytosol. As we learn more about how *T. gondii* antigens are processed and presented to CD8+ T cells, it is becoming clear that different antigens use distinct pathways based on their location and trafficking within host cells. Future studies to address the detailed mechanisms of these pathways will provide additional insight into the general problem of how exogenous and vacuolar antigens are cross-presented via MHC-I. Moreover, *T. gondii* shows considerable promise as a vaccine vector (Fox et al. 2017) and understanding the factors that lead to efficient processing and presentation of parasite antigens may also help to realize the full potential of this approach.

Much of our understanding of how CD8+ T cells respond to chronic infections is based on a limited number of mouse infection models, particularly the widely studied LCMV clone 13 model of chronic infection. The addition of the *T. gondii* infection model had broadened our perspective on this topic. *T. gondii* infection has contributed to our understanding of CD8+ T cell responses to infection in the central nervous system (CNS), as neurotropic viral mouse models are limited. Additionally, the difference in control of *T. gondii* infection between two strains of inbred mice provides the unique opportunity to compare CD8+ T cell function in a progressing disease setting *versus* a well-controlled chronic infection. Studies have identified a novel T cell population fundamental for control in the resistant setting, as well as cellular mechanisms leading to disease in susceptible mice.

One example demonstrating the potential of this system can be found in Salvioni et al. (2019), where the authors engineered a parasite strain expressing the OVA epitope in a manner similar to the immunodominant GRA6 epitope (Salvioni et al. 2019) (see Table 2). This system allowed the authors to recapitulate H-2^d-mediated protection in the typically susceptible H-2^b setting, highlighting the critical importance of antigen processing in generating parasite control. Similar efforts to take lessons from the H-2^d-restricted protective setting and manipulate the H-2^b-restricted susceptible setting to improve protective capacity may lead to exciting advancements in our understanding of CD8+ T cell function.

Table 1.1: Natural CD8+ T cell epitopes in *T. gondii*

Antigenic peptide	Source protein	MHC restriction	Subcellular location	T cell response
HPGSVNEFDF (HF10)	GRA6	H-2L^{d}	Constitutively secreted by dense granules in PV; localizes to PV membrane; C terminal epitope may extend into cytosol	Immunodominant response; responsible for protection in BALB/c mice
SPMNGGYYM (SM9)	GRA4	H-2L^{d}	Constitutively secreted by dense granules into PV lumen; localizes to intravacuolar network (IVN)	Subdominant response; not protective
YAVANYFFL (YAL9)	ROP5	H-2D^{b}	Secreted by rhoptries into host cell during invasion	Subdominant response; not protective
IPAAAGRFF (IF9)	ROP7	H-2L^{d}	Secreted by rhoptries into host cell during invasion	Subdominant response; not protective
SVLAFRRL (SVL8)	Tgd057	H-2K^{b}	Secreted by dense granules in PV lumen	High frequency of Tgd057-specific T cells post vaccination; adoptive transfer of CTLs protective against lethal parasite challenge

Table 1.2: Engineered CD8+ T cell antigens

Antigen	Description	Effect on antigen presentation and T cell response	Conclusion
SAG1ΔGPI-OVA	Model antigen OVA secreted by dense granules	OVA secreted into the PV results in efficient presentation; low $CD8^+$ T cell activation with nonsecreted OVA	Secreted antigen > nonsecreted antigen
Cytoplasmic β-galactosid-ase	Cytoplasmic expression of β-galactosidase under the tachyzoite-specific promoter, SAG1	No β-gal-specific $CD8^+$ T cell response	
Secreted β-galactosid-ase	β-galactosidase secreted into the PV lumen	Production of long-lasting dominant response against L^d restricted β-gal epitope	
GRA6-YAL9	YAL9 peptide targeted to dense granules instead of rhoptries	Increased presentation, higher $CD8^+$ T cell response	Dense granule targeting > rhoptry targeting
GRA6-ROP5	ROP5 protein targeted to dense granules instead of rhoptries	Increased presentation, 10- to 20-fold higher $CD8^+$ T cell response (more than GRA6-YAL9); better parasite control	
ROP5-HF10	HF10 peptide targeted to rhoptries instead of dense granules	Decreased presentation, 3- to 4-fold lower $CD8^+$ T cell response	
GRA6II-L, GRA6II-HA	GRA6 protein extended by a leucine or HA tag	HF10 presentation is lost; no T cell response; weaker protection	C terminal epitope position is important
GRA6II-SM9Cter	SM9 peptide at C terminus of GRA6 protein	Enhanced presentation; stronger $CD8^+$ T cell response; stronger parasite control	

TgRH GRA5-HF10	HF10 epitope at C terminus of GRA5 protein: HF10 inverted to face the PV lumen	Reduced presentation *in vitro*	Host cell cytosolic epitope > PV lumenal epitope
SAG1-GRA6-HF10	SAG1 N terminal domain with GRA6-HF10: converts to soluble protein	Reduced presentation	PV membrane localization > soluble within PV lumen
TgRH GRA6-HF10 gra2KO	GRA2 KO eliminates the IVN; GRA6 preferentially localizes to PV membrane	Enhanced presentation and $CD8^+$ T cell response	
Tg.pGRA6/ GRA6-OVA	OVA-derived SIINFEKL epitope at the C terminus of the GRA6 protein, under the GRA6 promoter	Antigen processed more efficiently than vacuolar SIINFEKL epitope from parental strain; lower parasite load in the brain; reduced brain inflammation	Dense granule targeting > soluble vacuolar localization
SAG1/GRA6-OVA	Same protein construct as above, but restricted to tachyzoites by SAG1 promoter	OVA-specific $CD8^+$ T cell response not significantly affected; effective parasite control in the CNS	Tachyzoite restricted antigen presentation is sufficient to confer protection

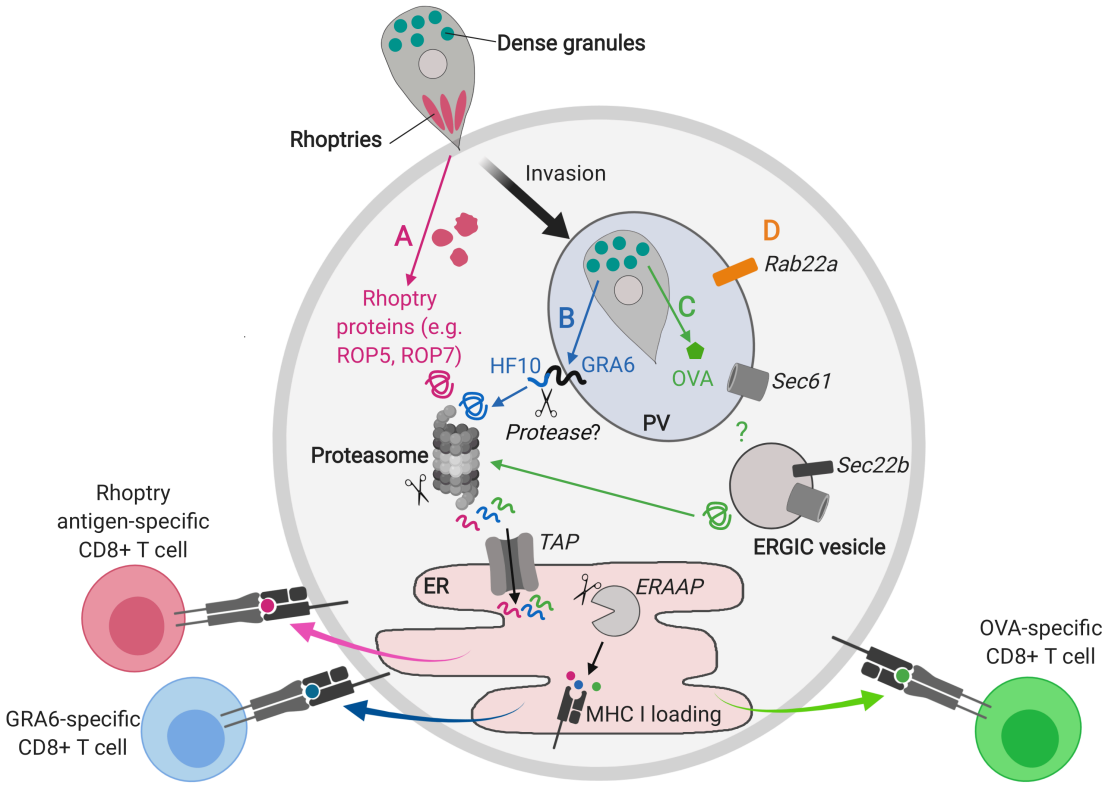

Figure 1.1: Modes of MHC-I presentation of vacuolar antigens.

Distinct pathways of MHC-I antigen processing and presentation are shown for different *T. gondii* antigens. **(A)** During host cell invasion or abortive invasion events, parasites secrete the contents of their rhoptries into the host cell cytosol, allowing rhoptry proteins to access the classical MHC-I presentation pathway. In the classical MHC-I pathway, antigens are cleaved by the proteasome and transported to the ER for further processing and loading onto MHC-I. MHC-I-peptide complexes are transported to the surface of the antigen-presenting cells (APC) to be presented to CD8+ T cells. **(B,C)** After invasion of the host cell, the parasite generates a parasitophorous vacuole (PV) and dense granules are constitutively secreted into the PV lumen. The dense granule antigen GRA6 (B) associates with the parasitophorous vacuole membrane (PVM) with the C-terminal antigenic peptide protruding into the host cell cytosol. Processing of this peptide requires components of the classical MHC I pathway. It has been hypothesized that a protease may cleave the C-terminal epitope. Soluble dense granule proteins such as the model antigen OVA (C) secreted from transgenic parasites localize within the PV lumen. The antigen may be trafficked to the host cytosol following fusion of ER-Golgi intermediate compartment (ERGIC) vesicles with the PV, mediated by the Sec22b SNARE protein, however this part of the pathway is not fully understood. **(D)** Additional proteins involved in cross-presentation like the Rab22a GTPase, which may play a role in recycling MHC-I molecules, accumulate on the PV in infected DCs. (Figure created with BioRender)

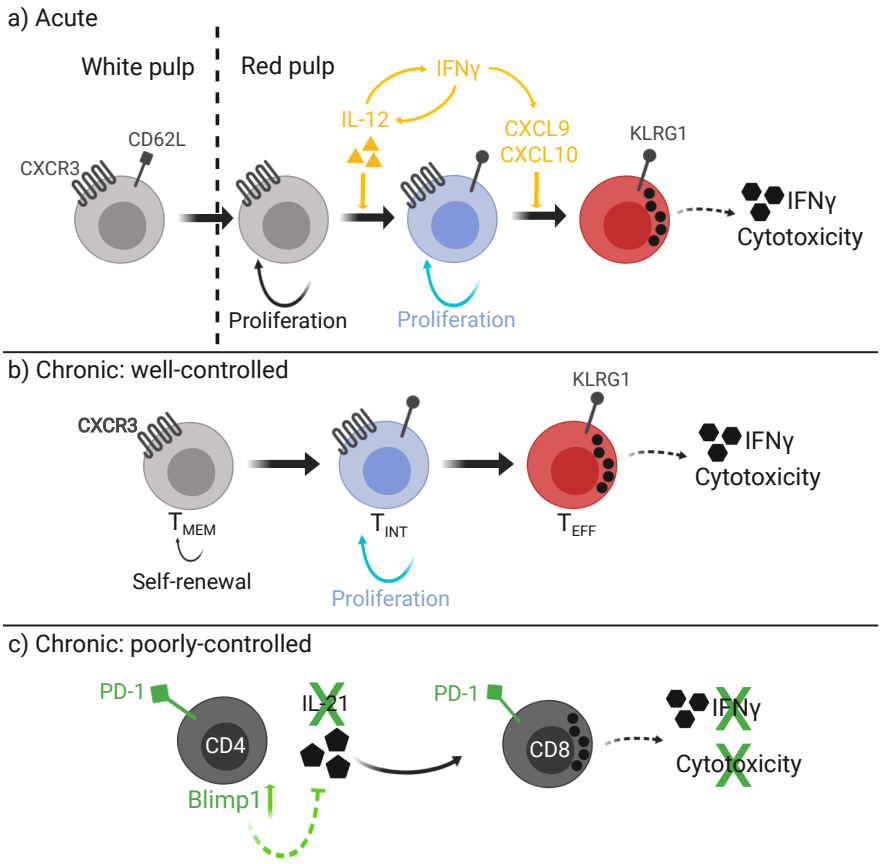

Figure 1.2: CD8+ T cell fate during *T. gondii* infection.

Features of CD8+ T cell differentiation and function are shown for the different settings of *T. gondii* responses in mice. **(A)** During an acute response or after vaccination, CD8+ T cell differentiation is linked to their migration and exposure to environmental signals. As naive cells are activated and differentiate into effector cells, they migrate from the white pulp of the spleen to the red pulp in a CXCR3:CXCL9/10-dependent manner. This migration results in exposure to a network of key cytokines like IL-12 and IFNγ (yellow) that drive changes in CXCR3 and KLRG1 expression (grey) and promote effector differentiation (Shah *et al.* 2015). **(B)** CD8+ T cells during well-controlled chronic infection give rise to three functionally distinct subsets of antigen-specific T cells. The differentiation of these populations shares many similarities to acute infection, including the expression pattern of surface receptors CXCR3 and KLRG1 on different subsets (grey) and a proliferative intermediate population (blue) that generates terminally differentiated effectors (red). However, unlike the vaccine setting, in which a single wave of T cell effector differentiation occurs, during well-controlled chronic infection, effector T cells are continuously replenished from memory and intermediate precursor populations. **(C)** During infection, CD4+ T cells provide help to CD8+ T cells in the form of key cytokines like IL-21. In the setting of poorly controlled progressing infection (green), CD4+ T cells become exhausted and lose their ability to produce these cytokines, resulting in subsequent CD8+ T cell exhaustion. (Figure created with BioRender)

1.3: Function of T cells with high and low self-reactivity

During T cell selection in the thymus, developing thymocytes receive signals from self-peptide MHC that will determine their fate. Most thymocytes will die by neglect or be clonally deleted through negative selection due to self-pMHC signals that are either too weak or too strong, respectively. T cells that receive a moderately strong signal will be positively selected and contribute to the mature T cell population in the periphery. The impact of self-pMHC interactions on T cell development, survival, and function has been studied extensively (Kim and Cho 2017).

Positively selected thymocytes can develop with varying levels of self-reactivity, depending on the extent of self-peptide MHC recognition they experience in the thymus. In order to distinguish T cell populations with differences in self-reactivity, expression of the cell-surface molecule CD5, which is directly proportional to the strength of TCR-self pMHC interactions, is used as a robust marker of self-reactivity (Azzam et al. 2001; Mandl et al. 2013; Persaud et al. 2014; Fulton 2015). CD5 negatively regulates and fine-tunes TCR signaling (Azzam et al. 2001) however its exact mechanism is not known. Recently, it has been appreciated that differing levels of sensitivity to self-pMHC allow for heterogeneity in T cell responsiveness to foreign antigens in the periphery (Hogquist and Jameson 2014).

Several studies have investigated the effects of self-reactivity on the intrinsic capacity of naïve T cells to respond to foreign antigens. First, Mandl et al. demonstrated that the self-reactivity of various CD4+ TCR transgenics predicts the strength of binding to their agonist peptide-MHCs (Mandl et al. 2013). However, much of this research was conducted on individual TCR transgenics specific for distinct antigens and later studies did not support this conclusion. Two studies further explored how self-reactivity influences responsiveness to foreign antigens using two TCR transgenic mice with CD4+ T cells that bind to the same immunodominant *Listeria monocytogenes* epitope. These TCR transgenics have similar affinity for the peptide-MHC but differing levels of self-reactivity. These studies demonstrated that the TCR transgenic with higher CD5 expression exhibited greater proliferation and intrinsic responsiveness after acute infection, however these T cells experienced TCR-driven cell death upon secondary challenge, suggesting that superior reactivity may come at the cost of susceptibility to elimination (Weber et al. 2012; Persaud et al. 2014). Furthermore, Persaud et al. demonstrated that basal signaling and responsiveness is set in the thymus during positive selection in response to TCR avidity for self-pMHC and is actively maintained in the periphery by self-pMHC signals (Persaud et al. 2014).

When these studies were extended to CD8+ T cells, it was demonstrated that $CD5^{high}$ CD8+ T cells exhibited enhanced reactivity to foreign peptide-MHC antigens, evidenced by advantages in initial activation and expansion in response to acute infection (Fulton et al. 2015). Importantly, CD5 levels did not predict the strength of binding to foreign peptide-MHC ligands, demonstrating that intrinsic properties of these T cells dictate their sensitivity to foreign antigen (Fulton et al. 2015). Additionally, $CD5^{high}$ CD8+ T cells exhibited greater responsiveness to cytokines compared with $CD5^{low}$ CD8+ T cells (Cho

et al. 2010; Palmer et al. 2011; Fulton et al. 2015; Cho et al. 2016). On the other hand, naïve $CD5^{low}$ CD8+ T cells had higher TCR sensitivity, modulated by TCR tuning via CD45 expression, as well as prolonged survival in the absence of homeostatic stimuli (Palmer et al. 2011; Cho et al. 2016).

Overall, these studies have led to a consensus in the field that $CD5^{high}$ T cells are superior in their acute responses to foreign antigens. However, none of these studies expanded their observations to chronic infection models so it is not known if these same distinctions apply in a setting with persistent antigen exposure. $CD5^{low}$ T cells are maintained in the naïve CD8+ T cell repertoire, so it is possible that they serve some other function, which has not been investigated. We hypothesize that $CD5^{low}$ CD8+ T cells may be uniquely poised to respond to chronic infections, able to avoid exhaustion and persist long-term. We investigate this hypothesis in Chapter 3.

1.4: References

Azzam, H.S. *et al.* (2001) Fine Tuning of TCR Signaling by CD5. J. Immunol. 166 (9): 5464–72

Barber, D.L. *et al.* (2006) Restoring function in exhausted CD8 T cells during chronic viral infection. Nature 439(7077), 682-687

Bertholet, S. *et al.* (2006) *Leishmania* antigens are presented to CD8+ T cells by a transporter associated with antigen processing-independent pathway *in vitro* and *in vivo*. J Immunol. 177(6), 3525-3533.

Betts, M. R. *et al.* (2006) HIV nonprogressors preferentially maintain highly functional HIV-specific CD8+ T cells. Blood 107, 4781–4789

Bhadra, R. *et al.* (2011) Control of *Toxoplasma* reactivation by rescue of dysfunctional CD8+ T-cell response via PD-1-PDL-1 blockade. PNAS 108, 9196-9201

Bhadra, R. *et al.* (2012) PD-1-mediated attrition of polyfunctional memory CD8+ T cells in chronic *toxoplasma* infection. J. Inf. Dis. 206, 125-134

Blackburn, S.D. *et al.* (2008) Selective expansion of a subset of exhausted CD8 T cells by anti-PD-L1 blockade. Proc. Natl Acad. Sci. USA 105, 15016–15021

Blackburn, S.D. *et al.* (2009) Coregulation of $CD8^+$ T cell exhaustion by multiple inhibitory receptors during chronic viral infection. Nat. Immunol. 10, 29–37

Blanchard, N. *et al.* (2008) Immunodominant, protective response to the parasite *Toxoplasma gondii* requires antigen processing in the endoplasmic reticulum. Nat. Immunol. *9*, 937-944

Blanco-Gelaz, M.A. *et al.* (2006) The amino acid at position 97 is involved in folding and surface expression of HLA-B27. Int. Immunol. 18, 211–220

Boni, C. *et al.* (2007) Characterization of hepatitis B virus (HBV)-specific T-cell dysfunction in chronic HBV infection. J Virol. 81(8):4215-25

Boothroyd, J.C. and Dubremetz, J.F. (2008) Kiss and split: the dual roles of *Toxoplasma* rhoptries. Nat. Rev. Microbiol. 6(1), 79-88

Bowen, D.G. and Walker, C.M. (2005) Adaptive immune responses in acute and chronic hepatitis C virus infection. Nature 436, 946–952

Brown, C.R. *et al.* (1995) Definitive identification of a gene that confers resistance against *Toxoplasma* cyst burden and encephalitis. Immunology 85, 419-428

Buaillon, C. *et al.* (2017) MHC I presentation of *Toxoplasma gondii* immunodominant antigen does not require Sec22b and is regulated by antigen orientation at the vacuole membrane. Eur. J. Immunol. 47, 1160-1170

Bucks, C.M. *et al.* (2009) Chronic Antigen Stimulation Alone Is Sufficient to Drive $CD8^+$ T Cell Exhaustion.J. Immunol. 182 (11) 6697-6708

Cabral, C.M. *et al.* (2016) Neurons are the primary target cell for the brain-tropic intracellular parasite *Toxoplasma gondii*. PLoS Pathog. 12(2), DOI: 10.1371/journal.ppat.1005447

Campanella *et al.* (2008) Chemokine receptor CXCR3 and its ligands CXCL9 and CXCL10 are required for the development of murine cerebral malaria. PNAS, 105(12):4814-9

Cebrian, I. *et al.* (2011) Sec22b regulates phagosomal maturation and antigen cross-presentation by dendritic cells. Cell 147(6), 1355-1368

Cebrian, I. *et al.* (2016) Rab22a controls MHC-I intracellular trafficking and antigen cross-presentation by dendritic cells. EMBO Rep. 17, 1753-1765

Chen, H. *et al.* (2012) TCR clonotypes modulate the protective effect of HLA class I molecules in HIV-1 infection. Nat. Immunol. 13, 691–700

Cho, J.H. *et al.* (2010) T cell receptor-dependent regulation of lipid rafts controls naive CD8+ T cell homeostasis. Immunity 32, 214–226

Cho, J.H. *et al.* (2016) CD45-Mediated Control of TCR Tuning in Naïve and Memory CD8+T Cells. Nature Communications 7: 1–15

Chu, H.H. *et al. (*2016) Continuous Effector CD8+ T cell Production in a Controlled Persistent Infection is Sustained by a Proliferative Intermediate Population. Immunity. 45(1), 159-171

Curtsinger, J.M. *et al.* (1999) Inflammatory cytokines provide a third signal for activation of naïve CD4+ and CD8+ T cells. J. Immunol. 162(6), 3256-62

Curtsinger, J.M. *et al.* (2005) Type I IFNs provide a third signal to CD8 T cells to stimulate clonal expansion and differentiation. J. Immunol. 174, 4465–4469

Day, C.L. *et al.* (2006) PD-1 expression on HIV-specific T cells is associated with T-cell exhaustion and disease progression. Nature 443(7109): 350

Delpoux, A. *et al.* (2017) FOXO1 opposition of $CD8^+$ T cell effector programming confers early memory properties and phenotypic diversity. PNAS, 114(42)

Dotiwala, F. *et al.* (2016) Killer lymphocytes use granulysin, perforin and granzymes to kill intracellular parasites. Nat. Med. 22, 210-216

Dupont, C.D. *et al.* (2014) Parasite Fate and Involvement of Infected Cells in the Induction of CD4+ and CD8+ T Cell Responses to *Toxoplasma gondii*. PLoS Pathog. 10(4), DOI: 10.1371/journal/ppat.1004047

Dzierszinski, F. *et al.* (2007) Presentation of *Toxoplasma gondii* antigens via the endogenous major histocompatibility complex class I pathway in nonprofessional and professional antigen-presenting cells. Infect. Immun. 75, 5200-5209

Fagerberg, T. *et al.* (2006) Structural prediction of peptides bound to MHC class I. J. Mol. Biol. 356, 521–546

Feliu, V. *et al.* (2013) Location of the CD8 T Cell Epitope within the Antigenic Precursor Determines Immunogenicity and Protection against the *Toxoplasma gondii* Parasite. PLoS Pathog. 9, DOI: 10.1371/journal.ppat.1003449

Ferguson, D.J. *et al.* (1994) A morphological study of chronic cerebral toxoplasmosis in mice: comparison of four different strains of *Toxoplasma gondii*. Parasitol. Res. 80(6), 493-501

Frickel, E.M. *et al.* (2008) Parasite stage-specific recognition of endogenous *Toxoplasma gondii*-derived CD8+ T cell epitopes. J. Inf. Dis. 198, 1625-1633

Fox, B. *et al.* (2017) Cancer therapy in a microbial bottle: Uncorking the novel biology of the protozoan *Toxoplasma gondii.* PLoS Pathog. 13(9); DOI: 10.1371/journal.ppat.1006523

Fulton, R.B. *et al.* (2015) The TCR's sensitivity to self peptide-MHC dictates the ability of naive CD8(+) T cells to respond to foreign antigens. Nat. Immunol. 16, 107–17

Grover, H.S. *et al.* (2014) Impact of regulated secretion on antiparasitic CD8 T cell responses. Cell Rep. *7*, 1716-1728

Goepfert, P.A. *et al.* (2000) A significant number of human immunodeficiency virus epitope-specific cytotoxic T lymphocytes detected by tetramer binding do not produce gamma interferon. J. Virol. 74(21), 10249-10255

Harris, T. *et al.* (2012) Generalized Levy walks and the role of chemokines in migration of effector CD8+ T cells. Nature 486, 545-548

He, R. *et al.* (2016) Follicular CXCR5-expressing $CD8^+$ T cells curtail chronic viral infection. Nature 537, 412–416

Hersperger, A.R. *et al.* (2011) Increased HIV-specific CD8+ T-cell cytotoxic potential in HIV elite controllers is associated with T-bet expression. Blood 117, 3799–3808

Hudson, W. *et al.* (2019) Proliferating Transitory T cells with an Effector-like Transcriptional Signature Emerge from PD-1+ Stem-like CD8+ T Cells during Chronic Infection. Immunity 51(6): 1043-1058

Hwang, S. *et al.* (2016) Blimp-1-mediated CD4 T cell exhaustion causes CD8 T cell dysfunction during chronic toxoplasmosis. J. Exp. Med. 213(9), 1799-1818

Im, S.J. *et al.* (2016) Defining CD8+ T cells that provide the proliferative burst after PD-1 therapy. Nature 537(7620), 417-421

Joffre, O. *et al.* (2012) Cross-presentation by dendritic cells. Nat. Rev. Immunol. 12, 557-569

Gallimore, A. *et al.* (1998) Induction and exhaustion of lymphocytic choriomeningitis virus-specific cytotoxic T lymphocytes visualized using soluble tetrameric major histocompatibility complex class I-peptide complexes. J. Exp. Med. 187, 1383–1393

Gigley, J.P. *et al.* (2011) CD8 T cells and Toxoplasma gondii: a new paradigm. J. Parasitol. Res. 2011, DOI: 10.1155/2011/243796

Gregg, B. *et al.* (2011) Subcellular Antigen Location Influences T-Cell Activation during Acute Infection with *Toxoplasma gondii*. PLoS One 6(7), DOI: 10.1371/journal.pone.0022936

Goldszmid, R.S. *et al.* (2009) Host ER-parasitophorous vacuole interaction provides a route of entry for antigen cross-presentation in *Toxoplasma gondii*-infected dendritic cells. J. Exp. Med. 206, 399-410

Goulder, P.J.R. and Walker, B.D. (2012) HIV and HLA Class I: An Evolving Relationship. Immunity 37, 426–440

Gubbels, M.J. *et al.* (2005) Class I major histocompatibility complex presentation of antigens that escape from the parasitophorous vacuole of *Toxoplasma gondii*. Infect. Immun. *73*, 703-711

Hogquist, K.A. and Jameson, S.C. (2014) The Self-Obsession of T Cells: How TCR Signaling Thresholds Affect Fate 'decisions' and Effector Function. Nature Immunology 15 (9): 815–23

Holtappels, R. *et al.* (2000) Enrichment of immediate-early 1 (m123/pp89) peptide-specific CD8 T cells in a pulmonary CD62L(lo) memory-effector cell pool during latent murine cytomegalovirus infection of the lungs. J. Virol. 74, 11495–11503

Hu, J.K. *et al.* (2011) Expression of chemokine receptor CXCR3 on T cells affects the balance between effector and memory CD8 T-cell generation. PNAS. 108(21) , E118-27

Im, S. *et al.* (2016) Defining $CD8^+$ T cells that provide the proliferative burst after PD-1 therapy. Nature 537, 417–421

Kaech S.M. and Wherry E.J. (2007) Heterogeneity and cell-fate decisions in effector and memory CD8+ T cell differentiation during viral infection. Immunity 27: 393-405

Karrer, U. *et al.* (2003) Memory Inflation: Continuous Accumulation of Antiviral CD8+ T Cells Over Time. J. Immunol. 170 (4): 2022–29

Kaslow, R. *et al.* (1996) Influence of combinations of human major histocompatibility complex genes on the course of HIV–1 infection. Nat Med 2, 405–411

Kim, H-O. and Cho, J-H. (2017) T Cell's Sense of Self: a Role of Self-Recognition in Shaping Functional Competence of Naïve T Cells. Immune Netw. 17(4): 201-213

Kirak, O. *et al.* (2010) Transnuclear mice with pre-defined T cell receptor specificities against *Toxoplasma gondii* obtained via SCNT. Science 328(5975), 243-248

Klein, R.S. *et al.* (2005) Neuronal CXCL10 directs CD8+ T-cell recruitment and control of West Nile virus encephalitis. J. Virol. 79(17), 11457-66

Kolumam, G.A. *et al.* (2005) Type I interferons act directly on CD8 T cells to allow clonal expansion and memory formation in response to viral infection. J. Exp. Med. 202, 637–50

Koshy, A. *et al.* (2012) *Toxoplasma* co-opts host cells it does not invade. PLoS Pathog. 8(7), DOI: 10.1371/journal.ppat.1002825

Košmrlj, A. *et al.* (2010) Effects of Thymic Selection of the T Cell Repertoire on HLA-Class I Associated Control of HIV Infection. Nature 465 (7296): 350–54

Krmpotic, A. *et al.* (2003) Pathogenesis of murine cytomegalovirus infection. Microbes and Infection, 5(13): 1263-1277

Kurachi, M. *et al.* (2011) Chemokine receptor CXCR3 facilitates CD8+ T cell differentiation into short-lived effector cells leading to memory degeneration. J. Exp. Med. 208(8), 1605-20

Kurtulus, S. *et al.* (2019) Checkpoint blockade immunotherapy induces dynamic changes in PD-1-CD8+ tumor-infiltrating T cells. Immunity 50(1), 181-194

Kwok, L.Y. *et al.* (2003). The induction and kinetics of antigen-specific CD8 T cells are defined by the stage specificity and compartmentalization of the antigen in murine toxoplasmosis. J. Immunol. 170, 1949-1957

Ladell, K. *et al.* (2013) A molecular basis for the control of preimmune escape variants by HIV-specific CD8 $^{+}$ T cells. Immunity 38(3): 425–36

Landrith, T.A. *et al.* (2015) Characteristics and critical function of CD8+ T cells in the *Toxoplasma*-infected brain. Semin. Immunopathol. 37(3), 261-70

Landrith, T.A. *et al.* (2017) CD103+ CD8 T cells in the *Toxoplasma*-infected brain exhibit a tissue-resident memory transcriptional profile. Font. Immunol. 8, 335

Lee, Y. *et al.* (2015) p62 plays a specific role in Interferon-g-induced presentation of a *Toxoplasma* vacuolar antigen. Cell Rep. 13(2), 223-233

Leong, Y. *et al.* (2016) CXCR5^{+} follicular cytotoxic T cells control viral infection in B cell follicles. Nat Immunol 17, 1187–1196

Loffredo, J.T. *et al.* (2007) Mamu-B*08-positive macaques control simian immunodeficiency virus replication. J Virol. 81(16): 8827-32

Lopez, J. *et al.* (2015) Intravacuolar membranes regulate CD8 T cell recognition of membrane-bound *Toxoplasma gondii* protective antigen. Cell Rep. 13(10), 2273-2286

Mandl, J.N. *et al.* (2013) T Cell-Positive Selection Uses Self-Ligand Binding Strength to Optimize Repertoire Recognition of Foreign Antigens. Immunity 38 (2): 263–74

Marple, A. *et al.* (2017) Cutting Edge: Helminth Coinfection Blocks Effector Differentiation of CD8 T Cells through Alternate Host Th2- and IL-10-Mediated Responses. J. Immunol. 198(2), 634-639

Matloubian, M., Concepcion, R.J. and Ahmed, R. (1994) CD4+ T cells are required to sustain CD8+ cytotoxic T-cell responses during chronic viral infection. Journal of Virology 68 (12) 8056-8063

Migueles, S.A. *et al.* (2000). HLA B*5701 is highly associated with restriction of virus replication in a subgroup of HIV-infected long term nonprogressors. Proc. Natl. Acad. Sci. USA 97, 2709–2714

Migueles, S.A. *et al.* (2002) HIV-specific CD8+ T cell proliferation is coupled to perforin expression and is maintained in nonprogressors. Nat. Immunol. 3, 1061–1068

Migueles, S.A. *et al.* (2008) Lytic granule loading of CD8+ T cells is required for HIV-infected cell elimination associated with immune control. Immunity 29, 1009–1021

Moretto, M.M. *et al.* (2017) Downregulated IL-21 Response and T Follicular Helper Cell Exhaustion Correlate with Compromised CD8 T Cell Immunity during Chronic Toxoplasmosis. Front. Immunol. 8, 1436

Munks, M.W. *et al.* (2006) Four Distinct Patterns of Memory CD8 T Cell Responses to Chronic Murine Cytomegalovirus Infection. J. Immunol. 177 (1) 450-458

Ndhlovu, Z.M. *et al.* (2015) Magnitude and Kinetics of CD8+ T Cell Activation during Hyperacute HIV Infection Impact Viral Set Point. Immunity 43(3):591-604

Norose, K. *et al.* (2001) Organ infectivity of *Toxoplasma gondii* in interferon-gamma knockout mice. J. Parasitol. 87(2):447-452

Ochiai, E. *et al.* (2015) CXCL9 is Important for Recruiting Immune T Cells into the Brain and Inducing an Accumulation of the T Cells to the Areas of Tachyzoite Proliferation to Prevent Reactivation of Chronic Cerebral Infection with *Toxoplasma gondii*. Am. J. Pathol. 185(2), 314-24

Palmer, M. *et al.* (2011) Signaling thresholds govern heterogeneity in IL-7-receptor-mediated responses of naïve CD8+ T cells. Immunology and Cell Biology 89, 581-594

Pardoll, D.M. (2012) The blockade of immune checkpoints in cancer immunotherapy. Nat. Rev. Cancer 12, 252–264

Parker, S.J. *et al.* (1991) CD8+ T cells are the major lymphocyte subpopulation involved in the protective immune response to *Toxoplasma gondii* in mice. Clin. Exp. Immunol. 84, 207-212

Pauken, K.E. & Wherry, E.J. (2015) Overcoming T cell exhaustion in infection and cancer. Trends Immunol. 36, 265–276

Pereyra, F. *et al.* (2010) The Major Genetic Determinants of HIV-1 Control Affect HLA Class I Peptide Presentation. Science 330 (6010): 1551–57

Persaud, S.P. *et al.* (2014) Intrinsic CD4+ T Cell Sensitivity and Response to a Pathogen Are Set and Sustained by Avidity for Thymic and Peripheral Complexes of Self Peptide and MHC. Nature Immunology 15 (3): 266–74

Petrovas, C. *et al.* (2006) PD-1 is a regulator of virus-specific CD8+ T cell survival in HIV infection. J Exp Med 203(10): 2281–92

Pohlmeyer, C.W. *et al.* (2013) $CD8^+$ T cells from HLA-B*57 elite suppressors effectively suppress replication of HIV-1 escape mutants. Retrovirology 10:152

Quinn, M. *et al.* (2015) Memory T Cells Specific for Murine Cytomegalovirus Re-Emerge after Multiple Challenges and Recapitulate Immunity in Various Adoptive Transfer Scenarios. J. Immunol. 194 (4): 1726-1736

Radziewicz, H. *et al.* (2007) Liver-infiltrating lymphocytes in chronic human hepatitis C virus infection display an exhausted phenotype with high levels of PD-1 and low levels of CD127 expression. J Virol. 81(6): 2545-53

Sa, Q. *et al.* (2017) Determination of a key antigen for immunolgical intervention to target the latent stage of *Toxoplasma gondii*. J. Immunol. 198(11), 4425-4434

Salvioni, A. *et al.* (2019) Robust control of a brain-persisting parasite through MHC I presentation by infected neurons. Cell Rep. 27(11), 3254-3268

Sanecka, A. *et al.* (2016) Transnuclear CD8 T cells specific for the immunodominant epitope Gra6 lower acute-phase *Toxoplasma gondii* burden. Immunology 149(3), 270-279

Sanecka, A. *et al.* (2018) T Cell Receptor-Major Histocompatibility Complex Interaction Strength Defines Trafficking and CD103(+) Memory Status of CD8 T Cells in the Brain. Front. Immunol. 9, 1290

Schaeffer, M. *et al.* (2009) Dynamic imaging of T cell-parasite interactions in the brains of mice chronically infected with *Toxoplasma gondii*. J. Immunol. 182, 6379-6393

Shah, S. *et al.* (2015) An extrafollicular pathway for the generation of effector CD8+ T cells driven by the proinflammatory cytokine, IL-12. eLife 4, DOI: 10.7554/eLife.09017

Shankar, P. *et al.* (2000) Impaired function of circulating HIV-specific CD8+ T cells in chronic human immunodeficiency virus infection. Blood 96, 3094-3101

Sharpe, A.H. *et al.* (2007) The function of programmed cell death 1 and its ligands in regulating autoimmunity and infection. Nat. Immunol. 8: 239-245

Smith, C.J., Turula, H. and Snyder, C.M. (2014) Systemic Hematogenous Maintenance of Memory Inflation by MCMV Infection. PLoS Pathog 10(7): e1004233

Snyder, C.M. *et al.* (2008) Memory inflation during chronic viral infection is maintained by continuous production of short-lived, functional T cells. Immunity 29, 650-659

Sorrentino, R., Bockmann, R.A. and Fiorillo, M.T. (2014) HLA-B27 and antigen presentation: At the crossroads between immune defense and autoimmunity. Mol. Immunol. 57, 22–27

Splitt, S.D. *et al.* (2018) PD-L1, TIM-3, and CTLA-4 Blockade Fails To Promote Resistance to Secondary Infection with Virulent Strains of *Toxoplasma gondii*. Infect. Immun. 86, DOI: 10.1128/IAI.00459-18

Streeck H. *et al*. (2008) Antigen Load and Viral Sequence Diversification Determine the Functional Profile of HIV-1-Specific CD8 T cells. PLOS Medicine 5(5): e100

Suzuki, Y. *et al.* (1988) Interferon-gamma: the major mediator of resistance against Toxoplasma gondii. Science 240(4851), 516-518

Suzuki, Y. and Remington, J.S. (1990) The effect of anti-IFN-gamma antibody on the protective effect of Lyt-2+ immune T cells against toxoplasmosis in mice. J. Immunol. 144(5), 1954-1956

Taborda-Vanegas, N., Zapata, W. and Rugeles, M.T. (2011) Genetic and Immunological Factors Involved in Natural Resistance to HIV-1 Infection. Open Virol J. 5:35-43

Trautmann, L. *et al.* (2006) Upregulation of PD-1 expression in HIV-specific T cells leads to reversible immune dysfunction. Nat Med. 12(10):1198-202

Urbani, S. *et al.* (2006) PD-1 expression in acute hepatitis C virus (HCV) infection is associated with HCV-specific CD8 exhaustion. J Virol. 80(22): 11398-403

Utzschneider, D.T. *et al.* (2016) T Cell Factor 1-Expressing Memory-like CD8+ T cells Sustain the Immune Response to Chronic Viral Infections. Immunity 45(2): 415-427

Virgin, H.W. *et al.* (2009) Redefining chronic viral infection. Cell 138, 30-50

Weber, K.S. *et al.* (2012) Distinct CD4+ Helper T Cells Involved in Primary and Secondary Responses to Infection. PNAS 109 (24): 9511–16

Wherry, E.J. *et al.* (2003) Viral persistence alters CD8 T-cell immunodominance and tissue distribution and results in distinct stages of functional impairment. J Virol 77(8): 4911-27

Wherry, E.J. (2011) T cell exhaustion. Nat. Immunol. 12, 492-499

Wilson, D. *et al.* (2008) IL-12 signaling drives CD8+ T cell IFNg production and differentiation of KLRG1+ effector subpopulations during *Toxoplasma gondii* infection. J. Immunol. 180(9), 5935-5945

Wilson, E.H. *et al.* (2009) Behavior of parasite-specific effector CD8+ T cells in the brain and visualization of a kinesis-associated system of reticular fibers. Immunity. 30(2), 300-311

Wilson, D.C. *et al.* (2010) Differential regulation of effector- and central-memory responses to *Toxoplasma gondii* Infection by IL-12 revealed by tracking of Tgd057-specific CD8+ T cells. PLoS Pathog. 6, DOI: 10.1371/journal.ppat.1000815

Wolchok, J.D. *et al.* (2013) Nivolumab plus ipilimumab in advanced melanoma. N. Engl. J. Med. 369, 122–133

Xiao, J. *et al.* (2018) PD-1 immune checkpoint blockade promotes brain leukocyte infiltration and diminishes cyst burden in a mouse model of *Toxoplasma* infection. J. Neuroimmunol. 319, 55-62

Zajac, A.J. *et al.* (1998) Viral immune evasion due to persistence of activated T cells without effector function. J. Exp. Med. 188, 2205–2213

Zander, R. *et al.* (2019) CD4+ T Cell Help is Required for the Formation of a Cytolytic CD8+ T Cell Subset that Protects against Chronic Infection and Cancer. Immunity 51(6): 1028-1042

Zhang, B. *et al.* (2008) CXCR3 mediates region-specific antiviral T cell trafficking within the central nervous system during West Nile virus encephalitis. J. Immunol. 180(4), 2541-9

Chapter 2: TCR Repertoire Analysis of Ld-Restricted CD8+ T Cells

2.1: Introduction

In mice infected with *Toxoplasma gondii*, an immunodominant CD8+ T cell response directed at a peptide derived from the parasite protein, GRA6, confers strong protection (Blanchard et al. 2008; Chu et al. 2016) This unusually potent T cell response may serve as a model for understanding the CD8+ T cell responses that underlie strong resistance to infection.

During thymic development, T cells generate a diverse repertoire of T cell receptor (TCR) sequences by random recombination of V, D, and J germline gene segments, as well as random addition or deletion of nucleotides at the junction, generating an estimated ~10^{18} unique αβ heterodimers (Arstila et al. 1999). The junction of the V(D)J segments forms the complementarity determining region 3 (CDR3), which has the highest diversity within the TCR and is responsible for recognizing the antigenic peptide. This great diversity allows for the recognition of virtually infinite foreign and self-antigens and provides protection against many different pathogens.

In the naïve T cell repertoire, T cells specific for a single antigen are present at a very low frequency, approximately 100-1,000 cells per mouse (Jenkins and Moon, 2012). When a naïve T cell encounters its cognate peptide-MHC, the T cell will clonally expand, generating effector T cells with identical TCRs. The TCR can be used to study dynamics of clonality and diversity of a T cell response. At the protein level, Vβ usage can be used to quantify diversity of the TCR repertoire. To quantify diversity at the sequence level, TCR CDR3 length can be measured, which will have a Gaussian distribution in a polyclonal population but will be skewed by clonal enrichment (De Simone et al. 2018). Paired sequencing of TCRα and TCRβ genes can give further information about clonality.

To further understand the factors that contribute to the robust GRA6-L^d specific T cell response, we characterized the TCR repertoire of this response after *T. gondii* infection. Here we show that the GRA6-L^d specific T cell response displays a TCR repertoire dominated by Vβ2, limited clonal diversity, a strongly selected CDR3β motif, and a public TCR. We also investigated whether other L^d-restricted responses had similar characteristics and demonstrated that the immunodominant F2-L^d specific response to Vaccinia virus also shows robust expansion, a Vβ2 preference, and a focused TCR repertoire.

2.2: Results and Discussion

T. gondii infection of genetically resistant (H-2^d) mice elicits a potent CD8+ T cell response directed against a single parasite-derived peptide which is associated with the continuous production of armed effector T cells in the chronic phase of persistent infection (Brown et al, 1995; Blanchard et al, 2008; Chu et al. 2016). Previous studies have shown that the secretion pattern of the antigenic precursor protein and the C-terminal location of the epitope contribute to, but do not fully account for, the strong

GRA6-L^d specific response during infection (Feliu et al. 2013; Grover et al. 2014). To examine the impact of TCR-pMHC interactions on the T cell response, we examined T cell responses in naïve mice upon immunization with peptide-loaded dendritic cells (DC) (Figure 1). T cells specific for GRA6-L^d expanded 4000x upon peptide-DC immunization, whereas T cells specific for the other *T. gondii* epitopes showed substantially lower expansion (Figure 1). These data indicate that the interactions between TCR and pMHC, as well as parasite biology and antigen presentation, contribute to the potency of the GRA6-L^d specific T cell response.

We previously showed a preferential usage of the Vβ2 variable chain in expanded GRA6-L^d specific CD8+ T cells from *T. gondii* infected mice (Blanchard et al. 2008). This preference for Vβ2 is also observed upon immunization of mice with DC loaded with the GRA6 epitope HF10, whereas T cell responses to other peptides displayed a Vβ profile that closely matched that of bulk CD8+ T cells (Figure 2A). GRA6-L^d specific T cells from naïve mice also showed a Vβ2 frequency significantly above that of bulk CD8+ T cells (Figure 2B) suggesting that a preference for Vβ2 is already evident after thymic selection and increases after T cell priming with the antigenic peptide.

GRA6-L^d is presented by an atypical MHC-1 molecule, L^d, which has been shown to have low surface expression and limited peptide binding compared to most MHC molecules (Potter et al. 1981; Lie et al. 1991; Narayanan and Kranz 2013). We wondered whether the unusual structure of L^d plays a role in generating this robust response, and therefore, if other L^d-restricted responses had similar characteristics. We searched the literature for L^d-restricted responses to other pathogens and quantified peptide binding strength of these peptides to L^d. All peptides tested bound to L^d with similar strength compared to the GRA6 peptide (Figure 3A). Next, we immunized mice with DC loaded with each peptide and quantified the expansion of tetramer+ CD8+ T cells (Figure 3B). No L^d-restricted response expanded better than the GRA6-L^d specific response, but the F2-L^d specific response, an immunodominant response to Vaccinia virus infection (Flesch et al. 2010), exhibited robust expansion as well (Figure 3B). We also observed a preference for Vβ2 in F2-L^d specific T cells, which was evident in naïve tetramer+ T cells but increased after priming, similar to what we see in GRA6-L^d specific T cells (Figure 3C-D). T cells specific for the NP peptide from LCMV showed a preference for the Vβ10 gene segment, though this data is only from one mouse (Figure 3C).

Given that we have identified two protective L^d-restricted responses with a strong Vβ2 preference, we speculated that the unusual structure of L^d may play a role in generating these robust responses. To investigate the structural features underlying the potent GRA6-L^d specific T cell response, our collaborators solved the crystal structure of GRA6-L^d together with a Vβ2-containing TCR specific for this peptide-MHC, TG6 (Wang, Tsitsiklis, et al., unpublished). We demonstrated that TG6 is a public TCR that provides a good representative of this response (Figure 4D-E), which validates the use of TG6 for structural studies. The structure revealed several unusual features of the peptide-MHC-TCR complex, including a reliance on several non-anchor residues for peptide binding, conserved Vβ2 specific germline contacts that stabilize TCR binding, and an unusual docking orientation of the TCR (Wang, Tsitsiklis, et al., unpublished). These characteristics of the structure suggest that Vβ2 may play a role in generating robust and

high affinity T cell responses, optimized for binding particular pMHC complexes and allowing for "jackpot" responses that provide strong protection for certain pathogens.

To further characterize the TCR repertoire of the GRA6-L^d specific response, we sequenced paired TCR α and β genes from 80 individual T cells from 2 different chronically infected mice, yielding 32 unique paired αβ TCR sequences. Analysis of the paired αβ sequences revealed that just a few clones dominated the GRA6-L^d specific response in each mouse (Figure 4A). Next, our collaborator (Paul Thomas, St. Jude Children's Hospital, TN) analyzed the unique sequences from this dataset using the TCRdist algorithm (Dash et al. 2017). The majority of T cells used the TRVB1 segment (which encodes Vβ2) together with TRBJ2-1 and displayed a strong selection for a GRG motif in the TCRβ CDR3 (Figure 4B). Our structural studies show that this highly selected arginine residue in the CDR3 makes an important contact with residue p9D of the peptide (Wang, Tsitsiklis, et al., unpublished). We also noted a preference for TCRβ CDR3 length of 13 amino acids, a trend that was particularly prominent for Vβ2 containing T cells (Figure 4C). This conservation of CDR3 length fits with the close wrapping around the predominant TCR contact residue, Glu7 of the GRA6 peptide, which we observed in our structural studies (Wang, Tsitsiklis, et al., unpublished). Therefore, the strong selection of the CDR3 loop seems to be related to important interactions with the peptide.

Since F2-L^d specific T cells also preferentially use Vβ2, we wondered whether the TCR repertoire is similarly focused. We performed the same single cell TCR αβ sequencing on F2-L^d specific T cells isolated from mice immunized with peptide-loaded DC. Analysis of 32 individual paired αβ sequences from 4 individual mice showed that the F2-L^d response is also dominated by a few clones, with a strongly selected TCRβ CDR3 motif (Figure 5A-B). Additionally, F2-L^d specific T cells showed a restricted CDR3 length of 12 amino acids, and this preference was exaggerated in Vβ2 containing T cells (Figure 5C). Interestingly, the F2 peptide (SPYAAGYDL) has a similar C-terminal sequence to the GRA6 peptide (HPGSVNEFDF). The F2-L^d specific TCRs also have a selected arginine within the CDR3, which likely forms a similar salt bridge with p8D of the F2 peptide. These data indicate that there may be similarities in the structure of peptide-MHC-TCR complexes that use L^d.

These data demonstrate that the response to GRA6-L^d exhibits a highly focused TCR repertoire dominated by Vβ2-containing TCRs. The unusual structural characteristics that we have observed with the TG6-GRA6-L^d complex may impose structural restraints on the possible GRA6-L^d specific TCRs that can recognize the peptide-MHC, resulting in limited diversity in the pre-immune repertoire. Furthermore, preferential expansion of particular T cell clones may further drive this TCR bias, resulting in an even more focused TCR repertoire after infection. Similar observations with the F2-L^d specific T cell response suggest that these highly focused T cell responses may be in part due to the unusual structural requirements of binding to the atypical MHC-1 molecule, L^d.

2.3: Materials and Methods

Animals

B6(C57BL/6) and B6.C (B6.C-H2d/bByJ) were obtained from The Jackson Laboratory (Bar Harbor, ME). TCR transgenic mice specific for GRA6-L^d (TG6) were bred in house. Detailed protocols for generation of TG6 mice are described in Chu et al., 2016. In order to monitor multiple *T. gondii* epitopes, F1 mice (B6xB6.c) expressing both the H-2^b and H-2^d MHC class I molecules were used for all experiments. 6-10 week old mice were used in all experiments.

Infection

Mice were injected intraperitoneally (i.p.) with $1x10^5$ live tachyzoites from the type II Prugniuad-tomato-OVA strain (Pru) (Chtanova et al., 2008). This strain harbors immunogenic T cell epitopes derived from the parasite proteins, GRA6 (Blanchard et al., 2008), GRA4 (Frickel et al., 2008), and ROP5 (Grover et al., 2014), and is engineered to express red fluorescent protein (RFP).

Flow Cytometry

All antibodies were from eBioscience (San Diego, CA), Biolegend (San Diego, CA), or Tonbo (San Diego, CA). All tetramers were obtained from the NIH tetramer facility (Atlanta, GA). The tetramers were made by conjugating the biotin-labeled monomers with PE-labeled streptavidin (Prozyme, Hayward, CA) according to protocols from the NIH tetramer facility. All flow cytometry data were acquired by BD LSR Fortessa analyzers (BD Biosciences) and were analyzed with FlowJo software (Tree Star, Ashland, OR). Fluorescent AccuCheck counting beads (Invitrogen) were used to calculate total numbers of live lymphocytes.

Immunization with peptide-loaded dendritic cells

Bone marrow derived dendritic cells were incubated with 1uM of peptide of interest for 3 hours at 37°C. Cells were washed and $5x10^6$ peptide-loaded dendritic cells were injected subcutaneously into naive F1 ($H2^{bxd}$) mice. Mice were sacrificed 7 days post immunization.

Vβ usage of *T. gondii* epitope specific CD8+ T cells

F1 ($H2^{bxd}$) mice were infected with Pru strain *T. gondii* parasites or immunized with bone marrow derived dendritic cells loaded with the indicated peptide. 3 weeks post infection or 1 week post immunization, RBC lysed splenocytes were stained for surface CD8, peptide-MHC-tetramer, CD44, and individual Vβs, and then analyzed by flow cytometry.

Single Cell TCR Sequencing

Mice were infected i.p. with the Pru strain of *T. gondii* or immunized with DC loaded with the F2 peptide. Spleens were harvested at 3 weeks post infection or 1 week post immunization, and GRA6-L^d or F2-L^d tetramer positive CD8+ T cells were single-cell sorted into 96-well plates. TCRα and TCRβ sequences were obtained by reverse transcription and nested PCRs according to Dash et al., 2011.

2.4: References

Arstila, T.P. *et al.* (1999) A direct estimate of the human alphabeta T cell receptor diversity. Science 286: 958-61

Blanchard, N. *et al.* (2008) Immunodominant, protective response to the parasite *Toxoplasma gondii* requires antigen processing in the endoplasmic reticulum. Nat Immunol 9, 937-944

Brown, C.R. *et al.* (1995) Definitive identification of a gene that confers resistance against Toxoplasma cyst burden and encephalitis. Immunology 85, 419-428

Chu, H.H. *et al.* (2016) Continuous Effector CD8(+) T Cell Production in a Controlled Persistent Infection Is Sustained by a Proliferative Intermediate Population. Immunity 45, 159-171

Dash, P. *et al.* (2011) Paired analysis of TCRα and TCRβ chains at the single-cell level in mice. J Clin Invest 121(1): 288-295

Dash, P. *et al.* (2017) Quantifiable predictive features define epitope-specific T cell receptor repertoires. Nature 547, 89-93

De Simone, M., Rossetti, G., and Pagani, M. (2018) Single Cell T Cell Receptor Sequencing: Techniques and Future Challenges. Frontiers in Immunology https://doi.org/10.3389/fimmu.2018.01638

Feliu, V. *et al.* (2013) Location of the CD8 T Cell Epitope within the Antigenic Precursor Determines Immunogenicity and Protection against the *Toxoplasma gondii* Parasite. PLoS Pathog. 9, DOI: 10.1371/journal.ppat.1003449

Flesch, I.E.A. *et al.* (2010) Altered CD8(+) T cell immunodominance after vaccinia virus infection and the naïve repertoire in inbred and F(1) mice. The Journal of Immunology, 184(1), 45-55

Grover, H.S. *et al.* (2014) Impact of regulated secretion on antiparasitic CD8 T cell responses. Cell Rep. *7*, 1716-1728

Jenkins, M.K. and Moon, J.J. (2012) The role of naïve T cell precursor frequency and recruitment in dictating immune response magnitude. Journal of Immunology, 188 (9) 4135-4140

Lie, W.R. *et al.* (1991) The Specific Binding of Peptide Ligand to Ld Class I Major Histocompatibility Complex Molecules Determines Their Antigenic Structure. Journal of Experimental Medicine 173 (2): 449–59.

Narayanan, S. and Kranz, D.M. (2013) The Same Major Histocompatibility Complex

Polymorphism Involved in Control of HIV Influences Peptide Binding in the Mouse H-2L^{d} System. Journal of Biological Chemistry 288 (44): 31784–94

Potter, T.A. *et al.* (1981) Flow Microfluorometric Analysis of H-2L Expression. Journal of Immunology 127 (2): 580–84

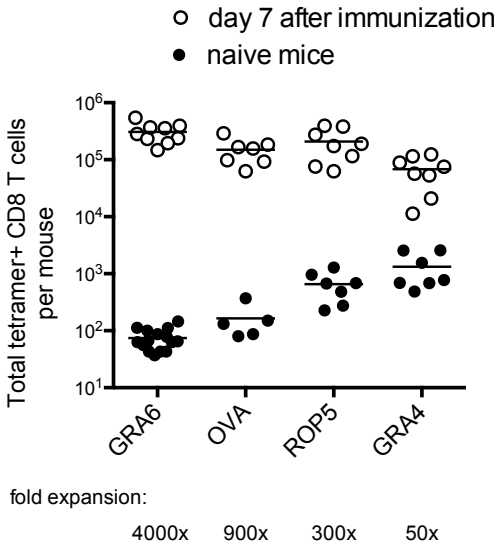

Figure 2.1: Expansion of *T. gondii* epitope specific CD8+ T cells after peptide immunization.

Mice were immunized with bone marrow-derived dendritic cells loaded with 1μM of the indicated peptides. Expanded GRA6-L^d, OVA-K^b, ROP5-D^b, and GRA4-L^d tetramer$^+$ CD8+ T cells were quantified by tetramer staining of splenocytes 7 days post immunization. Numbers of precursor tetramer$^+$ CD8+ T cells in the spleen were quantified by tetramer enrichment in naïve mice and were used to calculate the fold expansion of each antigen-specific T cell population.

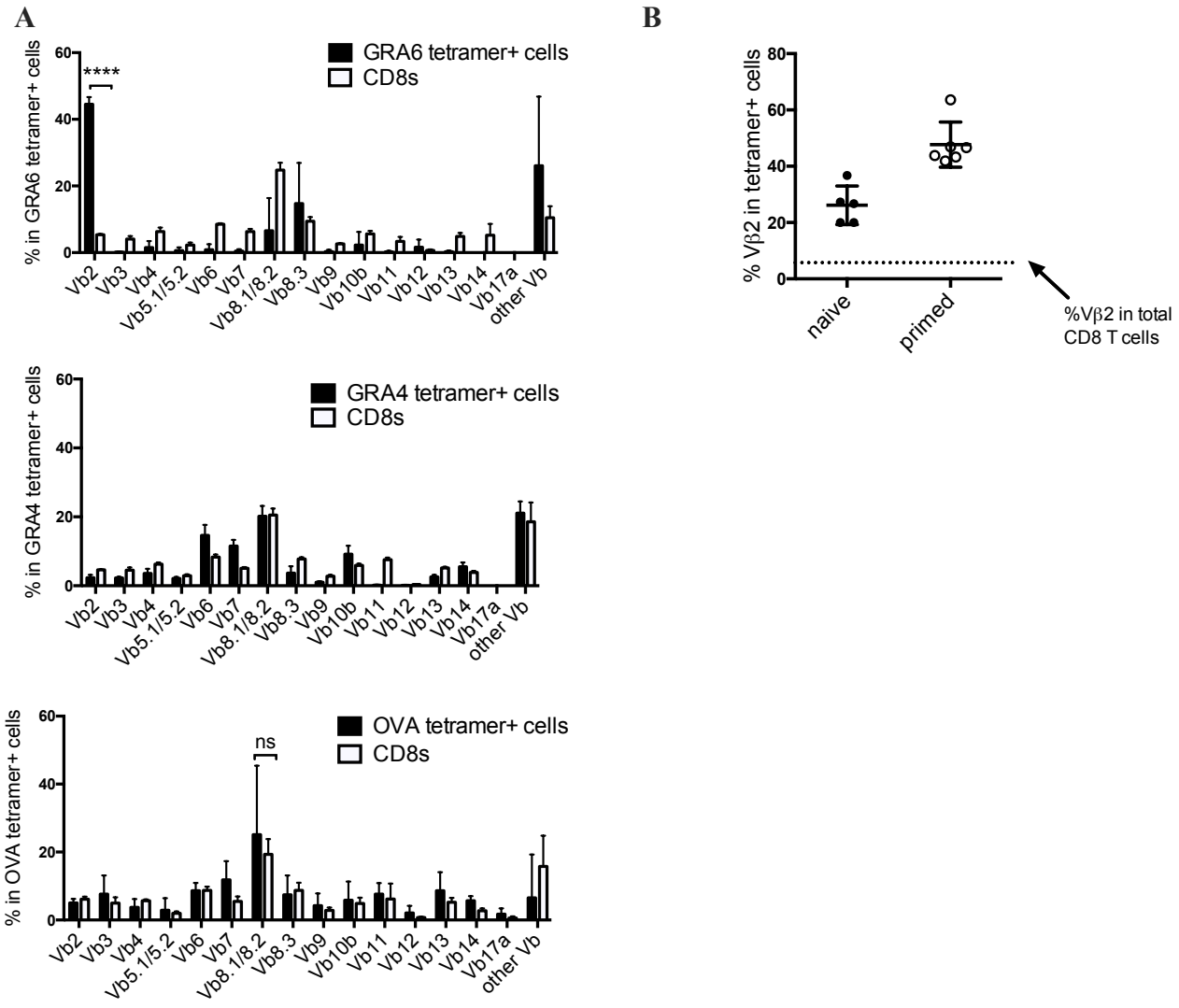

Figure 2.2: Vβ usage in epitope specific CD8+ T cells after *T. gondii* infection.

(A) Vβ usage of gated GRA6-L^d, GRA4-L^d, and OVA-K^b tetramer$^+$ splenic CD8+ T cells was determined by flow cytometry. Vβ usage in total splenic CD8+ T cells from the same mice is shown for comparison. Mice were infected i.p. with Pru strain *T. gondii* parasites and analyzed at 21 days post infection. **(B)** Vβ usage of expanded GRA6-L^d tetramer+ splenic CD8+ T cells or T cells tetramer-enriched from naïve mice. Each dot represents an individual mouse and the dashed line indicates the frequency of Vβ2 amongst total splenic CD8+ T cells (5.40%).

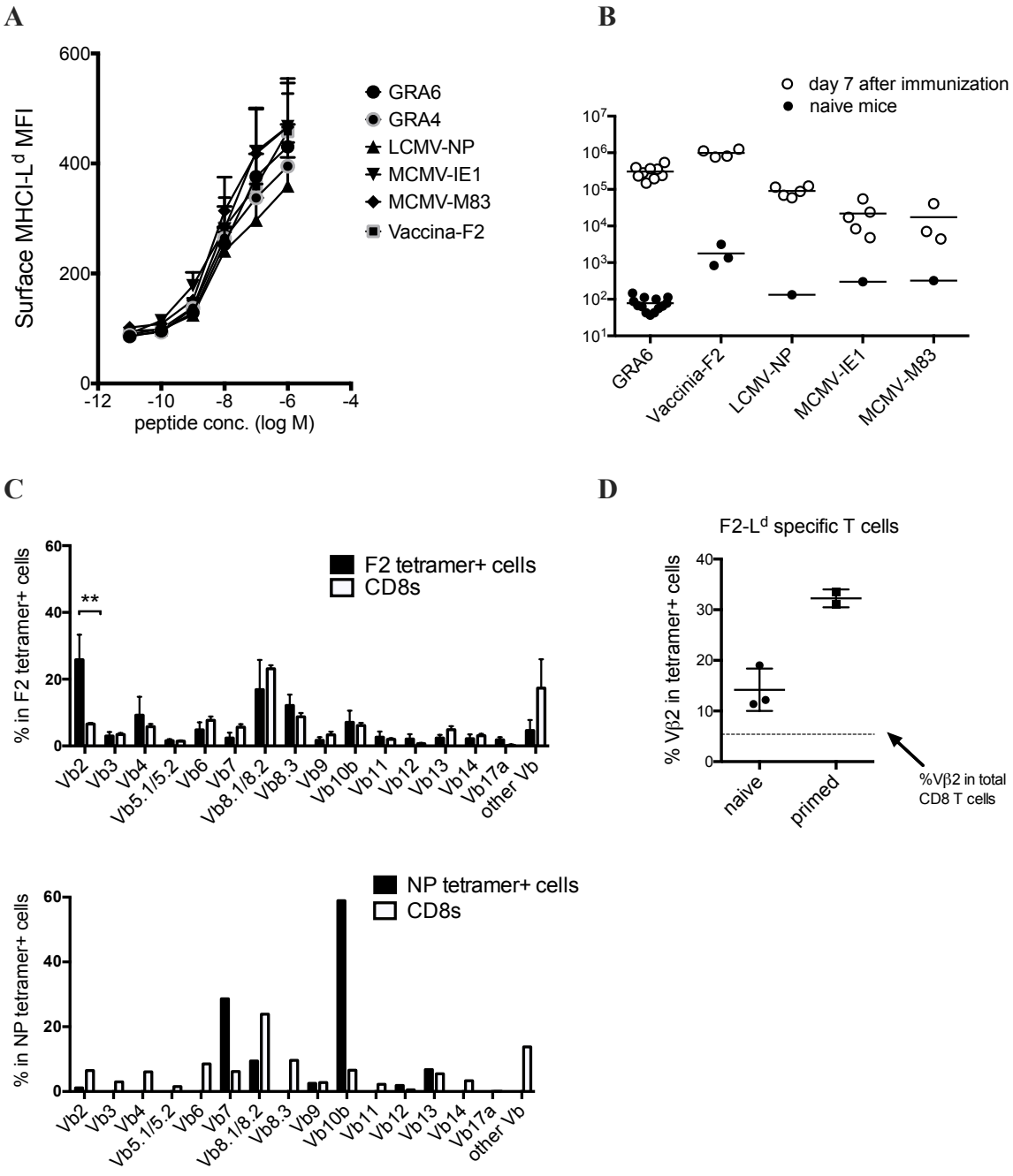
A
Surface MHCI-L^d MFI
peptide conc. (log M)
GRA6
GRA4
LCMV-NP
MCMV-IE1
MCMV-M83
Vaccina-F2
B
day 7 after immunization
naive mice
GRA6
Vaccinia-F2
LCMV-NP
MCMV-IE1
MCMV-M83
C
% in F2 tetramer+ cells
F2 tetramer+ cells
CD8s
**
% in NP tetramer+ cells
NP tetramer+ cells
CD8s
Vb2
Vb3
Vb4
Vb5.1/5.2
Vb6
Vb7
Vb8.1/8.2
Vb8.3
Vb9
Vb10b
Vb11
Vb12
Vb13
Vb14
Vb17a
other Vb
D
F2-L^d specific T cells
% Vβ2 in tetramer+ cells
naive
primed
%Vβ2 in total CD8 T cells

Figure 2.3: Peptide binding strength, T cell expansion and Vβ usage of other L^d-restricted CD8+ T cell responses.

(A) Strength of peptide binding to L^d was measured by an RMA-S assay. Peptide was added to TAP-/- RMA-S cells at the indicated concentrations, and L^d surface expression was measured. **(B)** Mice were immunized with bone marrow-derived dendritic cells loaded with 1μM of the indicated peptides. Expanded tetramer$^+$ CD8+ T cells were quantified by tetramer staining of splenocytes 7 days post immunization. Numbers of precursor tetramer$^+$ CD8+ T cells in the spleen were quantified by tetramer enrichment in naïve mice. **(C)** Vβ usage of gated F2-L^d and NP-L^d tetramer$^+$ splenic CD8+ T cells was determined by flow cytometry on splenocytes from immunized mice from (B). Vβ usage in total splenic CD8+ T cells from the same mice is shown for comparison. **(D)** Vβ usage of expanded F2-L^d tetramer+ splenic CD8+ T cells from immunized mice or T cells tetramer-enriched from naïve mice. Each dot represents an individual mouse and the dashed line indicates the frequency of Vβ2 amongst total splenic CD8+ T cells (5.40%).

A

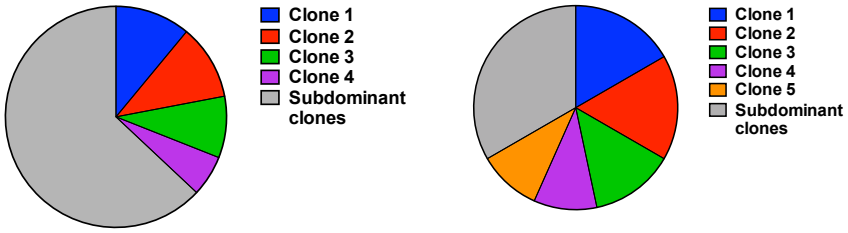

B



C

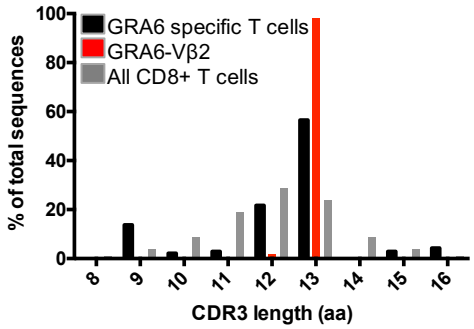

D

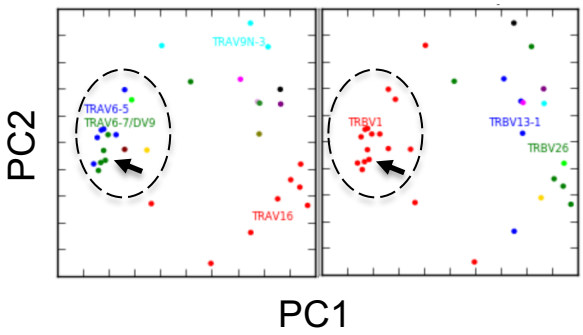

E

TG6 sequence:
TRAV6-7/DV9, TRAJ52*01, CDR3a CALGDPTGANTGKLTF
TRBV1, TRBJ2-1*01, CDR3b CTCSAGRGGYAEQFF

* indicates the identical TG6 sequence found in a new clone

Mouse 1:
Clone 1)
TRAV6-7/DV9, TRAJ30*01, CDR3a CALRIQDTNAYKVIF
*TRBV1, TRBJ2-1*01, CDR3b CTCSAGRGGYAEQFF

Clone 2)
TRAV6-7/DV9, TRAJ53*01, CDR3a CALSEGNSGGSNYKLTF
*TRBV1, TRBJ2-1*01, CDR3b CTCSAGRGGYAEQFF

Clone 3)
TRAV6-5, TRAJ32*01, CDR3a CPGSSGNKLIF
*TRBV1, TRBJ2-1*01, CDR3b CTCSAGRGGYAEQFF

Mouse 2:
Clone 1)
TRAV6-7/DV9, TRAJ52*01, CDR3a CALSDRDSGGSNYKLTF
*TRBV1, TRBJ2-1*01, CDR3b CTCSAGRGGYAEQFF

Clone 2)
*TRAV6-7/DV9, TRAJ52*01, CALGDPTGANTGKLTF
TRBV1, TRBJ2-1*01, CDR3b CTCSAGRGAHAEQFF

Figure 2.4: Clonal analyses of TCR α and β chains of GRA6-L^d specific T cells.

GRA6-L^d tetramer$^+$ CD8+ T cells were single-cell sorted from mice 3 weeks after i.p. infection with Pru strain parasites and TCRα and TCRβ genes from individual T cells were sequenced as described (Dash et al. 2011). (**A)** Frequency of top αβ clones in 2 individual mice. (**B)** Clonal diversity in GRA6-L^d specific CD8+ T cells was analyzed by a collaborator (Paul Thomas, St. Jude Children's Hospital, TN) using the TCRdist algorithm (Dash et al. 2017). Top-scoring CDR3β motif identified by a CDR3 motif discovery algorithm are shown using a TCR logo that summarizes V and J usage, CDR3 amino acid enrichment, and inferred rearrangement structures. The bottom panel shows the motif enriched by calculating against a background dataset of non-epitope specific TCR sequences. (**C)** Restricted TCRβ CDR3 length in GRA6-L^d specific T cells from 2 individual mice. The Vβ2$^+$ GRA6-L^d specific T cells include 57 total sequences, from 22 distinct clones, of which 21/22 have a TCRβ CDR3 length of 13aa. The distribution of TCRβ CDR3 length in bulk CD8+ T cells is provided for comparison. (**D)** Principal components analysis (PCA) projection of the TCRdist landscape colored by Vα (left panel) and Vβ (right panel) gene usage. The predominant cluster of TCRs that correspond to the top scoring CDR3β motif are indicated with a dashed circle, and the TG6 TCR, included in this cluster, is indicated with an arrow. (**E)** The TG6 TCRβ coding sequence from the original GRA6-L^d specific T cell hybridoma (Blanchard et al. 2008) was found independently in 2 additional mice, each time paired with a closely related TCRα. Likewise, the TCR α gene of the TG6 TCR was found independently in one additional mouse, paired with a closely related TCRβ gene.

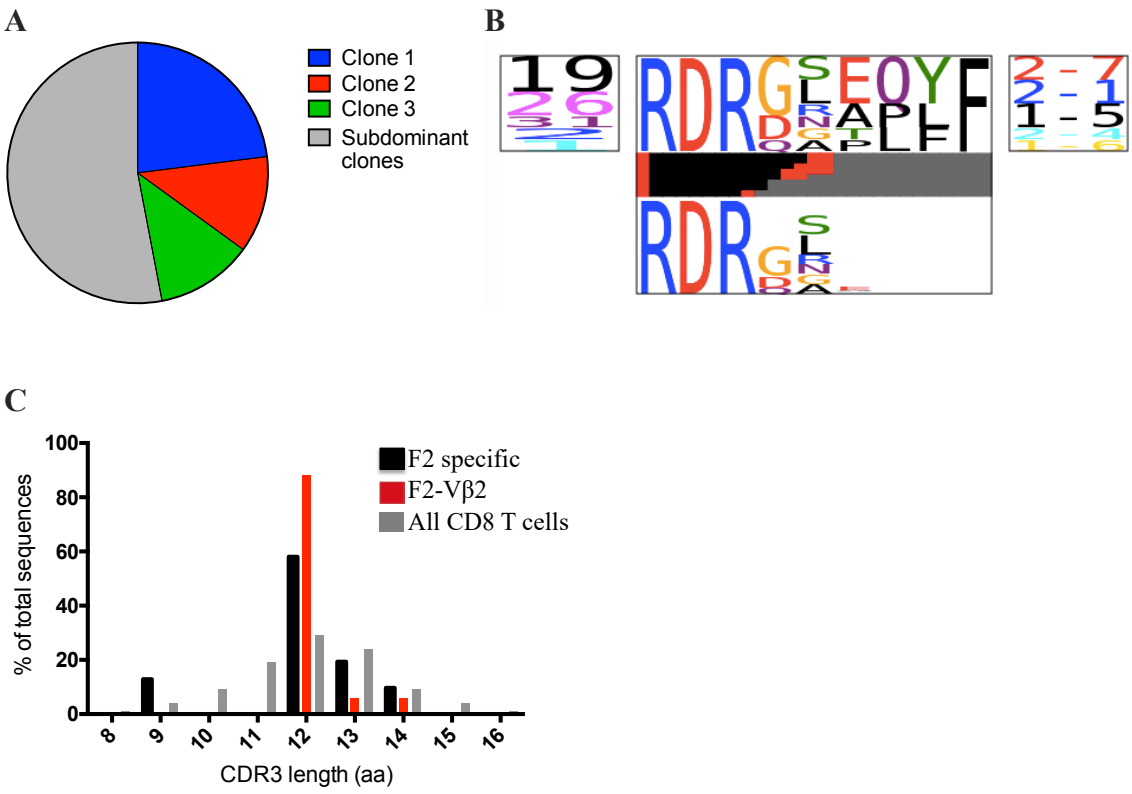

Figure 2.5: Clonal analyses of TCR α and β chains of F2-L^d specific T cells.

F2-L^d tetramer$^+$ CD8+ T cells were single-cell sorted from mice 1 week post immunization with peptide-loaded DC and TCRα and TCRβ genes from individual T cells were sequenced as described (Dash et al. 2011). (**A**) Frequency of top αβ clones in 2 individual mice. (**B**) Clonal diversity in F2-L^d specific CD8+ T cells was analyzed by a collaborator (Paul Thomas, St. Jude Children's Hospital, TN) using the TCRdist algorithm (Dash et al. 2017). Top-scoring CDR3β motif identified by a CDR3 motif discovery algorithm are shown using a TCR logo that summarizes V and J usage, CDR3 amino acid enrichment, and inferred rearrangement structures. The bottom panel shows the motif enriched by calculating against a background dataset of non-epitope specific TCR sequences. (**C**) Restricted TCRβ CDR3 length in F2-L^d specific T cells from 2 individual mice. The distribution of TCRβ CDR3 length in bulk CD8+ T cells is provided for comparison.

Chapter 3: An Unusual MHC Molecule Generates Protective CD8+ T Cell Responses to Chronic Infection

3.1: Abstract

The CD8+ T cell response to the intracellular parasite *Toxoplasma gondii* varies dramatically between mouse strains, resulting in stark differences in control of the parasite. Protection in BALB/c mice can be attributed to an unusually strong and protective MHC-1 L^d-restricted CD8+ T cell response directed against a peptide derived from the parasite antigen GRA6. The MHC-1 L^d molecule has limited peptide binding compared to conventional MHC molecules such as K^b or D^b, which correlates with polymorphisms associated with "elite control" of HIV in humans. To investigate the link between the unusual MHC-1 molecule L^d and the generation of "elite controller" CD8+ T cell responses, we compared the GRA6-L^d specific T cell response to the well-studied OVA-K^b specific response, and demonstrated that GRA6-L^d specific T cells are significantly more protective and resistant to exhaustion in chronic *T. gondii* infection. To further investigate the connection between limited peptide presentation and robust T cell responses, we used CRISPR/Cas9 to generate mice with a point mutation (W97R) in the peptide-binding groove of L^d that results in broader peptide binding. We investigated the effect of this L^d W97R mutation on another robust L^d-restricted response against the IE1 peptide during Murine Cytomegalovirus (MCMV) infection. This mutation leads to an increase in exhaustion markers in the IE1-L^d specific CD8+ T cell response. Our results indicate that limited peptide binding by MHC-1 L^d correlates with the development of robust and protective CD8+ T cell responses that may avoid exhaustion during chronic infection.

3.2: Introduction

Individuals differ dramatically in their ability to mount CD8+ T cell responses against intracellular infections, as exemplified by Human Immunodeficiency Virus (HIV) infected individuals who can control the virus without anti-retroviral therapy (Deeks and Walker 2007). HIV "elite control" is strongly correlated with polymorphisms in genes encoding the major histocompatibility complex (MHC) class I proteins (Goulder and Walker 2012). While the ability of elite control-associated alleles, such as Human Leukocyte Antigen (HLA)-B57 and B27, to induce strong CD8+ responses undoubtedly depends on their ability to bind particular viral peptides, these MHC alleles are also associated with autoimmunity and resistance to other infections, suggesting that more general properties of these molecules may underlie their ability to generate potent CD8+ T cell responses (Hraber, Kuiken, and Yusim 2007; Kim et al. 2011; Bowness 2015). Moreover, while potent CD8+ T cell responses are typically characterized by high affinity binding of T cell receptors (TCRs) for pathogen-derived peptides presented by MHC-1 proteins, other factors such as peptide affinity for MHC, T cell precursor frequency, and antigen density are also important (Tscharke et al. 2015; Jenkins and Moon 2015). Overall, the factors that determine the efficacy of CD8+ T cell responses, and why potent responses are linked to certain MHC-1 alleles, remains poorly understood.

Recent studies have revealed that the level of self-reactivity is another important factor in determining the strength of a T cell response. T cells undergo functional tuning in the thymus based on the strength of the self-pMHC signals they receive (Hogquist and Jameson 2014). CD5 is a key player in the tuning process, and also serves a robust marker of the degree of self-reactivity of naïve T cells (Azzam et al. 2001; Persaud et al. 2014; Fulton et al. 2015; Mandl et al. 2013). T cells with higher self-reactivity ($CD5^{high}$) are generally superior in their responses to foreign antigens, with higher antigen-driven expansion, IL-2 production, and reactivity to cytokines compared to T cells with low self-reactivity ($CD5^{low}$) (Weber et al. 2012; Mandl et al. 2013; Persaud et al. 2014; Fulton et al. 2015; Cho et al. 2016; Hogquist and Jameson 2014). In one study, a $CD5^{low}$ CD4+ T cell clone displayed resistance to activation-induced cell death and superior expansion during secondary challenge (Weber et al. 2012). This suggests that high versus low self-reactivity T cells may be designed to fulfill distinct roles in different infection settings. However, the role of CD8+ T cells with low self-reactivity remains unknown.

While different MHC alleles vary in their ability to bind to particular antigenic peptides, there are indications that other properties of MHC-1 molecules may also play a role in shaping T cell responses. Human HLA-B alleles differ in several properties including their dependence on components of the antigen processing machinery, stability in absence of peptides, peptide loading efficiency, and the broadness of their specificity for peptides (Yarzabek et al. 2018; Geng, Zaitouna, and Raghavan 2018; Košmrlj et al. 2010; Chappell et al. 2015). It has been proposed that, while the majority of MHC-1 molecules are "generalists" able to bind a large set of peptides and produce adequate CD8+ responses to a large number of pathogens, certain MHC-1 molecules with distinctive peptide binding properties may serve as "specialists" that sacrifice broad coverage in exchange for the potential to make potent T cell responses to specific pathogens (Chappell et al. 2015; Košmrlj et al. 2010). Notably, most mouse model studies of CD8+ T cell responses have been conducted on the C57BL/6 (B6) background, limiting studies to MHC-K^b and D^b restricted responses. Therefore, our knowledge of CD8+ T cells restricted to other mouse MHC-1 molecules is limited.

The CD8+ T cell response to the intracellular parasite *Toxoplasma gondii (T. gondii)* differs dramatically between mouse strains and determines whether or not mice eventually succumb to Toxoplasmic encephalitis. This difference is linked to MHC haplotype, with BALB/c ($H\text{-}2^d$) mice being resistant and B6 ($H\text{-}2^b$) mice being susceptible to infection. Resistance to *T. gondii* infection in $H\text{-}2^d$ mice is due to an unusually strong and protective CD8+ T cell response directed against a 10-mer peptide (HF10) derived from the parasite antigen GRA6, presented by the MHC-1 molecule L^d (Brown et al. 1995; Blanchard et al. 2008). The GRA6-L^d specific CD8+ T cell response is maintained by a proliferative intermediate population that gives rise to large numbers of armed effector T cells throughout chronic infection, and shows no signs of functional exhaustion (Chu et al. 2016). In contrast, high levels of CD8+ T cell dysfunction have been reported in B6 mice after infection with *T. gondii* (Bhadra et al. 2011; Bhadra, Gigley, and Khan 2012). Interestingly, the MHC-1 L^d molecule shares key polymorphic residues with protective HLA-B alleles in HIV "elite controllers" which correlate with

restricted peptide binding (Pereyra et al. 2010; Košmrlj et al. 2010; Narayanan and Kranz 2013).

Here we investigated the link between the atypical MHC-1 molecule L^d and the generation of "elite controller" CD8+ T cell responses. First, we compared the GRA6-L^d specific CD8+ cell response to the OVA-K^b specific response restricted to the conventional MHC-1 K^b molecule in their ability to protect against *T. gondii* infection. We also investigated the effect of a point mutation in MHC-1 L^d which leads to broader peptide binding, on another robust L^d-restricted response during chronic Murine Cytomegalovirus (MCMV) infection (Pahl-Seibert et al. 2005). In both systems, T cells restricted to MHC-1 L^d exhibited resistance to exhaustion compared to T cells restricted to an MHC-1 with broader peptide binding. Overall, our results indicate that limited peptide binding by MHC correlates with the development of CD8+ T cell responses that resist exhaustion, and are consistent with a model in which limited peptide binding by MHC-1 and the corresponding low self-reactivity of CD8+ T cells favor protective responses during chronic infections.

3.3: Results

The CD8+ T cell response to GRA6-L^d is protective and resistant to exhaustion

We previously showed that the GRA6-L^d specific CD8+ T cell response to *T. gondii* infection is immunodominant and highly protective (Blanchard et al. 2008; Chu et al. 2016). To further evaluate the protective capacity of this T cell response, we performed a direct comparison with the well-characterized and potent CD8+ T cell response to OVA-K^b (Pope et al. 2001; Kumar and Tarleton 2001; Radford et al. 2002; Braaten et al. 2005; Miyakoda et al. 2012). We used TCR transgenic mice expressing rearranged transgenes representative of either the GRA6-L^d (TG6) or OVA-K^b (OT-1) response (Chu et al. 2016; Hogquist et al. 1994). Both TCRs exhibit similarly strong binding to their respective peptide-MHC complexes (K_d of 0.5-6 micromolar) ((Alam et al. 1999; Rosette et al. 2001) and data not shown). We also used a *T. gondii* strain in which both the model antigen OVA and the endogenous parasite antigen GRA6 are secreted from the parasite via dense granules (Schaeffer et al. 2009).

We first compared the protective capacity of TG6 and OT-1 T cells during *T. gondii* infection. We transferred naïve splenic TG6 or OT-1 CD8+ T cells from TCR transgenic H-$2^{b/d}$ mice into T and B cell deficient H-$2^{b/d}$ (B6 Rag$2^{-/-}$ x BALB/c Rag$2^{-/-}$) mice one day prior to infection, and monitored parasite load and T cell responses 6-8 weeks later (Figure 3.1A). Mice that received OT-1 T cells had approximately 30-fold higher parasite load in the brain compared to mice that received TG6 T cells (Figure 3.1B). T cell numbers in the brains of OT-1 transferred mice were higher than in TG6 transferred mice, implying that reduced protection was not due to reduced T cell expansion or trafficking to the brain (Figure 3.1C). Interestingly, GRA6-L^d specific T cells could be readily detected by tetramer staining amongst donor T cells from OT-1 TCR transgenic mice (data not shown), suggesting that the outgrowth of GRA6-L^d specific T cells using endogenous TCR gene rearrangements could account for some protection in these mice.

Consistent with this interpretation, we observed even more striking differences in cyst load, and a change in mouse survival, when splenocytes from TG6 Rag2-/- or OT-1 Rag2-/- mice were used as the donor populations (Supplementary Figure 3.1).

We also observed that OT-1 T cells recovered from chronically infected mice were functionally impaired compared to TG6 T cells. OT-1 T cells in the spleen, lymph nodes and brain displayed significantly higher expression of the T cell exhaustion marker PD1 (Figure 3.1D). Additionally, OT-1 T cells in the spleen had a dramatically reduced capacity to produce the inflammatory cytokines IFNγ and TNFα compared to TG6 T cells (Figure 3.1E).

The increase in T cell exhaustion in mice transferred with OT-1 versus TG6 T cells could be due differences in parasite load, and/or T cell intrinsic differences. To control for the effects of parasite load, we co-transferred both T cell populations into wild type H-$2^{b/d}$ mice before infection with *T. gondii*. Again, we observed an increase in PD1 expression on OT-1 T cells compared to TG6 T cells in the spleen and lymph nodes of infected recipient mice (Supplementary Figure 3.2). This difference was less dramatic than that seen in Rag2-/- mice, likely due to the effective parasite control by the GRA6-L^d specific T cells. These data suggest that T cell-intrinsic differences contribute to the difference in exhaustion between OT-1 and TG6 T cells.

To extend these observations to a polyclonal T cell response, we used fluorochrome-labeled GRA6-L^d and OVA-K^b tetramers to detect endogenous T cell responses in wild type H-$2^{b/d}$ mice infected with OVA-expressing *T. gondii*. Both T cell populations expanded robustly in the spleen and lymph nodes of infected mice, although the GRA6-L^d specific population exhibited slightly better expansion, especially in the spleen (Figure 3.2A-C). As expected, given the effective control of parasites in mice harboring the H-2^d allele, inhibitory receptors remained generally low on CD8+ T cells in these mice. However, in approximately half of the mice, OVA-K^b specific T cells expressed significantly elevated levels of the inhibitory receptors PD1, Tim3 and Lag3, compared to GRA6-L^d specific T cells in both the spleen and lymph nodes (Figure 3.2D).

To confirm that the expression of inhibitory receptors on OVA-K^b specific T cells correlates with reduced functionality of these cells, we analyzed cytokine production by GRA6-L^d and OVA-K^b specific T cells. We re-stimulated splenocytes or lymph node cells from infected mice *ex vivo* with GRA6 or OVA peptide and measured IFNγ and TNFα production by flow cytometry. Stimulation with the GRA6 peptide resulted in slightly higher proportion of IFNγ producing cells compared to the OVA peptide (Figure 3.2E-F), which is likely a reflection of the relative size of the antigen-specific population (Figure 3.2B). To assess the functionality of antigen-specific T cells on a per cell basis, we determined the percentage of IFNγ+ cells that also produced TNFα. This proportion was lower amongst OVA-K^b specific T cells, particularly in those mice with relatively high (>5%) PD1 expression on T cells (Figure 3.2G-H). Thus, high PD1 expression correlated with reduced cytokine production in OVA-K^b specific T cells, indicating that OVA-K^b specific T cells are less functional compared to GRA6-L^d specific T cells from the same infected mice.

T cell exhaustion can be caused by chronic exposure to high levels of inflammatory signals or antigen (Wherry and Kurachi 2015). Differences in inflammatory signals are unlikely to account for the differences observed between GRA6-L^d and OVA-K^b responses when compared in the same infected mice. Therefore we tested whether differences in antigen levels could account for these differences. While both GRA6 and OVA precursor proteins are secreted by dense granules during infection, differences in the expression levels or antigen processing efficiency could lead to differences in the level of peptide presentation (Gubbels et al. 2005; Gregg et al. 2011; Lopez et al. 2015; Buaillon et al. 2017; Tsitsiklis, Bangs, and Robey 2019). To test this possibility, we used an *in vivo* antigen presentation assay. We transferred equal numbers of naïve CFSE-labeled TG6 and OT-1 CD8+ T cells from TCR transgenic mice into chronically infected mice and assessed their proliferation by CFSE dilution 2 or 3 days after transfer. We observed a similar proportion of proliferating cells in TG6 and OT-1 T cells recovered from the spleen and lymph nodes of infected mice (Figure 3.2I, Supplementary Figure 3.3A). As an additional measure of antigen stimulation, we also examined expression of Nur77, a TCR target gene whose induction is proportional to the strength of TCR stimulus (Moran et al. 2011). We did not observe a significant difference in Nur77 expression between TG6 and OT-1 T cells at 2 or 3 days after transfer, suggesting TG6 and OT-1 T cells are receiving similar amounts of antigen stimulation (Supplementary Figure 3.3B, C). The observation that OVA-K^b specific T cells show more exhaustion than GRA6-L^d specific T cells, in spite of exposure to similar levels of antigen and inflammatory signals and a similar affinity for peptide-MHC, suggested that there may be intrinsic differences between these two T cell populations that influence their susceptibility to functional exhaustion.

Limited peptide binding by L^d correlates with the selection of T cells with low self-reactivity

We considered that the unusual peptide binding characteristics of MHC-1 L^d might play a role in generating exhaustion-resistant T cell responses. Expression of L^d on the cell surface is 2- to 3-fold lower than that of other conventional MHC molecules, and several groups have reported that this is due to poor binding to endogenous (self) peptide ligands (Potter et al. 1981; Lie et al. 1991; Narayanan and Kranz 2013). Since L^d binds poorly to self-peptides, we might expect that positive selection on L^d would produce T cells with relatively low self-reactivity. To address this possibility, we examined expression of CD5, a robust surrogate marker for self-reactivity (Azzam et al. 2001; Fulton et al. 2015; Persaud et al. 2014) on T cells from TG6 transgenic mice. We found that CD5 surface expression on naïve splenocytes from TG6 TCR transgenic mice is relatively low compared to polyclonal CD8+ T cells (Figure 3.2J), supporting that TG6 T cells are less self-reactive than polyclonal CD8+ T cells. On the other hand, splenocytes from OT-1 TCR transgenic mice, which are selected on the conventional MHC molecule K^b, have relatively high CD5 expression, consistent with previously published literature that OT-1 T cells have high self-reactivity (Ge et al. 2004) (Figure 3.2J).

The L^d-restricted MCMV IE1 specific CD8+ T cell response has a proliferative CXCR3+KLRG1+ intermediate population

Given the unusual properties of L^d, we considered whether other L^d restricted CD8+ T cell responses might also be particularly robust during chronic infection. The IE1-L^d specific CD8+ T cell response to MCMV is one of a handful of "inflationary" responses that expands during chronic infection and provides strong protection (Pahl-Seibert et al. 2005; Rafaela Holtappels et al. 2002). During *T. gondii* infection, the GRA6-L^d CD8+ T cell response is maintained by an intermediate population (T_{int}), defined by dual expression of CXCR3 and KLRG1, which is highly proliferative and replenishes a short-lived effector (T_{eff}) population to allow for a long-lasting effector T cell response (Chu et al. 2016). Interestingly, we observed the same T_{int} population amongst IE1-L^d specific T cells in mice chronically infected with MCMV, whereas this population was less prominent in CD44+ tetramer- CD8+ T cells from the same mice (Figure 3.3A, B). The T_{int} population was also the most proliferative population within IE1-L^d specific T cells, as measured by Ki67 expression (Figure 3.3C), similar to what we previously observed in the GRA6-L^d specific response (Chu et al. 2016). Together, these data suggest that two robust L^d-restricted responses may be similarly maintained during chronic infection.

An H2-L^d variant with broader peptide binding is associated with increased expression of exhaustion markers by IE1-L^d specific T cells during MCMV infection

We next wanted to investigate whether limited or broad peptide binding in the context of H2-L could contribute to the exhausted T cell phenotype. Previous studies in cell lines have shown that an HIV-controller associated polymorphism at amino acid position 97 in the mouse H2-L gene impacts the broadness of peptide binding (R. Smith et al. 2002; Narayanan and Kranz 2013). To extend these studies to an *in vivo* setting, we used CRISPR-EZ (Chen et al. 2016) to generate mice in which the controller-associated tryptophan at position 97 of L^d is converted to a progressor-associated arginine residue (L^d W97R mutation) (Figure 3.4A) (Pereyra et al. 2010). As expected based on studies in cell lines (Narayanan and Kranz 2013), splenocytes from L^d 97R mice have higher surface expression compared to L^d 97W, consistent with the enhanced binding to self-peptides (Figure 3.4B). Additionally, while incubation with an antigenic peptide stabilized wild type (97W) L^d, this had little impact on the levels of 97R L^d (Figure 3.4D-E). In some cell types (e.g. CD4+ T cells) the levels of IE1 peptide-stabilized L^d 97W were equivalent to L^d 97R (Supplementary Figure 3.4). Thus, limited self-peptide binding by L^d 97W is reversed by the L^d W97R mutation, allowing for higher cell surface expression.

To further explore the connection between limited peptide binding by MHC and robust CD8+ T cell responses, we investigated the effect of the L^d W97R mutation in the setting of persistent infection. We focused on the MCMV IE1-L^d response, since this peptide, unlike the *T. gondii* GRA6 peptide, binds well to both 97R and 97W versions of L^d (Figure 3.4C and data not shown) (Narayanan and Kranz 2013). We infected L^d 97W and L^d 97R mice with MCMV and characterized the IE1-L^d specific CD8+ T cell response during chronic infection (11-16 weeks). IE1-L^d specific T cells expand robustly in L^d

97W mice, while expansion is weaker but still readily detectable in L^d 97R mice (Figure 3.4F). Furthermore, expression of the exhaustion markers PD1, Tim3 and Lag3 is significantly higher on IE1-L^d specific T cells in L^d 97R mice, in both the spleen and lymph nodes (Figure 3.4G). Interestingly, expression of exhaustion markers and the activation marker CD69 is markedly higher in the lymph nodes compared to the spleen in both L^d 97W and L^d 97R mice (Figure 3.4G; Supplementary Figure 3.5), although the IE1-L^d specific T cell population is smaller in the lymph nodes. This may be a result of higher antigen load in the lymph nodes during MCMV infection (Karrer et al. 2003; Torti et al. 2011), possibly pushing IE1-L^d specific T cells in the lymph nodes towards exhaustion and eventual deletion.

MCMV infected L^d 97W and L^d 97R mice have similar viral loads in the salivary glands (Supplementary Figure 3.6A), indicating that the difference in the IE1-L^d specific response is unlikely to be due to a difference in antigen load. To confirm that the changes in IE1-L^d specific T cells are a direct consequence of the W97R mutation, we examined another immunodominant response restricted to a different MHC-1 molecule (m164-D^d) (R. Holtappels et al. 2002). In contrast to IE1-L^d specific T cells, m164-D^d specific T cells do not exhibit an increase in expression of PD1, CD69, and Nur77 (Supplementary Figure 3.6B-D). Therefore, these data support our hypothesis that an intrinsic difference between T cells selected on MHCs with limited versus broad peptide binding may contribute to resistance to exhaustion.

3.4: Discussion

While MHC-1 molecules with limited peptide binding are associated with HIV control in humans and *T. gondii* control in mice, the link between the peptide binding characteristics of MHC and effective CD8+ T cell responses has not been experimentally examined. We used two parallel approaches to address this issue. First, we compared two high affinity CD8+ T cell responses, one restricted to an MHC molecule with limited peptide binding (L^d), and another restricted to a typical MHC-1 molecule (K^b) in the same *T. gondii*-infected mice. Second, we compared T cell responses to the same viral peptide presented by either L^d, or a single amino acid variant of L^d with broad peptide binding, during chronic MCMV infection. In both cases, T cells restricted to MHC-1 L^d showed fewer signs of exhaustion compared to T cells restricted to MHC-1 with broader binding to self-peptides. These data suggest that MHC molecules with limited peptide binding allow for the development of T cells with the ability to persist during chronic infection without becoming exhausted.

At first glance, the association between limited peptide binding and highly protective CD8+ T cell responses appears contradictory. However, while elite control associated MHC molecules bind less broadly to peptides in general, they nevertheless bind strongly to certain antigenic peptides (Narayanan and Kranz 2013; Schneidewind et al. 2008; Košmrlj et al. 2010). Importantly, MHC-1 L^d binds poorly to self-peptides, leading to lower cell surface expression and reduced stability of surface peptide-MHC complexes (Potter et al. 1981; Lie et al. 1991; Narayanan and Kranz 2013). The inability of L^d to bind strongly to self-peptides may explain the unusually low self-reactivity of TG6, a

public TCR representative of the CD8+ T cell response to the dominant *T. gondii* antigen GRA6 (data not shown). These data suggest that the combination of low reactivity to self, coupled with high reactivity to a pathogen-derived peptide may be a key feature of elite controller CD8+ T cell responses.

These considerations support a model in which MHC-1 molecules with restricted peptide binding properties may be considered "specialists", in contrast to the majority of "generalist" MHC-1 molecules with broad peptide binding (Supplementary Figure 3.7) (Chappell et al. 2015). During thymic development, generalist MHC molecules select T cells with relatively high self-reactivity, whereas specialist MHC molecules select T cells with relatively low self-reactivity due to weak binding to self-peptides (Supplementary Figure 3.7A-B). While most infections favor expansion of a broad set of T cells with relatively high self-reactivity, in settings where pathogen-derived peptides are able to bind to, and stabilize, specialist MHC-1 molecules, T cells with high reactivity to a pathogen-derived peptide, but low reactivity to self can expand, giving rise to elite controller CD8+ T cell responses (Supplementary Figure 3.7C-D).

Why might low self-reactivity favor elite controller T cell responses? As suggested previously (Košmrlj et al. 2010), T cells selected in the thymus on specialist MHC molecules may experience less stringent negative selection, allowing for the development of unusually high affinity T cells, which would have been deleted by a generalist MHC, to enter the mature T cell repertoire. Specifically, while negative selection primarily functions to remove highly cross-reactive thymocytes (Huseby et al. 2005, 2006; McDonald et al. 2015), modeling studies have predicted that limited self-peptide presentation by MHC allows for the selection of T cells with high cross-reactivity (Košmrlj et al. 2010). In support of this prediction, an MHC-2 molecule presenting a single peptide selects T cells with highly cross-reactive TCRs by taking advantage of high affinity germline interactions, as a result of minimal negative selection (Dai et al. 2008).

In addition to the selection of a distinctive TCR repertoire, specialist MHC molecules may also impact the functional tuning of T cells during their development in the thymus. Recent studies have shown that T cells tune their functional responsiveness based on their degree of self-reactivity, with higher self-reactivity ($CD5^{high}$) T cells exhibiting greater IL-2 production, more rapid expansion during acute infection, and greater responsiveness to cytokines (Weber et al. 2012; Mandl et al. 2013; Persaud et al. 2014; Fulton et al. 2015; Cho et al. 2016; Hogquist and Jameson 2014). While $CD5^{high}$ T cells are generally superior in their responses to pathogens, in one study $CD5^{low}$ CD4+ T cells were relatively resistant to activation induced cell death, and responded better upon secondary challenge (Weber et al. 2012). It is tempting to speculate that the reduced responsiveness of $CD5^{low}$ T cells to inflammatory environments may allow them to better avoid exhaustion during chronic infection.

In addition to functional tuning during T cell selection in the thymus, the degree of self-reactivity may also impact the tonic TCR signals that T cells experience in the periphery. Tonic signals have been shown to contribute to inhibitory receptor upregulation and

functional hyporesponsiveness in the absence of antigen-specific stimulation (Hsu et al. 2017; Ellestad et al. 2017). Recently, Duong et al. demonstrated that TCRs with higher affinity and higher CD5 expression were more susceptible to functional hyporesponsiveness after chronic exposure to self-peptide MHC (Duong et al. 2019). Higher tonic signaling may push $CD5^{high}$ T cells towards exhaustion, while $CD5^{low}$ T cells restricted to the specialist MHC-1 molecule L^d may experience lower levels of tonic signaling, contributing to their resistance to exhaustion during chronic infection.

While our model predicts that T cells restricted to specialist MHC molecules have the potential to generate high affinity responses to pathogen-derived peptides, it is unlikely that TCR signal strength alone can account for the lack of functional exhaustion in the L^d restricted responses examined in this study. TG6 and OT-1 TCRs have similarly high affinity for antigen-MHC ((Alam et al. 1999; Rosette et al. 2001) and data not shown) and show similar levels of the TCR signal strength reporter Nur77 in infected mice. Likewise, IE1-L^d specific T cells in L^d 97R and L^d 97W mice show comparable functional avidity based on peptide titration experiments **(**data not shown). Moreover, PD1 induction and functional exhaustion is associated with strong, persistent TCR signals, implying that stronger TCR reactivity would lead to more, not less, exhaustion. Thus, it seems likely that differences in functional tuning and tonic signals contribute, at least in part, to the propensity of T cells to become exhausted.

In addition to the T cell intrinsic factors explored here, it is clear that extrinsic factors such as persistent inflammatory signals and high antigen levels also play a role in driving T cell exhaustion. In the *T. gondii*-mouse infection model, the highly protective GRA6-L^d specific T cell response may contribute to a feedback mechanism to prevent exhaustion of other T cell responses by keeping antigen and inflammation levels low. Thus the OVA-K^b specific response exhibits less exhaustion in H-$2^{b/d}$ compared to H-2^b mice due the ongoing GRA6-L^d specific response and reduced parasite load. On the other hand, MCMV is well controlled in mice, even in the absence of a particularly protective T cell response, which may explain the overall low level of T cell exhaustion in this model. Finally, for infections where pathogen levels and inflammation remain high in spite of strong T cell responses, extrinsic factors may be able to overcome the intrinsic resistance of certain T cells to exhaustion. Consistent with this notion, the L^d-restricted CD8+ T cell response to NP peptide during mouse infection with LCMV clone 13 infection exhibited high levels of PD1 and functional exhaustion (data not shown).

In summary, we have used two experimental systems to demonstrate that limited peptide binding by MHC-1 L^d is associated with the generation of exhaustion-resistant CD8+ T cell responses. T cell intrinsic factors linked to the peptide binding properties of restricting MHC molecules may combine with T cell extrinsic factors, such as high antigen levels and persistent inflammatory signals, to determine the outcome of infection. Future studies should directly explore the role of TCR repertoire, T cell tuning, and tonic TCR signaling in T cell susceptibility to exhaustion. Furthermore, extensions to human studies may help to identify additional MHC-1 specialist molecules and may provide insight into protective responses to HIV and other persistent infections, which would have valuable therapeutic implications.

3.5: Materials and Methods

Mice

B6 (C57BL/6), B6 Rag2-/- (B6-Cg-Rag2$^{tm1.1Cgn}$/J), B6.C (B6.C-*H2d*/bByJ), BALB/c, BALB/c Rag2-/- (C.B6(Cg)-Rag2 $^{tm1.1Cgn}$/J), and TCR transgenic mice specific for OVA-K^{b} (OT-1; C57BL/6-Tg(TcraTcrb)1100Mjb/J) were originally purchased from The Jackson Laboratory (Bar Harbor, ME, USA) and then bred in the AAALAC accredited animal facility at University of California, Berkeley. TCR transgenic mice specific for GRA6-L^{d} (TG6) were previously generated in our lab as described (Chu et al. 2016). F1 mice (B6xB6.C or B6 Rag2-/- x BALB/c Rag2-/-) were used for all *T. gondii* experiments in order to monitor multiple *T. gondii* epitopes. L^{d} W97R mutant mice were generated in our lab (described below). Mice were infected at 6-8 weeks old, and sacrificed at indicated times post infection. All mouse procedures were approved by the Animal Care and Use Committee (ACUC) of the University of California.

Infection

For *T. gondii* infections, C57BL/6 Rag2-/- x BALB/c Rag2-/- (H-2$^{b/d}$) or intact C57BL/6 x B6.C (H-2$^{b/d}$) mice were injected intraperitoneally (i.p.) with 2,000 or 10^5 live tachyzoites of the type II Prugniuad-tomato-OVA strain (Pru-OVA) *T. gondii* (Schaeffer et al. 2009), respectively. *T. gondii* brain cysts were quantified by imaging of homogenized brain samples stained with fluorescein-conjugated *Dolichos biflorus* agglutinin (Vector Laboratories) to stain the cell wall with a protocol adapted from (S.-K. Kim and Boothroyd 2005). For MCMV infections, L^{d} 97W or 97R B6.C (H-2^{d}) mice were injected i.p. with 10^6 pfu Smith strain MCMV (L. M. Smith et al. 2008). MCMV viral titers were measured using quantitative PCR.

Flow Cytometry

Cells were stained with various fluorophore-labeled antibodies from BD Biosciences (San Diego, CA), Biolegend (San Diego, CA), or Tonbo Biosciences (San Diego, CA) at 4°C. For intracellular staining, cells were fixed and permeabilized using the eBioscience FoxP3 Fixation/permeabilization buffer kit (for Nur77 and Ki67) or the BD Biosciences Cytofix/Cytoperm kit (for cytokines) according to manufacturer protocols. Biotinylated peptide-MHC monomers were obtained from the NIH Tetramer Facility (Atlanta, GA). Tetramers were made by conjugating the biotin-labeled monomers with PE-labeled or APC-labeled streptavidin (Agilent) according to protocols from the NIH tetramer facility. A tetramer with the WR97 mutation in L^{d} was generated by the NIH Tetramer Facility and used for staining the IE1-L^{d} tetramer specific populations in 11/14 of the L^{d} 97R mice. No significant differences were observed when using the L^{d} 97W versus 97R tetramer. Data were acquired on BD LSR Fortessa and analyzed using FlowJo software (Ashland, OR). Statistical analyses were conducted using GraphPad Prism (San Diego, CA).

Ex Vivo Stimulation with Peptides for Quantification of Cytokine Production

Spleen or lymph node cells from infected mice were plated at a density of 1-3x10^5 cells per well in 96-well round-bottom tissue culture plates and incubated with 1μM of the indicated peptide (Peptide 2.0 Inc.) in media for 3 hours in the presence of protein transport inhibitor cocktail (eBioscience). Cells were then harvested for surface and intracellular antibody staining before flow cytometry analysis.

Antigen Presentation Detection *in Vivo*

Lymph nodes and spleen of TG6 (Ly5.2/5.2) or OT-1 (Ly5.1/5.2) TCR transgenic (H-$2^{b/d}$) mice were harvested and cells were labeled with the cell proliferation dye CFSE (5μM). Cells were washed twice with RPMI and twice with PBS. Cells were then counted and mixed in equal proportions prior to transfer. 5x10^5 TG6 and 5x10^5 OT-1 cells were transferred by intravenous tail-vein injection into previously infected mice (Ly5.1/5.1) and proliferation dye dilution was examined 2 or 3 days after transfer by gating on congenic markers to identify each donor population. Relative antigen presentation is expressed as the percentage of donor TG6 or OT-1 cells that diluted the proliferation dye.

Generation of L^d W97R mutant mouse by CRISPR/Cas9

Single guide RNAs (sgRNAs) were designed using MIT's CRISPR RNA guide design tool (crispr.mit.edu). A homology directed repair (HDR) donor DNA oligo with the desired mutation was synthesized by Life Technologies Co., with a single T→C point mutation that converts a tryptophan (TGG) to arginine (CGG) at position 97 in the L^d gene. Cas9-sgRNA RNP was prepared and incorporated together with the HDR donor DNA oligo and electroporated into mouse zygotes from H-2^d (B6.C) mice as described (Chen et al. 2016; Modzelewski et al. 2018). Resulting mice were genotyped by sequencing. Mice were backcrossed to WT B6.C mice for several generations.

MHC-1 stabilization assay

RMA-S cells were infected with the VSV.G plasmid expressing the 97W or 97R version of L^d and sorted for L^d-positive cells using the Thy1.1 marker. The MHC-1 stabilization assay was performed as described (Feliu et al. 2013). In brief, RMA-S.L^d (97W or 97R) cells or splenocytes from L^d 97W and 97R mice were incubated at room temperature overnight to increase surface MHC-1 expression. The next day, cells were washed with PBS and plated at 3×10^5 cells per well in a 96-well round-bottom tissue culture plate. Peptides of interest (Peptide 2.0 Inc.) were added to the cells at indicated concentrations. The cells were incubated for 1 hour at room temperature and 3 hours at 37°C. Cells were stained with the 30-5-7 antibody (specific for conformed, peptide-bound L^d) and a goat anti-mouse IgG phycoerythrin (PE)-conjugated secondary antibody and analyzed by flow cytometry.

3.6: References

Alam, S. *et al.* (1999) Qualitative and Quantitative Differences in T Cell Receptor Binding of Agonist and Antagonist Ligands. Immunity 10 (2): 227–37

Azzam, H.S., *et al.* (2001) Fine Tuning of TCR Signaling by CD5. Journal of Immunology 166 (9): 5464–72

Bhadra, R. *et al.* (2011) Control of Toxoplasma Reactivation by Rescue of Dysfunctional CD8+ T-Cell Response via PD-1-PDL-1 Blockade. PNAS 108 (22): 9196–9201

Bhadra, R. *et al.* (2012) PD-1-Mediated Attrition of Polyfunctional Memory CD8+ T Cells in Chronic Toxoplasma Infection. The Journal of Infectious Diseases 206 (1): 125–34

Blanchard, N. *et al.* (2008) Immunodominant, Protective Response to the Parasite Toxoplasma Gondii Requires Antigen Processing in the Endoplasmic Reticulum. Nature Immunology 9 (8): 937–44

Bowness, P. (2015) HLA B27. Annual Review of Immunology 33: 29–48

Braaten, D.C. *et al.* (2005) An Optimized CD8+ T-Cell Response Controls Productive and Latent Gammaherpesvirus Infection. Journal of Virology 79 (4): 2573–83

Brown, C.R. *et al.* (1995) Definitive Identification of a Gene That Confers Resistance against Toxoplasma Cyst Burden and Encephalitis. Immunology 85 (3): 419–28

Buaillon, C. *et al.* (2017) MHC I Presentation of Toxoplasma Gondii Immunodominant Antigen Does Not Require Sec22b and Is Regulated by Antigen Orientation at the Vacuole Membrane. European Journal of Immunology 47 (7): 1160–70

Chappell, P. *et al.* (2015) Expression Levels of Mhc Class i Molecules Are Inversely Correlated with Promiscuity of Peptide Binding. ELife 2015 (4): 1–22

Chen, S. *et al.* (2016) Highly Efficient Mouse Genome Editing by CRISPR Ribonucleoprotein Electroporation of Zygotes. Journal of Biological Chemistry 291 (28): 14457–67

Cho, J.H. *et al.* (2016) CD45-Mediated Control of TCR Tuning in Naïve and Memory CD8+T Cells. Nature Communications 7: 1–15

Chu, H.H. *et al.* (2016) Continuous Effector $CD8^+$ T Cell Production in a Controlled Persistent Infection Is Sustained by a Proliferative Intermediate Population. Immunity 45 (1)

Dai, S. *et al.* (2008) Crossreactive T Cells Spotlight the Germline Rules for Alphabeta T

Cell-Receptor Interactions with MHC Molecules. Immunity 28 (3): 324–34

Deeks, S.G. and Walker, B.D. (2007) Human Immunodeficiency Virus Controllers: Mechanisms of Durable Virus Control in the Absence of Antiretroviral Therapy. Immunity 27 (3): 406–16

Duong, M.N. *et al.* (2019) Chronic TCR-MHC (Self)-Interactions Limit the Functional Potential of TCR Affinity-Increased CD8 T Lymphocytes. Journal for ImmunoTherapy of Cancer 7 (1): 1–17

Ellestad, K.K. *et al.* (2017) PD-1 Controls Tonic Signaling and Lymphopenia-Induced Proliferation of T Lymphocytes. Frontiers in Immunology 8 (OCT)

Feliu, V. *et al.* (2013) Location of the CD8 T Cell Epitope within the Antigenic Precursor Determines Immunogenicity and Protection against the Toxoplasma Gondii Parasite. PLoS Pathogens 9(6)

Fulton, R.B. *et al.* (2015) The TCR's Sensitivity to Self Peptide-MHC Dictates the Ability of Naive CD8(+) T Cells to Respond to Foreign Antigens. Nature Immunology 16 (1): 107–17

Ge, Q. *et al.* (2004) Competition for Self-Peptide-MHC Complexes and Cytokines between Naive and Memory CD8+ T Cells Expressing the Same or Different T Cell Receptors. Proceedings of the National Academy of Sciences of the United States of America 101 (9): 3041–46

Geng, J., Zaitouna, A.J., and Raghavan, M.. (2018) Selected HLA-B Allotypes Are Resistant to Inhibition or Deficiency of the Transporter Associated with Antigen Processing (TAP). PLoS Pathogens 14 (7): 1–22

Goulder, P.J. and Walker, B.D. (2012) HIV and HLA Class I: An Evolving Relationship. Immunity 37 (3): 426–40

Gregg, B. *et al.* (2011) Subcellular Antigen Location Influences T-Cell Activation during Acute Infection with *Toxoplasma Gondii*. PLoS ONE 6 (7): 1–7

Gubbels, M.J. *et al.* (2005) Class I Major Histocompatibility Complex Presentation of Antigens That Escape from the Parasitophorous Vacuole of *Toxoplasma Gondii*. Infection and Immunity 73 (2): 703–11

Hogquist, K.A. *et al.* (1994) T Cell Receptor Antagonist Peptides Induce Positive Selection. Cell 76 (1): 17–27

Hogquist, K.A. and Jameson, S.C. (2014) The Self-Obsession of T Cells: How TCR Signaling Thresholds Affect Fate 'Decisions' and Effector Function. Nature Immunology 15 (9): 815–23

Holtappels, R. *et al.* (2002) “Two Antigenic Peptides from Genes M123 and M164 of Murine Cytomegalovirus Quantitatively Dominate CD8 T-Cell Memory in the H-2d Haplotype.” Journal of Virology 76 (1): 151–64

Holtappels, R. *et al.* (2002) Two Antigenic Peptides from Genes M123 and M164 of Murine Cytomegalovirus Quantitatively Dominate CD8 T-Cell Memory in the H-2d Haplotype. Journal of Virology 76 (1): 151–64

Hraber, P., Kuiken, C., and Yusim, K. (2007) Evidence for Human Leukocyte Antigen Heterozygote Advantage against Hepatitis C Virus Infection. Hepatology 46 (6): 1713–21

Hsu, L.Y. *et al.* (2017) Destabilizing the Autoinhibitory Conformation of Zap70 Induces Up-Regulation of Inhibitory Receptors and T Cell Unresponsiveness. The Journal of Experimental Medicine 214 (3): 833–49

Huseby, E.S. *et al.* (2006) Interface-Disrupting Amino Acids Establish Specificity between T Cell Receptors and Complexes of Major Histocompatibility Complex and Peptide. Nature Immunology 7 (11): 1191–99

Huseby, E.S. *et al.* (2005) How the T Cell Repertoire Becomes Peptide and MHC Specific. Cell 122 (2): 247–60

Jenkins, M.K. and Moon, J.J. (2015) The Role of Naive T Cell Precursor Frequency and Recruitment in Dictating Immune Response Magnitude. Journal of Immunology, 188 (9): 4135–40

Karrer, U. *et al.* (2003) Memory Inflation: Continuous Accumulation of Antiviral CD8+ T Cells Over Time. The Journal of Immunology 170 (4): 2022–29

Kim, A.Y. *et al.* (2011) Spontaneous Control of HCV Is Associated with Expression of HLA-B *57 and Preservation of Targeted Epitopes. Gastroenterology 140 (2): 686-696

Kim, S-K. and Boothroyd, J.C. (2005) Stage-Specific Expression of Surface Antigens by Toxoplasma Gondii as a Mechanism to Facilitate Parasite Persistence. The Journal of Immunology 174 (12): 8038–48

Košmrlj, A. *et al.* (2010) Effects of Thymic Selection of the T Cell Repertoire on HLA-Class I Associated Control of HIV Infection. Nature 465 (7296): 350–54

Kumar, S. and Tarleton, R.L. (2001) Antigen-Specific Th1 But Not Th2 Cells Provide Protection from Lethal Trypanosoma Cruzi Infection in Mice. The Journal of Immunology 166 (7): 4596–4603

Lie, W.R. *et al.* (1991) The Specific Binding of Peptide Ligand to Ld Class I Major

Histocompatibility Complex Molecules Determines Their Antigenic Structure. Journal of Experimental Medicine 173 (2): 449–59.

Lopez, J. *et al.* (2015) Intravacuolar Membranes Regulate CD8 T Cell Recognition of Membrane-Bound *Toxoplasma Gondii* Protective Antigen. Cell Reports, 2273–86

Mandl, J.N. *et al.* (2013) T Cell-Positive Selection Uses Self-Ligand Binding Strength to Optimize Repertoire Recognition of Foreign Antigens. Immunity 38 (2): 263–74

McDonald, B.D. *et al.* (2015) Crossreactive Aβ T Cell Receptors Are the Predominant Targets of Thymocyte Negative Selection. Immunity 43 (5): 859–69

Miyakoda, M. *et al.* (2012) Development of Memory CD8 + T Cells and Their Recall Responses during Blood-Stage Infection with Plasmodium Berghei ANKA. The Journal of Immunology 189 (9): 4396–4404

Modzelewski, A.J. *et al.* (2018) Efficient Mouse Genome Engineering by CRISPR-EZ Technology. Nature Protocols 13 (6): 1253–74

Moran, A.E. *et al.* (2011) T Cell Receptor Signal Strength in Treg and INKT Cell Development Demonstrated by a Novel Fluorescent Reporter Mouse. Journal of Experimental Medicine 208 (6): 1279–89

Narayanan, S. and Kranz, DM. (2013) The Same Major Histocompatibility Complex Polymorphism Involved in Control of HIV Influences Peptide Binding in the Mouse H-2L^{d} System. Journal of Biological Chemistry 288 (44): 31784–94

Pahl-Seibert, M.-F. *et al.* (2005) Highly Protective In Vivo Function of Cytomegalovirus IE1 Epitope-Specific Memory CD8 T Cells Purified by T-Cell Receptor-Based Cell Sorting. Journal of Virology 79 (9): 5400–5413

Pereyra, F. *et al.* (2010) The Major Genetic Determinants of HIV-1 Control Affect HLA Class I Peptide Presentation. Science 330 (6010): 1551–57

Persaud, S.P. *et al.* (2014) Intrinsic CD4+ T Cell Sensitivity and Response to a Pathogen Are Set and Sustained by Avidity for Thymic and Peripheral Complexes of Self Peptide and MHC. Nature Immunology 15 (3): 266–74

Pope, C. *et al.* (2001) Organ-Specific Regulation of the CD8 T Cell Response to Listeria Monocytogenes Infection. The Journal of Immunology 166 (5): 3402–9

Potter, T.A. *et al.* (1981) Flow Microfluorometric Analysis of H-2L Expression. Journal of Immunology 127 (2): 580–84

Radford, K.J. *et al.* (2002) A Recombinant E. Coli Vaccine to Promote MHC Class I-Dependent Antigen Presentation: Application to Cancer Immunotherapy. Gene Therapy 9

(21): 1455–63

Rosette, C. *et al.* (2001) The Impact of Duration versus Extent of TCR Occupancy on T Cell Activation. Immunity 15 (1): 59–70

Schaeffer, M. *et al.* (2009) Dynamic Imaging of T Cell-Parasite Interactions in the Brains of Mice Chronically Infected with *Toxoplasma Gondii*. Journal of Immunology, 182: 6379–93

Schneidewind, A. *et al.* (2008) Structural and Functional Constraints Limit Options for Cytotoxic T-Lymphocyte Escape in the Immunodominant HLA-B27-Restricted Epitope in Human Immunodeficiency Virus Type 1 Capsid. Journal of Virology 82 (11): 5594–5605

Smith, L.M. *et al.* (2008) Laboratory Strains of Murine Cytomegalovirus Are Genetically Similar to but Phenotypically Distinct from Wild Strains of Virus. Journal of Virology 82 (13): 6689–96

Smith, R.A. *et al.* (2002) Polymorphism at Position 97 in MHC Class I Molecules Affects Peptide Specificity, Cell Surface Stability, and Affinity for Beta2-Microglobulin. Journal of Immunology, 169 (6): 3105–11

Torti, N. *et al.* (2011) Non-Hematopoietic Cells in Lymph Nodes Drive Memory CD8 t Cell Inflation during Murine Cytomegalovirus Infection. PLoS Pathogens 7 (10)

Tscharke, D.C. *et al.* (2015) Sizing up the Key Determinants of the CD8+ T Cell Response. Nature Reviews Immunology 15 (11): 705–16

Tsitsiklis, A., Bangs, D.J. and Robey, E.A. (2019) CD8+ T Cell Responses to Toxoplasma Gondii: Lessons from a Successful Parasite. Trends in Parasitology 35 (11): 887–98

Weber, K.S. *et al.* (2012) Distinct CD4+ Helper T Cells Involved in Primary and Secondary Responses to Infection. Proceedings of the National Academy of Sciences of the United States of America 109 (24): 9511–16

Wherry, E.J. and Kurachi, M. (2015) Molecular and Cellular Insights into T Cell Exhaustion. Nature Reviews Immunology 15 (8): 486–99

Yarzabek, B. *et al.* (2018) Variations in HLA-B Cell Surface Expression, Half-Life and Extracellular Antigen Receptivity. Elife 7: e34961

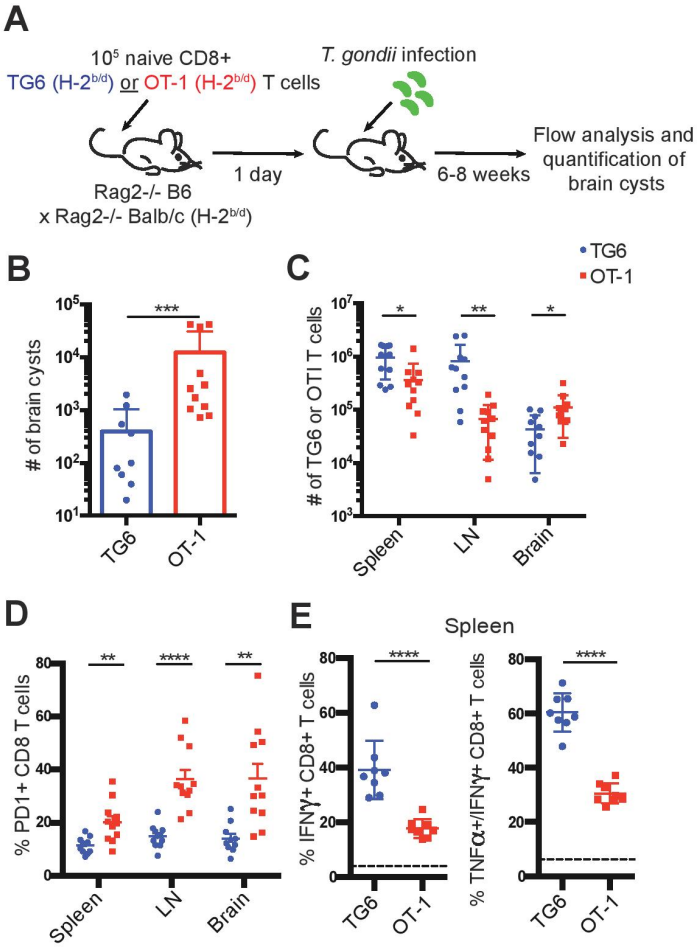

Figure 3.1: TG6 T cells are more protective and resistant to exhaustion compared to OT-1 T cells.

(A) Experimental design to compare the protective capacity of TG6 or OT-1 T cells. B6 Rag2-/- x BALB/c Rag2-/- mice were injected intravenously (i.v.) with 10^5 naïve CD8+ T cells from TG6 (n=11) or OT-1 (n=11) TCR transgenic mice, infected one day later with 2,000 *T. gondii* Pru-OVA parasites, and analyzed at 6-8 weeks post infection. **(B)** Number of brain cysts in mice transferred with TG6 (avg. 397 cysts) or OT-1 (avg. 12,453 cysts) CD8+ T cells. **(C)** Numbers of TG6 or OT-1 T cells recovered in the spleen, lymph nodes and brain determined by flow cytometry. **(D)** Frequency of PD1 expression on TG6 or OT-1 CD8+ T cells. **(E)** Production of IFNγ and TNFα cytokines by TG6 or OT-1 CD8+ T cells isolated from the spleen (n=8). Splenocytes were stimulated *ex vivo* with the HF10 (GRA6) or SIINFEKL (OVA) peptides in culture for 3 hours, and cells were analyzed for cytokine production by flow cytometry. Values indicate the percentage of IFNγ+ CD8+ T cells (left) or the percentage of TNFα producing cells among the IFNγ+ CD8+ T cells (right), following stimulation with peptide. Dotted line indicates background cytokine staining in un-stimulated cells from the same mice. Graphs show the summary of two independent experiments. Statistical significance was measured by a Mann-Whitney test in (B) and a t-test in (C)-(E) (*p<0.05, **p<0.01, ***p<0.001, and ****p<0.0001).

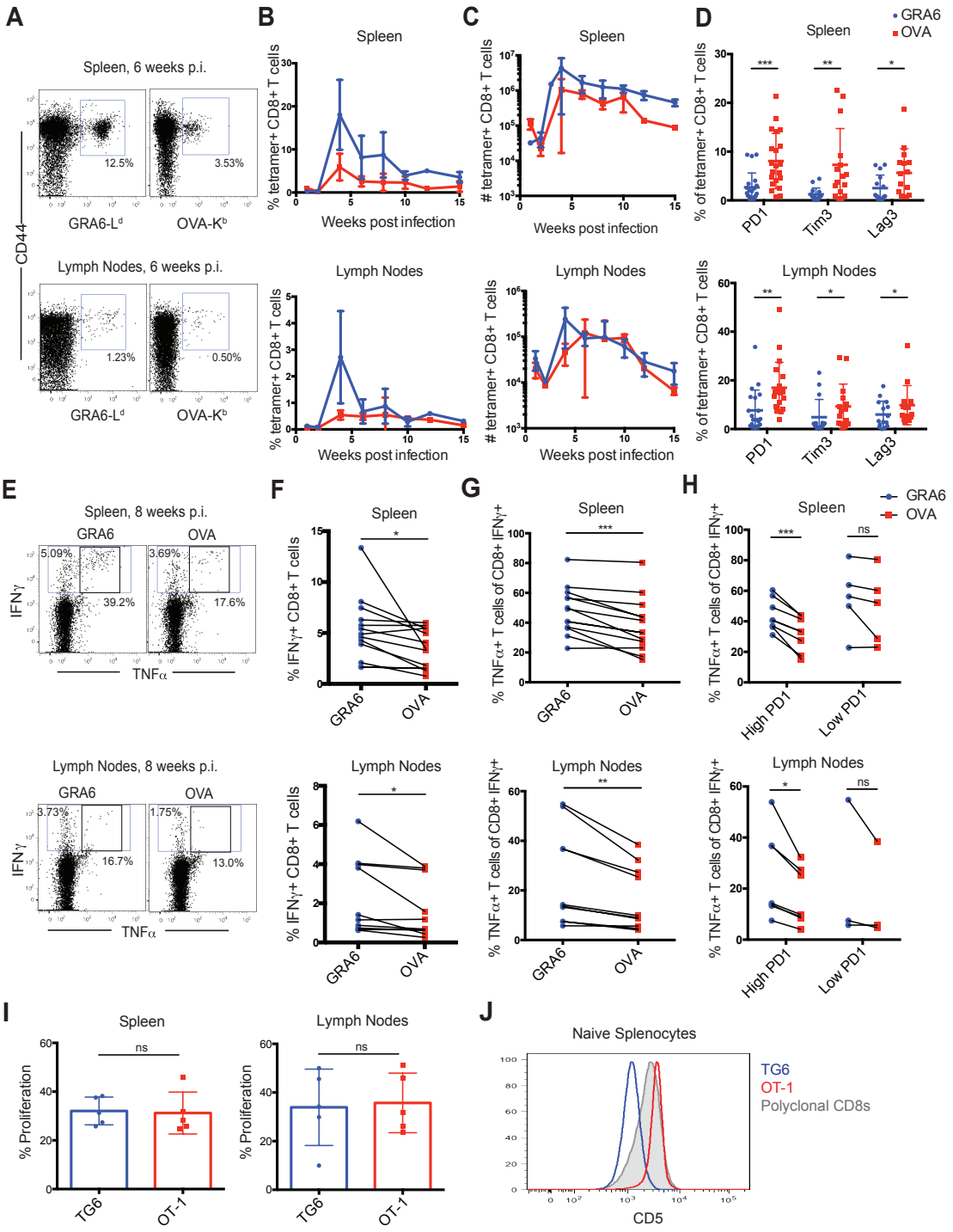
A
Spleen, 6 weeks p.i.
12.5%
3.53%
GRA6-L^d
OVA-K^b
CD44
Lymph Nodes, 6 weeks p.i.
1.23%
0.50%
GRA6-L^d
OVA-K^b
B
Spleen
% tetramer+ CD8+ T cells
Weeks post infection
Lymph Nodes
% tetramer+ CD8+ T cells
Weeks post infection
C
Spleen
tetramer+ CD8+ T cells
Weeks post infection
Lymph Nodes
tetramer+ CD8+ T cells
Weeks post infection
D
Spleen
GRA6
OVA
% of tetramer+ CD8+ T cells
PD1
Tim3
Lag3
Lymph Nodes
% of tetramer+ CD8+ T cells
PD1
Tim3
Lag3
E
Spleen, 8 weeks p.i.
GRA6
OVA
5.09%
39.2%
3.69%
17.6%
IFNγ
TNFα
Lymph Nodes, 8 weeks p.i.
GRA6
OVA
3.73%
16.7%
1.75%
13.0%
IFNγ
TNFα
F
Spleen
% IFNγ+ CD8+ T cells
GRA6
OVA
Lymph Nodes
% IFNγ+ CD8+ T cells
GRA6
OVA
G
Spleen
% TNFα+ T cells of CD8+ IFNγ+
GRA6
OVA
Lymph Nodes
% TNFα+ T cells of CD8+ IFNγ+
GRA6
OVA
H
Spleen
GRA6
OVA
% TNFα+ T cells of CD8+ IFNγ+
High PD1
Low PD1
Lymph Nodes
% TNFα+ T cells of CD8+ IFNγ+
High PD1
Low PD1
I
Spleen
% Proliferation
TG6
OT-1
Lymph Nodes
% Proliferation
TG6
OT-1
J
Naive Splenocytes
TG6
OT-1
Polyclonal CD8s
CD5

Figure 3.2: The OVA-K^b specific CD8+ T cell response to *T. gondii* infection shows signs of functional exhaustion.

(A-H) H-2$^{b/d}$ mice were infected intra-peritoneally (i.p.) with 10^5 *T. gondii* Pru-OVA parasites and were sacrificed during the chronic infection (3-15 weeks). **(A)** Representative flow cytometry plots gated on live, singlet, CD8+ T cells and **(B)** compiled data showing percentage and **(C)** absolute numbers of GRA6-L^d (blue) and OVA-K^b (red) tetramer+ CD8+ T cells from the spleens and lymph nodes of infected mice. Graphs in (B)-(C) represent a total of 2-6 mice at each time point (n=26 (spleen), n=22 (lymph nodes)), and graphs display mean values with error bars depicting the SEM. **(D)** Expression of T cell exhaustion markers PD1, Tim3 and Lag3 on GRA6-L^d and OVA-K^b tetramer+ CD8+ T cells in the spleen and lymph nodes (n=21 (PD1), n=15 (Tim3/Lag3). **(E-H)** Production of IFNγ and TNFα cytokines by GRA6-L^d or OVA-K^b specific T cells isolated from the spleens (n=13) or lymph nodes (n=10) of infected mice. Splenocytes or lymph node cells were stimulated *ex vivo* with the HF10 (GRA6) or SIINFEKL (OVA) peptides at 1μM in culture for 3 hours, and cells were analyzed for cytokine production by flow cytometry. **(E)** Representative flow cytometry plots of IFNγ and TNFα in CD8+ T cells from the spleen or lymph node. Compiled data showing the percentage of IFNγ+ cells among CD8+ T cells **(F)**, or the percentage of TNFα producing cells among the IFNγ+ CD8+ T cells in the spleen and lymph nodes **(G)**. **(H)** Data shown in (G) are separated based on PD1 expression in each mouse, with "high PD1" defined as >5% PD1+ in GRA6-L^d or OVA-K^b CD8+ T cells. Data points from the same animal are indicated by connecting lines. Graphs in (D) and (F-H) are the summary of >5 independent experiments, with data from all chronic time points (3-15 weeks) graphed together. **(I)** GRA6 and OVA antigen presentation in the spleens and lymph nodes of mice infected with *T. gondii* Pru-OVA. H-2$^{b/d}$ mice were infected i.p. with 10^5 *T. gondii* Pru-OVA parasites. At 6 weeks post infection, mice were injected i.v. with naïve CFSE-labeled splenocytes consisting of 10^6 TG6 and 10^6 OT-1 CD8+ T cells and analyzed by flow cytometry 2 days post T cell transfer. Transferred T cells were distinguished by a congenic marker together with Vβ2 (TG6) or Vβ5 (OT-1). Proliferation of TG6 and OT-1 CD8+ T cells was assessed by dilution of CFSE in the spleen and lymph nodes. Values are the percent proliferated cells out of the transferred T cell population. Graphs in (I) show data from one independent experiment (n=5), representative of 5 independent experiments (see Supplemental Figure 3A). **(J)** CD5 expression on splenic CD8+ T cells from TG6 (blue) and OT-1 (red) TCR transgenic mice. CD5 expression on polyclonal CD8+ T cells is shown for comparison (grey). Histogram is representative of >5 independent experiments. Statistical significance was measured by a t-test in (D, I) and a paired t-test in (F-H) with data from the same mouse paired (*$p<0.05$, **$p<0.01$, and ***$p<0.001$, ns is not significant).

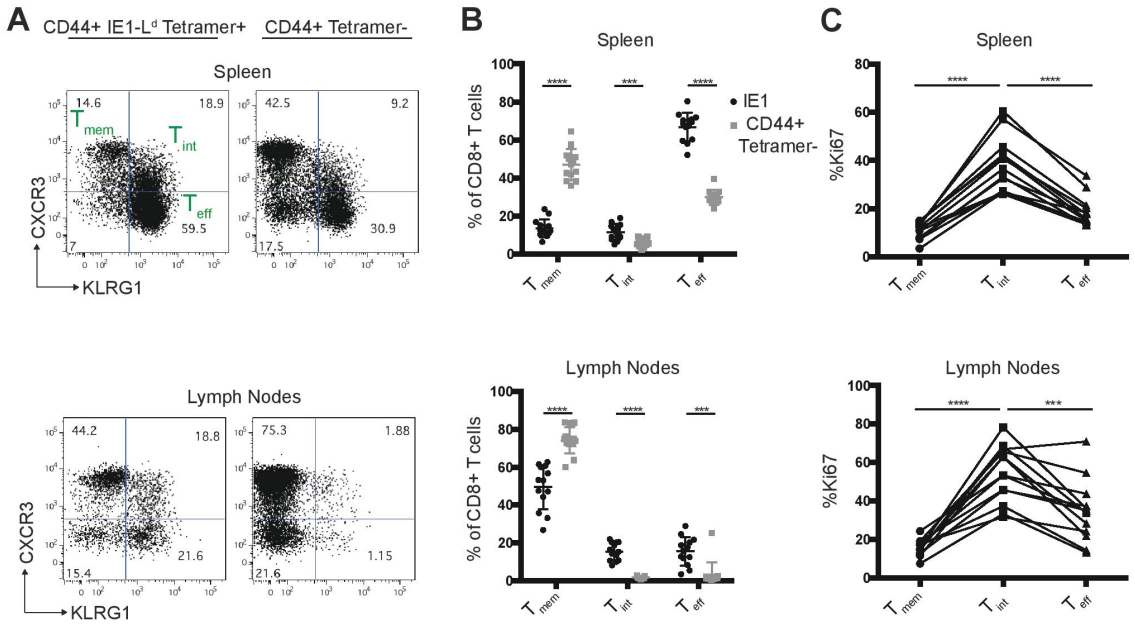

Figure 3.3: The L^d-restricted MCMV IE1 response has a proliferative intermediate population.

H-$2^{d/d}$ mice were infected i.p. with 10^6 pfu MCMV and cells from the spleens and lymph nodes were analyzed by flow cytometry 11-16 weeks post infection. **(A)** Representative flow cytometry plots show CXCR3 and KLRG-1 expression within CD44+ IE1-L^d and CD44+ tetramer- CD8+ T cells in the spleens and lymph nodes of MCMV infected mice. **(B)** Percentage of CXCR3+KLRG1- (T_{mem}), CXCR3+KLRG-1+ (T_{int}), and CXCR3-KLRG-1+ (T_{eff}) cells within IE1-L^d (black) and CD44+ tetramer- (grey) CD8+ T cells. **(C)** Percentage of Ki67+ cells within the indicated subset defined by CXCR3 and KLRG-1 expression in IE1-L^d CD8+ cells in the spleens and lymph nodes. Data points from the same animal are indicated by connecting lines. Graphs are the summary of 3 independent experiments (n=13). Statistical significance was determined by a t-test in (B) and a one-way ANOVA in (C) (*$p<0.05$, **$p<0.01$, ***$p<0.001$, and ****$p<0.0001$).

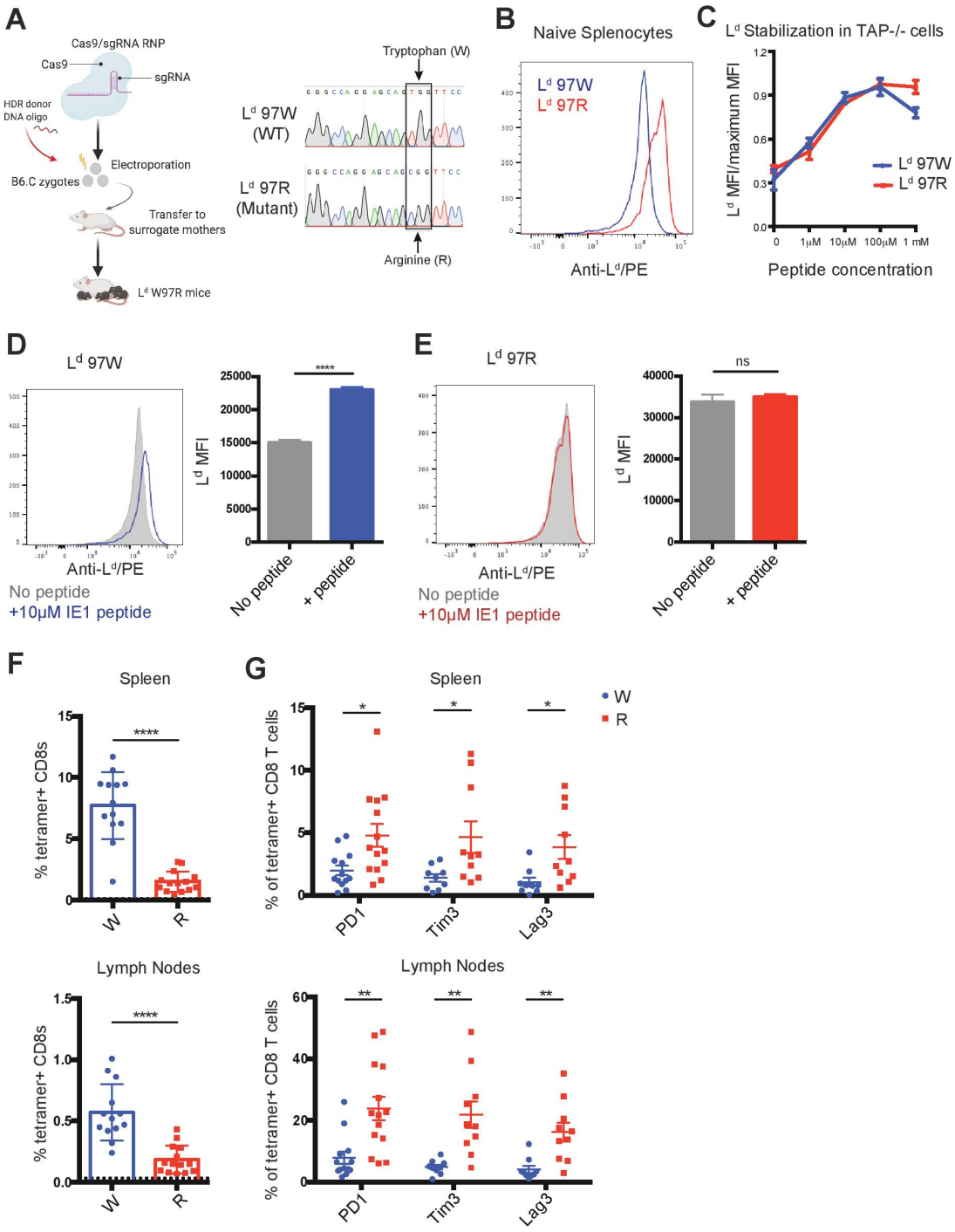
A
Cas9/sgRNA RNP
Cas9
sgRNA
HDR donor DNA oligo
Electroporation
B6.C zygotes
Transfer to surrogate mothers
Ld W97R mice
Tryptophan (W)
Ld 97W (WT)
Ld 97R (Mutant)
Arginine (R)
B
Naive Splenocytes
Ld 97W
Ld 97R
Anti-Ld/PE
C
Ld Stabilization in TAP-/- cells
Ld MFI/maximum MFI
Ld 97W
Ld 97R
0 1μM 10μM 100μM 1 mM
Peptide concentration
D
Ld 97W
Anti-Ld/PE
No peptide
+10μM IE1 peptide
Ld MFI
****
No peptide
+ peptide
E
Ld 97R
Anti-Ld/PE
No peptide
+10μM IE1 peptide
Ld MFI
ns
No peptide
+ peptide
F
Spleen
% tetramer+ CD8s
****
W
R
Lymph Nodes
% tetramer+ CD8s
****
W
R
G
Spleen
% of tetramer+ CD8 T cells
*
*
*
PD1
Tim3
Lag3
W
R
Lymph Nodes
% of tetramer+ CD8 T cells
**
**
**
PD1
Tim3
Lag3

Figure 3.4: Polymorphism in H2-L^d increases self-peptide binding and correlates with increased expression of exhaustion markers on IE1-L^d specific CD8+ T cells.

(A) Generation of L^d W97R mutant mouse by CRISPR-EZ (Chen et al. 2016; Modzelewski et al. 2018). Cas9-sgRNA ribonucleoprotein (RNP) was prepared and incorporated together with the HDR donor DNA oligo and electroporated into mouse zygotes from H-2^d (B6.C) mice. A single T→C point mutation that converts a tryptophan (TGG) to arginine (CGG) at position 97 in the L^d gene was generated. Sequences show an example of a wild-type B6.C mouse compared to an L^d W97R mutant mouse generated by sequencing DNA from the tail. **(B)** Surface expression of H2-L^d on naïve splenocytes from L^d W97 (blue) or L^d R97 mice (red). H2-L^d surface expression was measured by flow cytometry using an antibody that binds peptide-bound L^d. Data is representative of 3 independent experiments. **(C)** IE1 peptide binding strength to H-2L^d. Binding strength was measured using the ability of peptide to stabilize surface L^d expression on the TAP deficient RMA-S cell line expressing either the WT (97W) or mutated (97R) version of H2-L^d. The mean fluorescent intensity (MFI) of peptide-bound H2-L^d was measured after incubating the cells with increasing concentrations of peptide for 3 hours. Graph shows representative data from 2 independent experiments. **(D-E)** Surface expression of H2-L^d on naïve splenocytes from L^d 97W (D) or L^d 97R (E) mice with (color) or without (grey) the addition of 10μM IE1 peptide. Experimental groups consisted of 3 samples, and data is representative of 2 independent experiments. **(F-G)** L^d 97W (n=13) or L^d 97R (n=14) mice were infected with 10^6 pfu MCMV and sacrificed at 11-16 weeks post infection. **(F)** IE1-L^d tetramer+ CD8+ T cells were quantified in the spleen and lymph nodes of infected mice. Dotted line indicates background IE1-L^d tetramer staining in CD4+ T cells. **(G)** Expression of exhaustion markers PD1, Tim3, and Lag3 on IE1-L^d tetramer+ CD8+ T cells in the spleen and lymph nodes in L^d 97W and 97R mice. Graphs are pooled data from 3 independent experiments. Statistical significance was determined by a t-test (*$p<0.05$, **$p<0.01$, and ****$p<0.0001$).

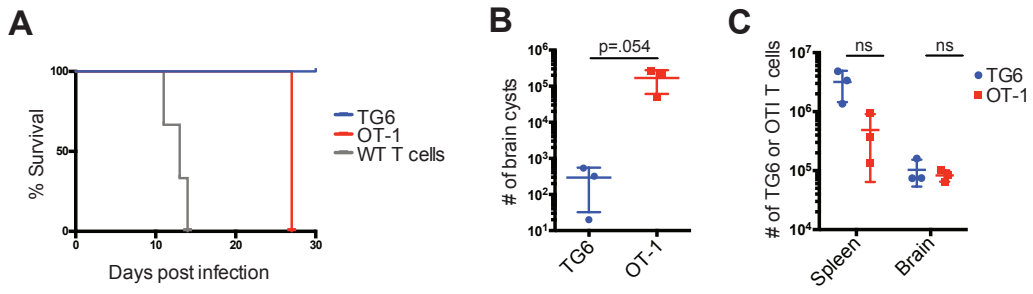

Supplementary Figure 3.1: TG6 T cells are more protective compared to OT-1 T cells.

B6 Rag2-/- x BALB/C Rag2-/- (H-$2^{b/d}$) mice were injected i.v. with 10^6 naïve TG6 Rag2-/- (n=6), OT-1 Rag2-/- (n=3) or wild type B6xBALB/c (n=3) splenocytes. The next day, mice were infected i.p. with 2,000 *T. gondii* Pru-OVA parasites, and then monitored for signs of illness and analyzed at day 27 post infection. **(A)** Survival curve indicating when mice were sacrificed due to illness. TG6 transferred mice remained healthy and were sacrificed together with OT-1 transferred mice for analysis. Survival of OT-1 transferred mice was significantly different from TG6 transferred mice (p=0.0047). **(B)** The number of brain cysts measured at 27 days post infection. **(C)** Numbers of TG6 or OT-1 CD8+ T cells recovered from the spleen and brain of recipient mice as measured by flow cytometry. Statistical significance was determined by a Gehan-Breslow-Wilcoxon test in (A), and a t-test in (B) and (C) (*p<0.05, **p<0.01, ns is not significant).

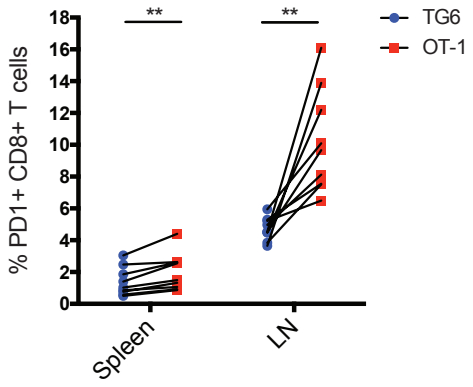

Supplementary Figure 3.2: OT-1 T cells express higher levels of PD1 after infection.

H-$2^{b/d}$ mice were injected i.v. with splenocytes consisting of 10^6 TG6 and 10^6 OT-1 CD8+ T cells from TCR transgenic mice. Mice were infected i.p. with 10^5 OVA-expressing *T. gondii* parasites the next day. Expression of PD1 on TG6 or OT-1 CD8+ T cells in the spleen and lymph nodes was quantified 6-12 weeks post infection (n=9). Data points from the same mouse are indicated by connecting lines. Statistical significance was determined by a paired t-test, with data from the same mouse paired (**$p<0.01$).

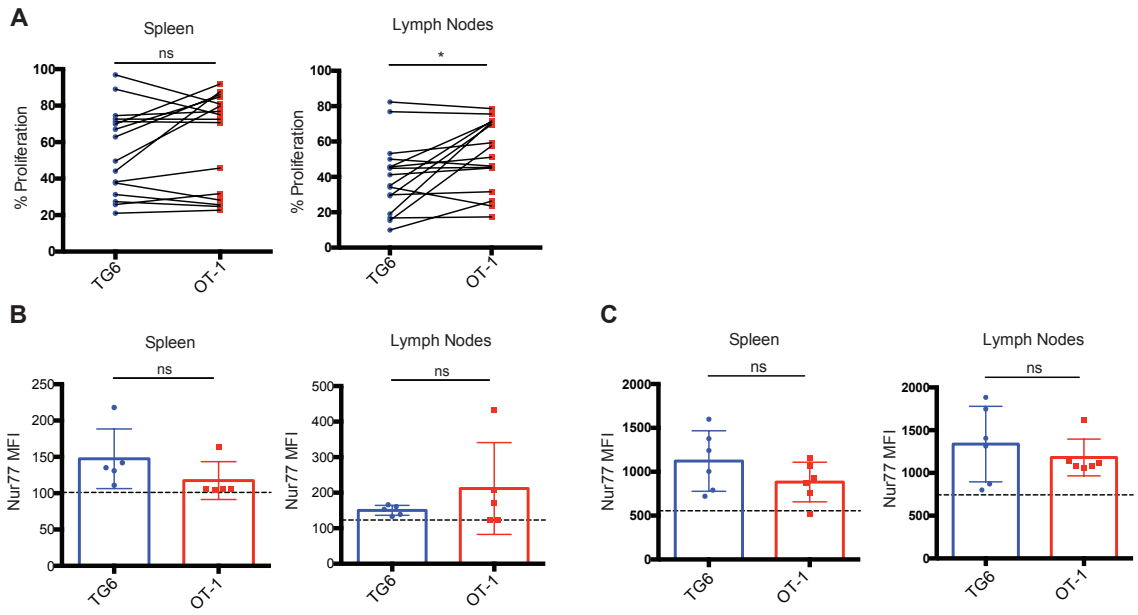

Supplementary Figure 3.3: TG6 and OT-1 T cells experience similar levels of antigenic stimulation after transfer to infected mice.

H-$2^{b/d}$ mice were infected i.p. with 10^5 *T. gondii* Pru-OVA parasites. At 3-8 weeks post infection, mice were injected i.v. with naïve CFSE-labeled splenocytes consisting of 10^6 TG6 and 10^6 OT-1 CD8+ T cells and analyzed by flow cytometry 2 or 3 days post T cell transfer. Transferred T cells were distinguished by a congenic marker, as well as either Vβ2 (for TG6) or Vβ5 (for OT-1). **(A)** Proliferation of TG6 and OT-1 CD8+ T cells was assessed by dilution of CFSE in the spleen and lymph nodes. Values are the percent proliferated cells out of the transferred T cell population. Graphs in A show compiled data from 5 independent experiments: 4 at day 3 post transfer and 1 at day 2 post transfer (n=16). This includes data shown in Figure 2I. Data points from the same mouse are indicated by connecting lines **(B-C)** Graphs show mean fluorescence intensity (MFI) of intracellular Nur77 on CD44+ TG6 and CD44+ OT-1 CD8+ T cells in the spleen and lymph nodes at day 2 (B) or day 3 (C) post transfer. Dotted line indicates Nur77 expression in CD44- CD8+ cells from the same samples. Data in (B) are from 1 independent experiment (n=5), and data in (C) are compiled from 2 independent experiments (n=6). Statistical significance was measured by a paired t-test in (A) and an unpaired t-test in (B-C) (*$p<0.05$, ns is not significant).

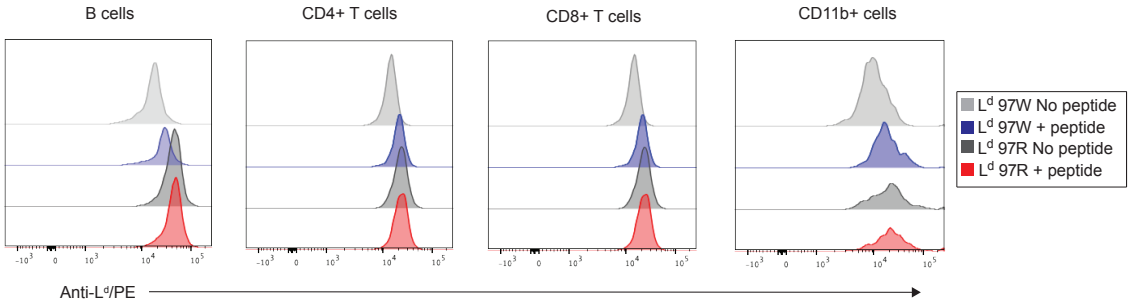

Supplementary Figure 3.4: H2-L^d expression in L^d 97W mice is stabilized by peptide in different cell types.

Surface expression of H2-L^d on **(A)** CD4+ T cells, **(B)** CD8+ T cells, **(C)** B cells, or **(D)** macrophages from splenocytes of L^d 97W or L^d 97R mice with or without the addition of 10μM IE1 peptide. Histograms are representative of 2 independent experiments.

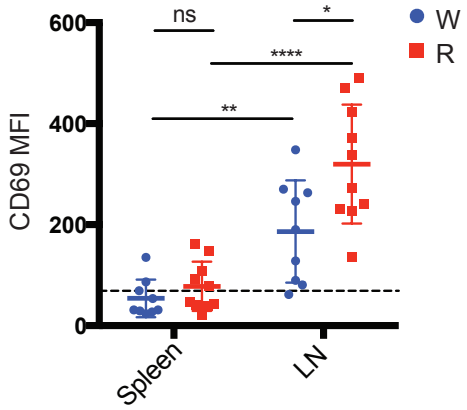

Supplementary Figure 3.5: IE1-L^d specific CD8+ T cells express higher levels of CD69 in the lymph nodes compared to the spleen in L^d 97W and L^d 97R mice.

L^d 97W or L^d 97R mice were infected with 10^6 Pfu MCMV and sacrificed at 11-16 weeks post infection. CD69 expression on IE1-L^d specific CD8+ T cells was quantified by flow cytometry. Dotted line indicates CD69 expression in CD44- CD8+ T cells in the same mice. Data is compiled from 2 independent experiments. Statistical significance was determined by a t-test (*p<0.05, **p<0.01, ***p<0.001, and ****p<0.0001, ns is not significant).

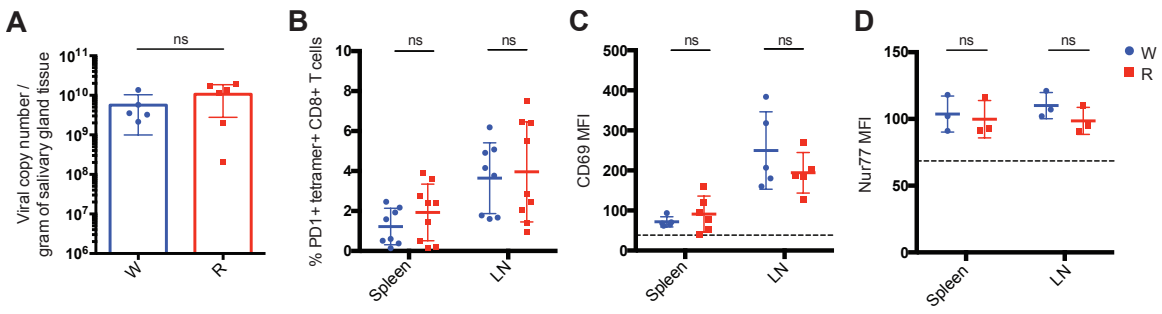

Supplementary Figure 3.6: Antigen levels are similar between L^d 97W and L^d 97R mice after MCMV infection.

L^d 97W or L^d 97R mice were infected with 10^6 Pfu MCMV and sacrificed at 11-16 weeks post infection. **(A)** MCMV viral copy number in the salivary glands of L^d 97W and L^d 97R mice 14 weeks post infection was quantified by qPCR. Expression of **(B)** PD1, **(C)** CD69, and **(D)** Nur77 on m164-D^d specific CD8+ T cells quantified by intracellular staining and flow cytometry. Dotted lines in (C-D) indicate CD69 or Nur77 expression in CD44- CD8+ T cells in the same mice. Statistical significance was determined by a t-test (*$p<0.05$, ns is not significant).

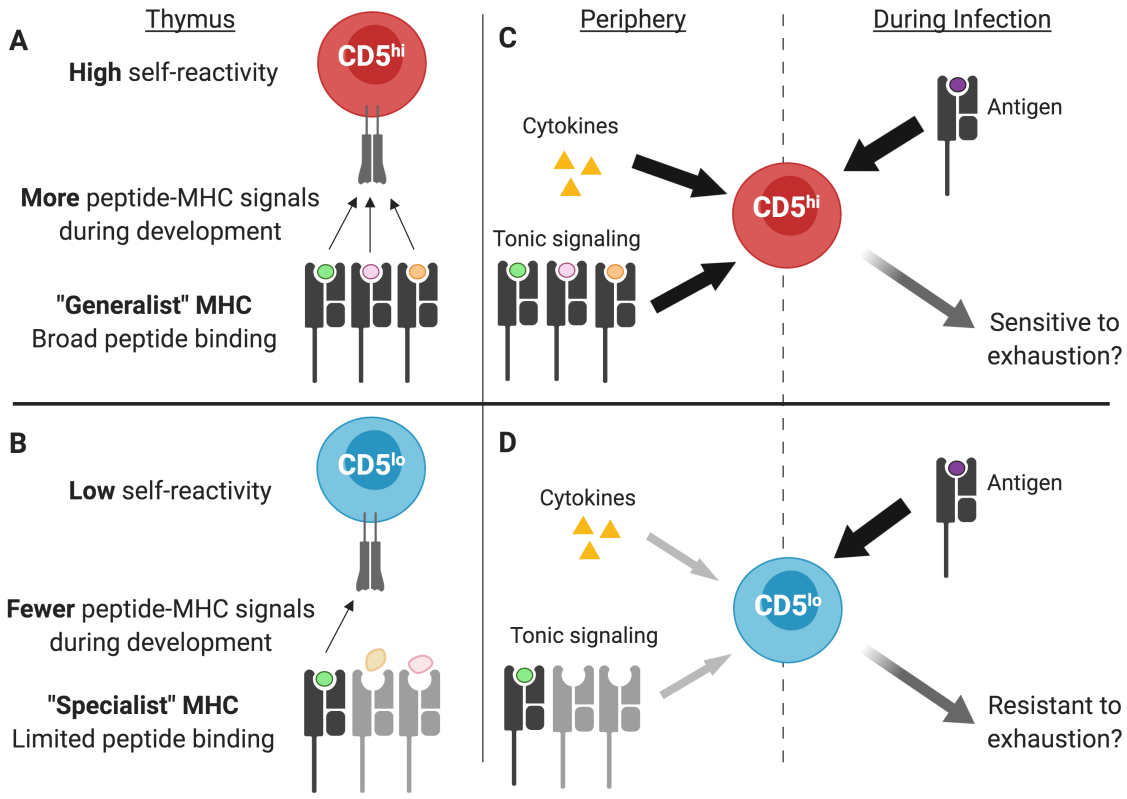

Supplementary Figure 3.7: Model for MHC-1 specialists and CD8+ elite control.

(A) MHC-1 generalists bind a large set of self-peptides allowing for positive selection of T cells with relatively high self-reactivity ($CD5^{high}$). **(B)** MHC-1 specialists display low and unstable surface expression due to poor binding of self-peptides, resulting in the positive selection of T cells with low self-reactivity ($CD5^{low}$). **(C)** CD8+ T cells with high self-reactivity are more responsive to cytokines and may experience greater TCR tonic signaling in the periphery, which may promote exhaustion during chronic infection. **(D)** In contrast, CD8+ T cells with low self-reactivity are less responsive to inflammatory environments and may receive lower tonic signals, allowing them to persist without becoming exhausted during chronic infection. Figure created with BioRender.

Chapter 4: Studying CD8+ T Cells with High or Low Self-Reactivity

4.1: Introduction

In Chapter 3 we demonstrated that T cells selected on a "specialist" MHC-1 molecule, L^d, may be better suited to provide protection against chronic infection, and speculated that this may be due to their relatively low self-reactivity. T cells sense and adjust to the level of self-reactivity they experience during development, and this tunes their functional response in the periphery. While CD8+ T cells with high self-reactivity have been shown to respond better during acute infections (Fulton et al. 2015), the function of CD8+ T cells with low self-reactivity has not been studied. We hypothesized that limited peptide binding by MHC-1 L^d selects T cells with low self-reactivity, and that CD8+ T cells with low-self reactivity are resistant to functional exhaustion in the context of a chronic infection. Our data from Chapter 3 support these hypotheses. Here we describe 4 different attempts to address specific aspects of these hypotheses.

4.2: Results and Discussion

4.2.1 Analysis of CD5 expression on naïve GRA6-L^d specific T cells and bulk T cells from different mouse strains

CD5 is a robust marker for self-reactivity on the surface of naïve T cells and has been used extensively to distinguish T cells with differing self-reactivity within bulk T cell populations as well as TCR transgenics (Azzam et al. 2001; Persaud et al. 2014; Fulton et al. 2015). We have shown that splenocytes from the GRA6-L^d specific TCR transgenic, TG6, have relatively low CD5 expression (Chapter 3), so we attempted to measure the CD5 expression on polyclonal GRA6-L^d specific T cells to determine if these cells also have relatively low self-reactivity. We pooled several naïve mice and performed tetramer enrichment in order to have sufficient tetramer+ cells to analyze. However, CD5 expression was not significantly different on GRA6-L^d specific T cells compared to bulk naïve T cells (Figure 4.1A). This may be because the naïve tetramer positive population does not accurately represent the T cells that respond to *T. gondii* infection. Not all tetramer positive cells are able to signal (Sibener et al. 2018) and we have observed a strong Vβ2 preference in expanded GRA6-L^d specific T cells after infection that is only slightly present in naïve tetramer positive cells (Chapter 2), indicating that only a small subset of the naïve population respond to infection.

Next we hypothesized that if L^d selects T cells with relatively low self-reactivity, CD5 expression on CD8+ T cells may be different in mouse strains with and without L^d. Therefore, we measured CD5 expression on naïve CD8+ T cells from B6 (H-2^b), B6.C (H-2^d) and B6.C L^d W97R mice (Chapter 3). However, CD5 levels did not differ based on the presence of the L^d MHC molecule (Figure 4.1B-C).

4.2.2 *In vitro* and *in vivo* assays to compare self-reactivity of TG6 and OT-1 CD8+ T cells

We have observed that CD5 levels on CD8+ T cells change after stimulation (data not shown), so CD5 is no longer a reliable marker of self-reactivity after T cell activation. Therefore, we aimed to find a measure other than CD5 that correlates with self-reactivity and would retain a correlation after antigen stimulation, so that we could determine self-reactivity of polyclonal T cell populations after infection. To begin, we aimed to develop assays that could distinguish between T cells with high and low self-reactivity, using naïve T cells from the TG6 and OT-1 TCR transgenics as representative T cells with relatively low and high self-reactivity, respectively. We hoped to then use these assays on activated T cells as well as polyclonal T cell populations to measure their relative self-reactivity. To this end, we looked in the literature for phenotypes that have been shown to distinguish between T cells with high and low self-reactivity.

Palmer et al. 2011 showed that T cells with high self-reactivity proliferate more in the presence of IL7 but are unable to survive as well in its absence, compared with T cells with low self-reactivity. To reproduce these differences with our TCR transgenic T cells, we measured survival and proliferation of TG6 and OT-1 T cells with or without the addition of IL7 *in vitro*. We cultured splenocytes from naïve TG6 and OT-1 transgenic mice in media (+/- IL7) for 3 days. As expected, TG6 T cells survived better in culture without IL7 compared to OT-1 T cells (Figure 4.2A). Additionally, in the presence of IL7, both TG6 and OT-1 T cells survived well, and OT-1 T cells exhibited greater proliferation compared to TG6 T cells, as measured by CFSE dilution and Ki67 expression (Figure 4.2B-C).

Next we attempted to extend these observations to activated T cells. To this end, we transferred TG6 and OT-1 T cells to naïve $F1^{b/d}$ mice prior to immunization with GRA6 and OVA peptides. Two weeks post immunization we performed the same *in vitro* assays. However, the differences we observed with the naïve T cells were no longer apparent: survival and proliferation were equal between TG6 and OT-1 T cells (Figure 4.3A-B). We thought the cells might need to rest after the immunization before these phenotypes could be seen, so we tried to perform the same experiments 4, 6, and 8 weeks post immunization. However, at these later time-points, the numbers of TG6 and OT-1 T cells recovered from the spleens of immunized mice were very low, and therefore the experiments were inconclusive. Further attempts to measure *in vitro* survival of endogenous GRA6-L^d tetramer+ CD8+ T cells were also inconclusive due to low cell numbers (data not shown).

Lastly, we wondered whether survival *in vivo* would distinguish our two T cell populations after antigen stimulation. We measured population size over time and proliferation by Ki67 expression in GRA6-L^d and OVA-K^b tetramer+ CD8+ T cells after peptide-DC immunization by bleeding a cohort of mice approximately every 5 days (Figure 4.4A-B). However, similar to the previous experiments, the tetramer+ populations were very small in the blood after immunization, so these experiments were also inconclusive. Therefore, we determined that survival and/or responsiveness to IL7

was not the appropriate measure for this purpose. In the end, we concluded that these experiments were not effective because we were not able to obtain a large enough population of tetramer+ T cells in these settings. It is significantly harder to track a small polyclonal antigen specific population compared to TCR transgenic T cells, which hindered the analysis of these experiments.

4.2.3 Transfer of CD5^{high} and CD5^{low} T cells to determine relative CD5 expression of polyclonal GRA6-L^{d} and OVA-K^{b} specific CD8+ T cells

Since CD5 is not a reliable marker of self-reactivity after antigen stimulation, we attempted to determine whether GRA6-L^{d} or OVA-K^{b} specific T cells were preferentially found in naïve CD5^{high} or CD5^{low} subsets by a sort and co-transfer experiment. We sorted the top 25% and bottom 25% on CD5 expression within CD62L+CD44- CD8+ T cells from naïve H-2$^{b/d}$ mice and co-transferred 1.8-2.4x10^{6} cells of each population into naïve H-2$^{b/d}$ F1 recipient mice, with congenic markers that would allow both transferred populations to be distinguished from the endogenous cells (Figure 4.5A). We then infected these mice with *T. gondii* or Listeria monocytogenes expressing both GRA6 and OVA the next day and sacrificed them 1-2 weeks later. We predicted that GRA6-L^{d} specific T cells would preferentially come from the CD5^{low} transferred population, while OVA-K^{b} specific T cells would emerge primarily from the CD5^{high} population. Tetramer staining revealed that while this was the case in several mice, there was a high level of mouse-to-mouse variability (Figure 4.5B-C), and unfortunately, we could not make any conclusions about the self-reactivity of these polyclonal T cell populations from this experiment. We hypothesize that this may be due to the fact that the precursor frequency of GRA6-L^{d} specific T cells is quite low, approximately 60 cells per mouse, which comes out to just 2 cells per million CD8+ T cells (assuming that a mouse spleen has approximately 3x10^{7} CD8+ T cells). Therefore, it is possible that with a transfer of 2x10^{6} CD8+ T cells, some mice may not have received any, or very few, GRA6-L^{d} specific T cells in the transfer. This experiment may be more successful with transfers of greater cell numbers, however this would require a large amount of mice to sort from, which would make the experiment technically challenging.

4.2.4 Analysis of activation and exhaustion of bulk CD5^{high} and CD5^{low} CD8+ T cells after infection

We also wondered whether we could make observations about the function of bulk CD8+ T cells with high and low CD5 expression in acute and chronic infection. We hypothesized that T cells with high and low self-reactivity have distinct functions during infection. Specifically, CD5^{high} T cells may be more responsive in acute infection, while CD5^{low} T cells may be able to avoid exhaustion and remain functional in a chronic infection. While we have shown these differences in certain antigen-specific populations (Chapter 3), we wondered whether these differences could also be observed in bulk CD5^{high} and CD5^{low} T cells.

To compare bulk CD5^{high} and CD5^{low} CD8+ T cells, we performed the same sort experiment described above, and looked at all CD8+ T cells after infection. In our first

attempt at this experiment, we transferred $CD5^{high}$ and $CD5^{low}$ T cells into RagKO recipient mice and waited several weeks to allow for the transferred cells to expand. Bleeding the recipient mice over time revealed that the $CD5^{high}$ T cells dominated, leading to a loss of the $CD5^{low}$ population (Figure 4.6). Therefore, we decided that a transfer into intact mice would be preferable for these experiments.

Next we transferred $CD5^{high}$ and $CD5^{low}$ T cells into $F1^{b/d}$ mice and infected them the following day with either Listeria monocytogenes or *T. gondii* expressing the GRA6 and OVA antigens. After infection, we tracked the T cell populations in the blood before sacrificing the mice and analyzing the spleen and lymph nodes. We sacrificed the listeria-infected mice at 1-week post infection for an acute time point, and sacrificed *T. gondii*-infected mice at either 2 weeks or 6-8 weeks post infection for acute and chronic time points. As expected, at 1 week post infection with listeria (data not shown) or 2 weeks post infection with *T. gondii* (Figure 4.7A-B), $CD5^{high}$ CD8+ T cells were more activated than $CD5^{low}$ cells, demonstrated by a higher percentage of CD44+ CD62L- CD8+ T cells within the transferred population in the spleen and lymph nodes. We expected to see that the $CD5^{low}$ CD8+ T cells were more active at chronic time points, however this was not the case. We observed a high level of mouse-to-mouse variation, but altogether we saw a trend towards higher activation for the $CD5^{high}$ T cells (Figure 4.7C). Additionally, PD1 expression was not significantly higher in $CD5^{high}$ T cells (Figure 4.7D). When this data was subdivided based on Ly5.1 or Ly5.2 expression, it became clear that the congenic marker was influencing the data. When either the $CD5^{high}$ or $CD5^{low}$ transferred cells were Ly5.1, they were more active and express more PD1 than the Ly5.2 population (data not shown). This was one factor that complicated the data and led us to determine that these experiments would not be successful.

Another potential problem with these experiments is that we did not have a way to detect only the *T. gondii*-specific activated cells. In the spleen and blood, most CD8+ T cells are CD44+, but not all of these cells are specific for *T. gondii* antigens. We predict that if we had a better way to identify the responding cells, the data may have been clearer. One potential solution to this problem would be to re-stimulate splenocytes *ex vivo* with *T. gondii*-infected APCs.

Additionally, it is likely that not all $CD5^{low}$ CD8+ cells are better during the chronic infection. Most $CD5^{low}$ T cells are likely cells with weak affinity for antigen and therefore will not respond as well during any stage of infection. We have identified a population of T cells with low self-reactivity (GRA6-L^d specific T cells) that are robust in the chronic infection, but this may be a rare situation in which low self-reactivity is combined with high affinity. Therefore, studies of bulk $CD5^{high}$ and $CD5^{low}$ T cells may not reveal the differences that we have predicted.

4.3: References

Azzam, H.S. *et al.* (2001) Fine Tuning of TCR Signaling by CD5. J. Immunol. 166 (9): 5464–72

Fulton, R.B. *et al.* (2015) The TCR's sensitivity to self peptide-MHC dictates the ability of naive CD8(+) T cells to respond to foreign antigens. Nat. Immunol. 16, 107–17

Palmer, M. *et al.* (2011) Signaling thresholds govern heterogeneity in IL-7-receptor-mediated responses of naïve CD8+ T cells. Immunology and Cell Biology 89, 581-594

Persaud, S.P. *et al.* (2014) Intrinsic CD4+ T Cell Sensitivity and Response to a Pathogen Are Set and Sustained by Avidity for Thymic and Peripheral Complexes of Self Peptide and MHC. Nature Immunology 15 (3): 266–74

Sibener, L. *et al.* (2018) Isolation of a Structural Mechanism for Uncoupling T Cell Receptor Signaling from Peptide-MHC Binding. Cell 174(3): 672-687

A

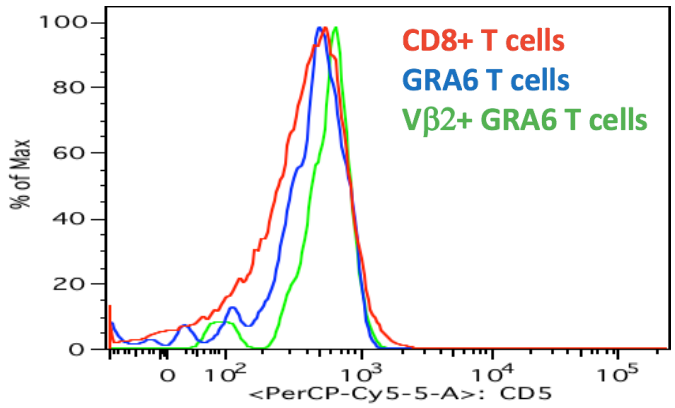

B Spleen C Thymus

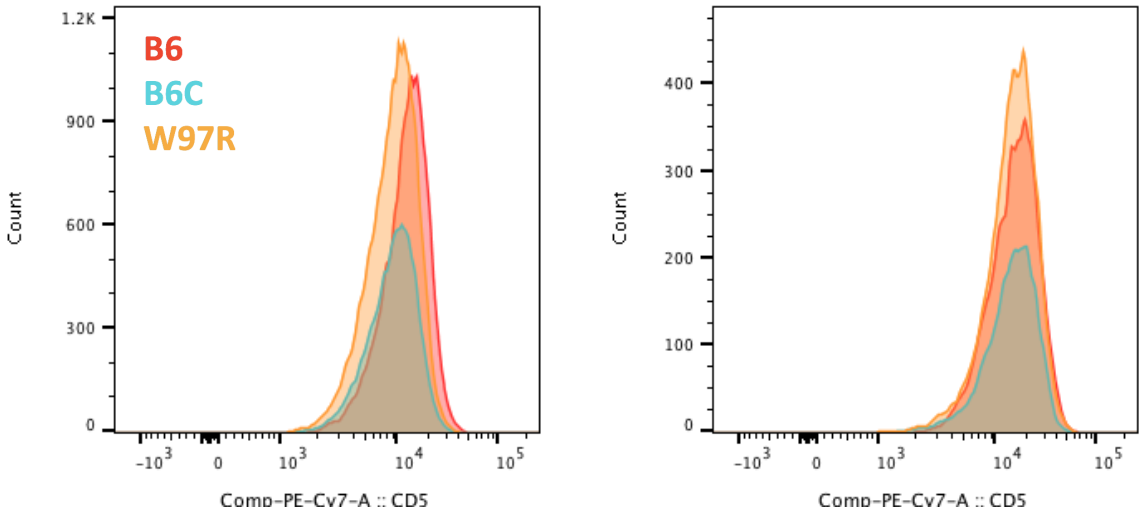

Figure 4.1: Analysis of CD5 expression on naïve GRA6-L^d specific T cells and bulk T cells from different mouse strains

(A) Splenocytes from 4 naïve B6.C mice were pooled and enriched for GRA6-L^d specific T cells by tetramer enrichment. CD5 expression was measured on tetramer+ CD8+ T cells, and Vβ2 specific tetramer+ CD8+ T cells. **(B-C)** CD5 expression on (B) splenocytes and (C) thymocytes from B6, B6.C and L^d W97R mice.

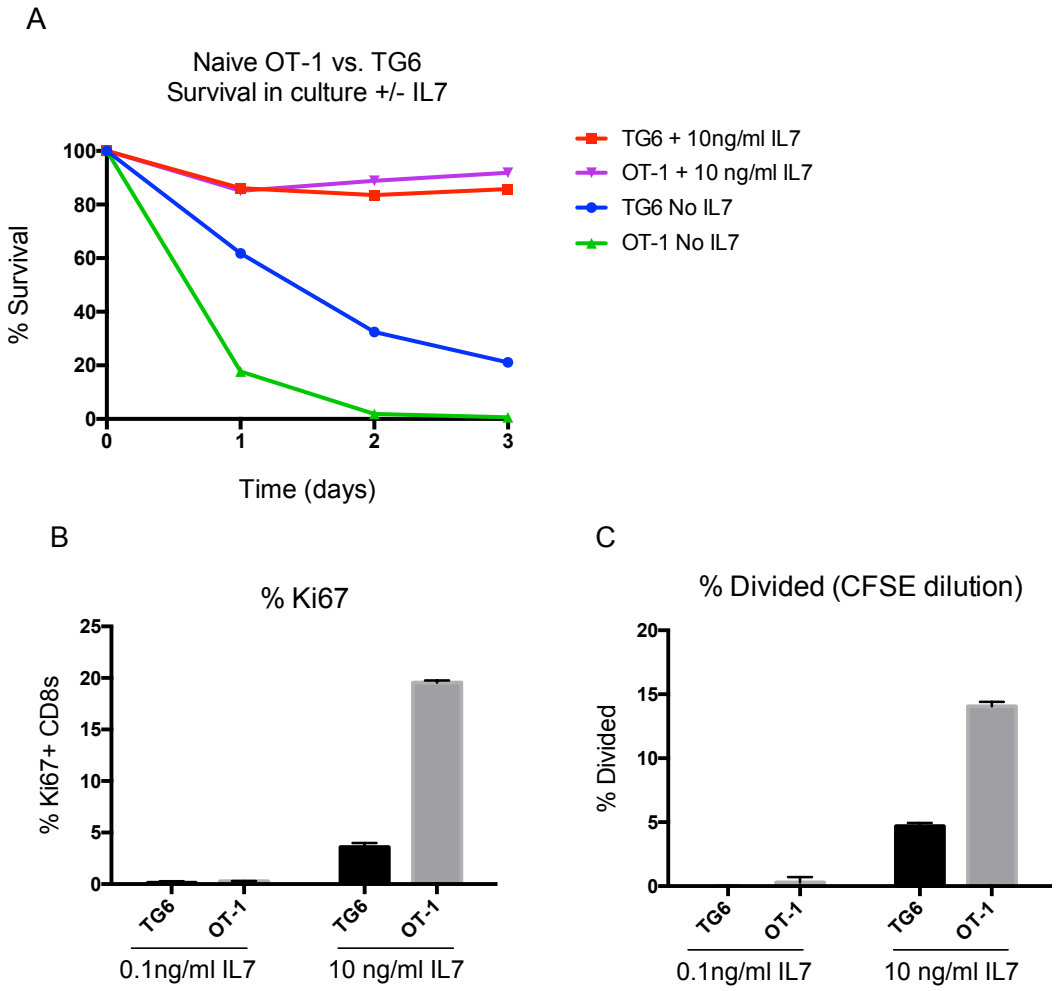

Figure 4.2: Survival and proliferation of naïve TG6 and OT-1 T cells *in vitro* with and without IL7.

Splenocytes from naïve TG6 or OT-1 mice were cultured *ex vivo* and IL7 was added at 10ng/ml at day 0. Cells were collected and analyzed by flow cytometry each day. **(A)** Survival was measured by staining with a live/dead dye. **(B)** Proliferation was measured by Ki67 expression at day 3. **(C)** At day 0, some cells were dyed with the proliferation dye CFSE, and added to separate wells. CFSE dilution was measured at day 3 as another measure of proliferation.

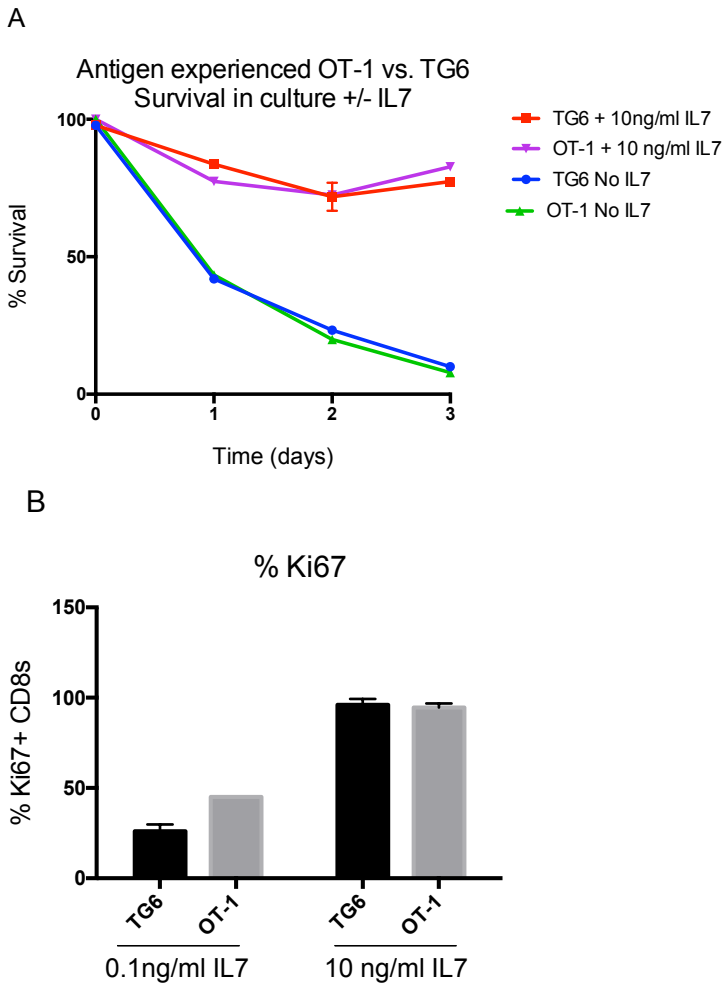

Figure 4.3: Survival and proliferation of antigen experienced TG6 and OT-1 T cells *in vitro* with and without IL7.

TG6 or OT-1 splenocytes from naïve mice were transferred into naïve $F1^{b/d}$ mice. Recipient mice were immunized with bone marrow derived dendritic cells loaded with 1μM of either the GRA6 or OVA peptide. Mice were sacrificed 1 week post immunization and splenocytes were cultured with or without IL7 for 3 days. **(A)** Survival was measured by staining with a live/dead dye. **(B)** Proliferation was measured by Ki67 expression at day 3.

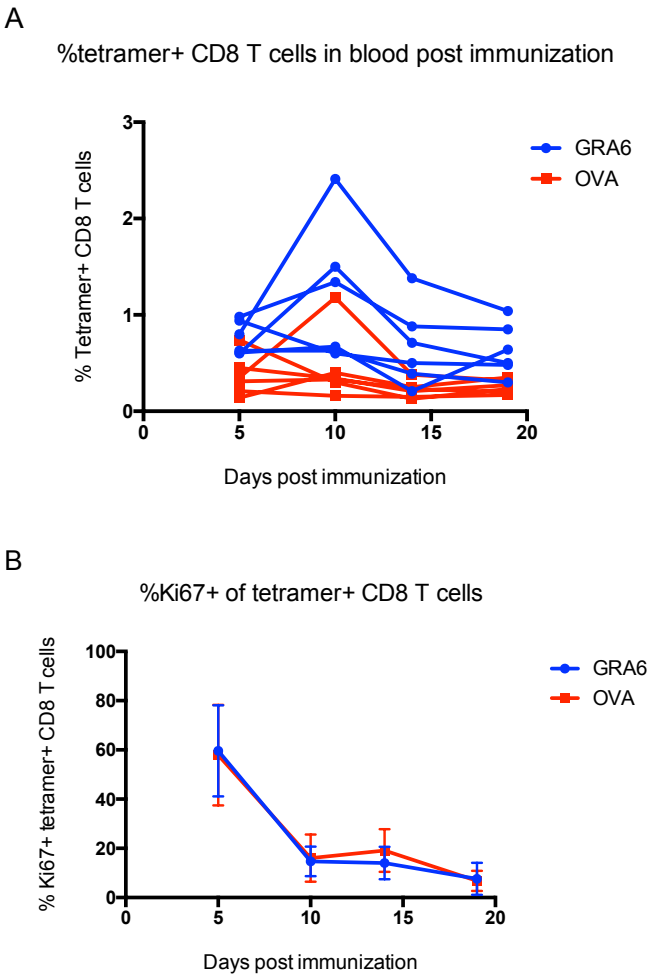

Figure 4.4: Tracking GRA6-L^{d} and OVA-K^{b} specific CD8+ T cell populations in the blood after peptide-DC immunization.

Bone marrow derived dendritic cells were loaded with 1μM GRA6 peptide or 1μM OVA peptide and mixed before immunization of B6xB6c F1 mice. Immunized mice were bled at indicated time points post immunization and cells were analyzed by flow cytometry. Size **(A)** and proliferation **(B)** of GRA6-L^{d} and OVA-K^{b} tetramer+ CD8+ T cell populations in blood of immunized mice over time.

A

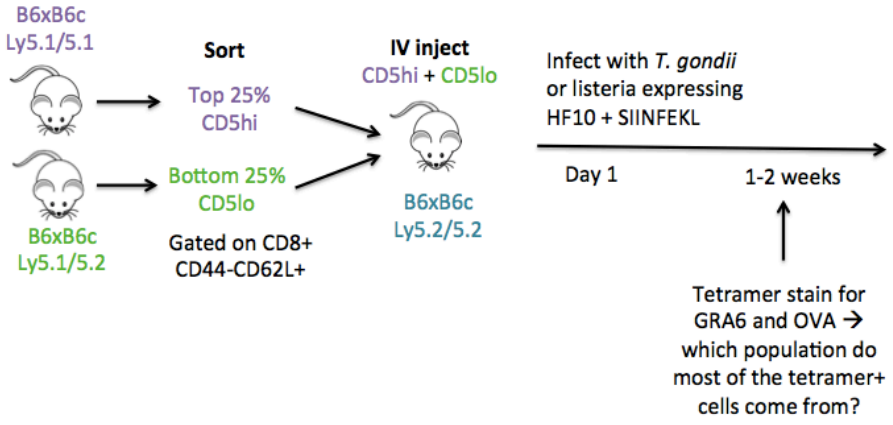

B

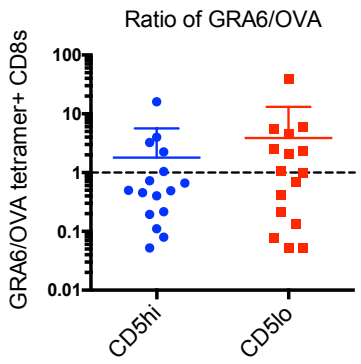

C

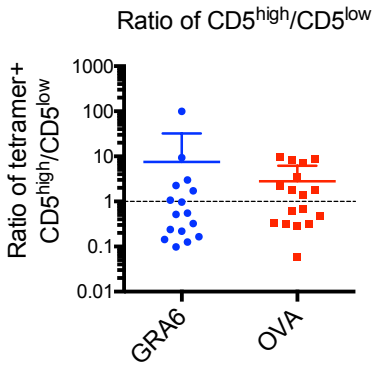

Figure 4.5: GRA6-L^{d} and OVA-K^{b} specific T cells in CD5^{high} or CD5^{low} CD8+ T cell transfer

CD62L+ **(A)** CD44- CD8+ T cells were sorted on CD5 expression from naïve F1$^{b/d}$ mice. The top 25% and bottom 25% of cells were collected and transferred into naïve F1$^{b/d}$ recipient mice with congenic markers to distinguish each population. The next day, mice were infected with *T. gondii* parasites or Listeria expressing both GRA6 and OVA. Mice were sacrificed two weeks post infection with *T. gondii* or 1 week post infection with Listeria. **(B-C)** Splenocytes were stained with GRA6 and OVA tetramers to determine the proportion of tetramer+ cells coming from each transferred population. (B) Data is represented as the ratio of GRA6-L^{d} tetramer+ CD8+ T cells/OVA-K^{b} tetramer+ CD8 T cells in either the CD5^{high} or CD5^{low} transferred population. (C) Data is represented as the ratio of tetramer+ CD8s in the CD5^{high} population/tetramer+ CD8s in the CD5^{low} population for either the GRA6-L^{d} or OVA-K^{b} specific T cells.

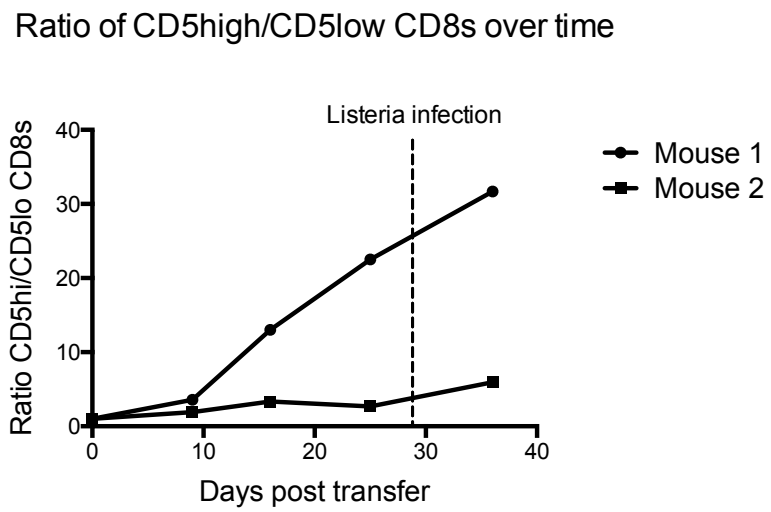

Figure 4.6: Ratio of CD5^{high} to CD5^{low} transferred CD8+ T cells in blood over time.

CD62L+ CD44- CD8+ T cells were sorted on CD5 expression from naïve F1$^{b/d}$ mice. The top 25% and bottom 25% of cells were collected and transferred into two naïve B6xBalb/c Rag2KO mice with congenic markers to distinguish each population. Mice were bled at various time points post infection and the ratio of CD5^{high} to CD5^{low} T cells present in the blood was tracked. The mice were infected with listeria expressing both GRA6 and OVA proteins at 28 days post transfer.

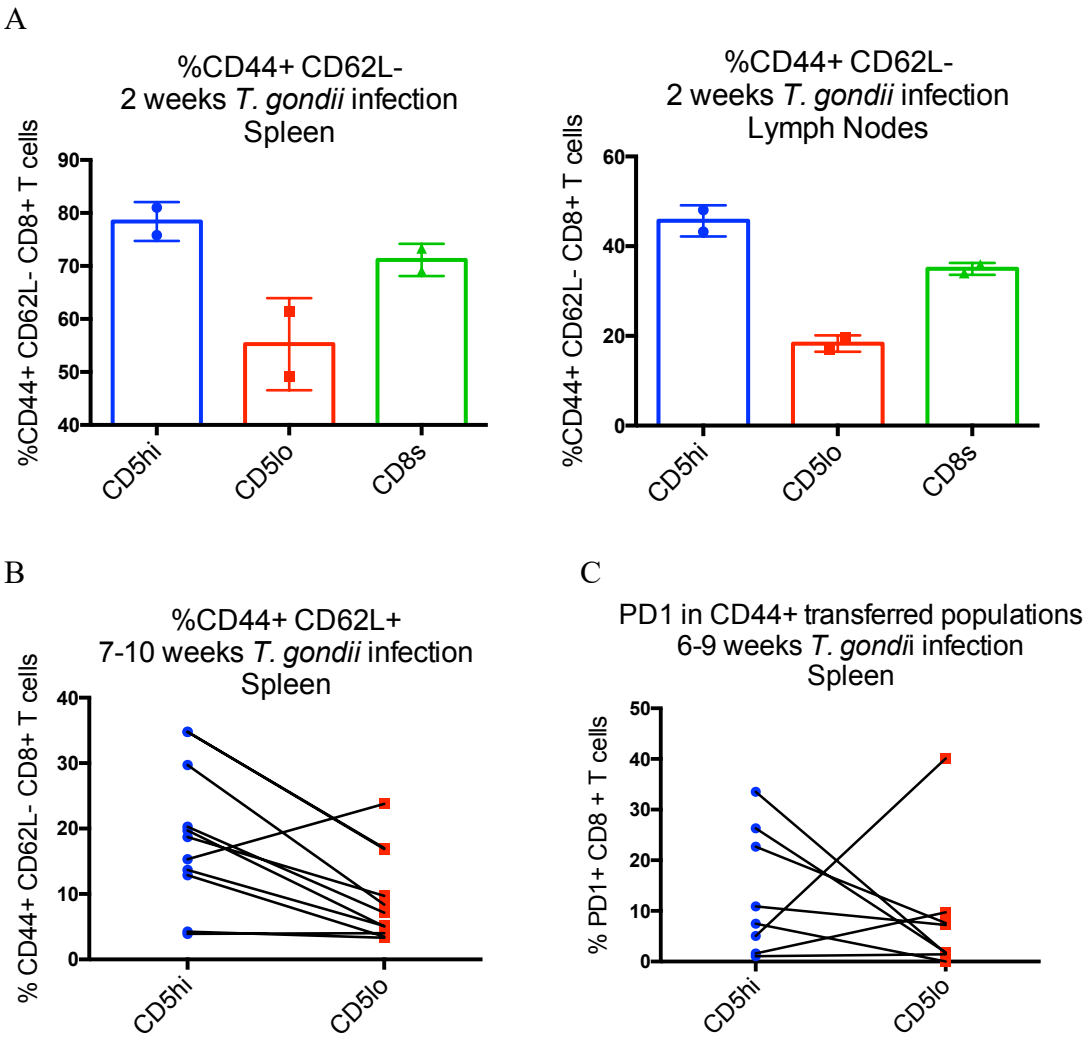

Figure 4.7: Activation and PD1 expression of transferred CD5^{high} and CD5^{low} T cells in *T. gondii* infected mice.

CD62L+ CD44- CD8+ T cells were sorted on CD5 expression from naïve F1$^{b/d}$ mice. The top 25% and bottom 25% of cells were collected and transferred into naïve F1$^{b/d}$ recipient mice with congenic markers to distinguish each population. The next day, mice were infected with *T. gondii* parasites expressing OVA. Mice were sacrificed at either 2 or 7-10 weeks post infection and cells were analyzed by flow cytometry. **(A)** Activation of transferred CD5^{high} and CD5^{low} T cells 2 weeks post infection, with endogenous CD8 T cells as a comparison, in the spleen and lymph nodes. **(B)** Activation of CD5^{high} and CD5^{low} T cells in the spleen 7-10 weeks post infection. **(C)** PD1 expression in CD44+ CD5^{high} and CD5^{low} T cells in the spleen 6-9 weeks post infection. Lines connect data from the same mouse.